

# Introduction à l'optique non-linéaire

Paul Mandel  
Université Libre de Bruxelles  
Faculté des Sciences Appliquées  
(PHYS 327)

Août 2004

©2004 Paul Mandel

This file contains the course *Introduction to Nonlinear Optics* given at the Applied Science Faculty of the Université Libre de Bruxelles during the academic year 2004-2005. Its content is copyright protected. Copies can be made by students if it is not for commercial purposes.

# Contents

Preface	i
<b>I Nonlinear propagation</b>	<b>1</b>
<b>1 Two-level medium</b>	<b>1</b>
1.1 Electric field equation . . . . .	1
1.2 Material equations . . . . .	2
1.3 Phenomenology: incoherent pumping and decay . . . . .	5
<b>2 Propagation regimes</b>	<b>7</b>
2.1 Linear propagation regime . . . . .	7
2.2 Nonlinear susceptibility . . . . .	10
2.3 Nonlinear steady propagation . . . . .	13
2.4 Group and phase velocity . . . . .	14
<b>3 Ultrashort pulse propagation</b>	<b>17</b>
3.1 Introduction . . . . .	17
3.2 Self-induced transparency . . . . .	17
3.3 Sine-Gordon equation . . . . .	23
3.4 $2\pi$ solitons . . . . .	25
3.5 References . . . . .	27
<b>II Cavity nonlinear optics</b>	<b>28</b>
<b>4 Laser theory</b>	<b>29</b>
4.1 Introduction . . . . .	29
4.2 Single mode ring laser . . . . .	34
4.3 Steady states . . . . .	35
4.4 Rate equations . . . . .	36
4.5 Good cavity limit . . . . .	39

4.6	References . . . . .	40
<b>5</b>	<b>Optical Bistability I</b>	<b>41</b>
5.1	Introduction . . . . .	41
5.2	Steady state solutions . . . . .	42
5.3	Optical devices . . . . .	43
5.4	Generic description . . . . .	45
5.5	Nonlinear stability . . . . .	47
5.6	References . . . . .	49
5.7	Appendix: The Schmitt trigger . . . . .	50
<b>6</b>	<b>Optical Bistability II</b>	<b>52</b>
6.1	Delay-differential equations . . . . .	52
6.2	Discrete map equations . . . . .	53
6.3	Deterministic chaos . . . . .	55
6.4	References . . . . .	59
<b>III</b>	<b>Weakly nonlinear systems</b>	<b>61</b>
<b>7</b>	<b>Frequency mixing</b>	<b>62</b>
7.1	Tensor $\rightarrow$ vector $\rightarrow$ scalar description . . . . .	62
7.2	Multiple time-scales . . . . .	63
7.3	$\chi^{(2)}$ media . . . . .	64
7.4	References . . . . .	67
<b>8</b>	<b>Second harmonic generation</b>	<b>68</b>
8.1	Formulation . . . . .	68
8.2	Free running SHG . . . . .	70
8.3	Intracavity SHG . . . . .	79
<b>9</b>	<b>Sum &amp; difference frequency generation</b>	<b>85</b>
9.1	Sum frequency generation . . . . .	85
9.1.1	Formulation . . . . .	85
9.1.2	Free running SFG . . . . .	86
9.2	Difference frequency generation . . . . .	90
9.2.1	Two intense input fields . . . . .	91
9.2.2	One intense input field . . . . .	92
<b>10</b>	<b>Optical parametric oscillator</b>	<b>95</b>
10.1	Formulation . . . . .	95
10.2	Threshold condition . . . . .	96

10.3 Degenerate OPO . . . . . 97  
10.4 Ring and Fabry-Perot cavities . . . . . 101  
10.5 References . . . . . 102

**IV Quantum interference 103**

**11 Coherence and atomic interference 104**  
11.1 Atomic interference . . . . . 104  
11.2 Semiclassical formulation . . . . . 107  
11.3 Electromagnetically induced transparency (EIT) . . . . . 109  
11.4 Slow light . . . . . 112



# Préface

Le but de ces notes de cours est d'introduire l'étudiant aux notions de base de l'optique non-linéaire. Ceci implique deux aspects qu'il faut traiter simultanément: la physique non-linéaire de l'interaction matière-lumière et les mathématiques requises pour résoudre les équations auxquelles conduit la description physique des phénomènes étudiés. J'ai essayé, autant que faire se peut, de trouver un équilibre entre ces deux aspects qui me paraissent également importants, mais il est inévitable que certains chapitres ressemblent plus à un cours de mathématiques appliquées qu'à un cours de physique, pour la bonne raison que la frontière entre ces deux disciplines est floue. On ne s'étonnera donc pas de trouver de nombreux exemples de bifurcations: d'une part, les bifurcations sont l'une des signatures naturelles des non-linéarités; d'autre part, elles sont le mécanisme de choix par lequel des solutions de nouvelle nature peuvent apparaître. Typiquement, les bifurcations les plus simples décrivent l'émergence de solutions périodiques dans le temps et/ou l'espace au départ d'une solution stationnaire et spatialement homogène.

La base de l'optique nonlinéaire telle qu'elle est développée dans ces notes est la théorie électromagnétique de Maxwell. C'est une théorie difficile à assimiler car le champ électromagnétique est un concept unificateur mais abstrait<sup>1</sup>. La théorie de Maxwell est le premier exemple d'une théorie unifiée du champ. La difficulté majeure à laquelle on se heurte est que les équations de Maxwell pour le champ électromagnétique sont linéaires, ce qui les rend conceptuellement simples, tandis que les grandeurs accessibles à l'expérience (énergie, intensité, puissance, ...) sont des fonctions bilinéaires en les champs. Contrairement à la théorie de Newton, qui manipule directement les grandeurs mesurables et permet donc de formuler les relations fondamentales sous une forme simple (force = masse×accélération,

---

<sup>1</sup>Pour rappel, l'article fondateur de Maxwell *A dynamical theory of the electromagnetic field* est paru dans les *Philosophical Transactions of the Royal Society* en 1865. Un physicien américain, Michael Pupin, raconte qu'il est venu à Cambridge en 1883 (soit quatre ans après le décès de Maxwell) pour apprendre la théorie électromagnétique et n'a trouvé personne qui puisse l'aider. Ce n'est qu'en Allemagne, à Berlin, qu'il trouvera en H. von Helmholtz un maître qui lui enseignera la théorie de Maxwell.

action = réaction, ...), la théorie de Maxwell manipule des champs qui vérifient des équations aux dérivées partielles. L'ajout des relations matérielles complique à souhait le problème. On peut voir l'optique non-linéaire comme une chronique de la stratégie développée pour transformer les équations de Maxwell en équations explicites pour des grandeurs mesurables dans le visible. On retrouve le même niveau de difficulté lorsque l'on essaie d'exprimer les lois de la mécanique classique à partir de la mécanique quantique.

Il est généralement impossible de déterminer les limites réelles d'un sujet: certaines d'entre elles paraissent si évidentes que l'on juge inutile de les mentionner, jusqu'à ce qu'un nouveau résultat montre à quel point elles sont importantes. L'optique non-linéaire vient d'être le sujet d'un tel bouleversement. Les chapitres abordés dans les deux premières parties de ces notes ne concernent que l'interaction entre un champ et un milieu matériel qui peut être décrit comme un milieu à deux niveaux. Les chapitres de la troisième partie traitent le milieu matériel comme un milieu caractérisé par une susceptibilité du deuxième ou du troisième ordre constante. Par contre, dans la quatrième partie, j'ai introduit un chapitre qui traite des phénomènes d'interférences atomiques. Actuellement, la conséquence la plus spectaculaire en est la transparence induite par voie électromagnétique et sa conséquence, la lumière lente. Il s'agit là d'un effet purement quantique puisqu'il est lié à l'aspect ondulatoire de la matière.

L'optique non-linéaire souffre d'un défaut parfois considéré comme rédhibitoire: il n'est pas possible de la formuler au départ de principes premiers sans introduire des hypothèses phénoménologiques. Aussi ne me suis-je pas embarrassé de longs développements théoriques visant à justifier ces hypothèses: ces théories existent, souffrent de nombreux défauts et aboutissent toutes, en première approximation, au même résultat que l'approche phénoménologique.

Ce cours s'articule en quatre parties complémentaires:

- La première partie est consacrée à l'étude de la propagation du champ dans des systèmes fortement non-linéaires mais dont le milieu matériel peut être décrit au moyen d'un modèle à deux niveaux.
- La deuxième partie est consacrée à l'étude des mêmes systèmes mais placés dans des cavités résonantes.
- Dans la troisième partie, les systèmes sont faiblement non-linéaires et le milieu matériel est décrit par une polarisation atomique nonlinéaire qui est une fonction bilinéaire du champ électrique.
- Enfin, la quatrième partie aborde les effets d'interférence atomique qui peuvent apparaître lorsque deux voies de désexcitation sont disponibles.

Le choix des chapitres développés dans ce cours résulte à la fois de la contrainte de temps imposée à ce cours (deux modules<sup>2</sup>) et de mes centres d'intérêts. Pour une information complémentaire, l'étudiant pourra consulter avec profit les ouvrages parus sur ce sujet. Voici une brève liste de livres, récents ou classiques, qui traitent de l'optique non-linéaire:

- N. Bloembergen, *Nonlinear optics* (Benjamin, New York, 1965).
- A. Yariv and P. Yeh, *Optical waves in crystals* (Wiley, New York, 1984).
- Y.R. Shen, *The principles of nonlinear optics* (Wiley, New York, 1984).
- P.N. Butcher and D. Cotter, *The elements of nonlinear optics* (Cambridge University Press, 1991).
- A.C. Newell and J.V. Moloney, *Nonlinear optics* (Addison-Wesley, Reading, 1992).
- P. Mandel, *Theoretical problems in cavity nonlinear optics* (Cambridge University Press, 1997).
- R.W. Boyd, *Nonlinear Optics 2<sup>nd</sup> Edition* (Academic Press, New York, 2003).

Cette liste n'est pas exhaustive. À la fin de certains chapitres, j'ai ajouté une liste de références et/ou une bibliographie qui renvoient à des articles originaux et/ou à des livres spécialisés.

Finalement, un mot de précaution: dans chaque chapitre, la notation est cohérente, mais le même symbole peut être utilisé avec des sens différents d'un chapitre à l'autre.

---

<sup>2</sup>La notion de module semble relativement stable car parfaitement indéfinie. Par contre, sa traduction en terme d'heures de cours a subi des fluctuations gigantesques.



# Part I

## Nonlinear propagation



# Chapter 1

## Two-level medium

In this chapter, we review some properties of an electric field  $E$  interacting with a collection of  $N$  identical two-level atoms in the semiclassical formulation. The purpose of this chapter is to show that a nonlinear response is the rule rather than the exception in physics. However, we shall also see that the nonlinear response characterizing the light-matter interaction is usually small. It is only in special circumstances that the nonlinear response becomes a relevant feature.

### 1.1 Electric field equation

Our starting point is Maxwell's equation for the electric field

$$\left( \frac{\partial^2}{\partial x^2} - \frac{1}{c^2} \frac{\partial^2}{\partial t^2} \right) E_{tot} = \frac{1}{\epsilon_0 c^2} \partial_{tt}^2 P_{eff} \quad (1.1)$$

where  $P_{eff}$  is the atomic polarization induced by the field  $E_{tot}$ ,  $c$  is the velocity of light in vacuum and  $\epsilon_0 = 8.85 \times 10^{-12}$  F/m is the vacuum permittivity.

All the problems which are analyzed in these lecture notes share the property that the field will interact with active atoms embedded in a passive and linear medium. For instance, the passive medium can be an inert buffer gas needed to stabilize the active gas, it can be a solvent in which the active liquid is diluted, or it can be the host crystal doped by the active atoms. The total atomic polarization will then be the sum of the polarization generated by the linear passive medium and the polarization, linear and nonlinear, generated by the active medium:  $P_{eff} = P_{pass} + P_{act}$ . We may assume a linear dependence on the field  $P_{pass} = \epsilon_0 \chi_{pass} E_{tot}$  which is the material relation needed to close the Maxwell equation with respect to the passive medium.

It is assumed that the coefficient  $\chi_{pass}$  is real and constant in space and time. This leads to the field equation

$$\left( v^2 \frac{\partial^2}{\partial x^2} - \frac{\partial^2}{\partial t^2} \right) E_{tot} = \frac{1}{\varepsilon'_0} \partial_{tt}^2 P_{act} \quad (1.2)$$

In this equation, the effective velocity of light in the passive medium is defined as  $v = c/n_{pass} \leq c$  where  $n_{pass}^2 = 1 + \chi_{pass}$  is the refractive index of the passive medium, the permittivity  $\varepsilon'_0 = n_{pass}^2 \varepsilon_0$  now refers to the passive medium and the polarization is that of the active atoms only.

We introduce the decompositions

$$E_{tot} = \frac{1}{2} \left[ E e^{i(k_f x - \omega_f t)} + c.c. \right], \quad P_{act} = N \left[ P e^{i(k_f x - \omega_f t)} + c.c. \right] \quad (1.3)$$

where the optical frequency  $\omega_f$  and the wave number  $k_f$  are related by the dispersion relation  $\omega_f = v k_f$ .

In the absence of light-matter interaction, a solution of Maxwell's equation is given by an electric field amplitude  $E$  which is constant in space and time. This is no longer true, in general, in the presence of light-matter interaction. Therefore, we seek solutions  $E(x, t)$  which, due to the atom-field interaction, vary slowly in space and time, compared with the optical space and time variation

$$\omega_f |P| \gg |\partial P / \partial t|, \quad \omega_f |E| \gg |\partial E / \partial t|, \quad k_f |E| \gg |\partial E / \partial x| \quad (1.4)$$

This is usually justified by the fact that the residual variation of the complex field amplitude  $E(x, t)$  is related to the atomic temporal variations, which occur in a much longer time scale. For solid state and semiconductor materials, slow atomic relaxation processes range from 1 to  $10^{-6}$  sec whereas fast atomic relaxation processes range from  $10^{-6}$  to  $10^{-12}$  sec. By contrast, the optical time scale in the visible range is about  $10^{-14}$  to  $10^{-15}$  sec. With these elements, it is easy to derive a propagation equation for the complex field amplitude

$$(v \partial_x + \partial_t) E = (i N \omega_f / \varepsilon'_0) P \quad (1.5)$$

The final step in this derivation is to relate the polarization per atom,  $P$ , with the microscopic properties of the medium. This will be done in the next section.

## 1.2 Material equations

The last equation we have obtained for the electric field is still an open equation since we need a closure relation of the form  $P = P(E)$ . For this,

we have to introduce a model of the atomic system in order to express the reaction of the medium to the applied field. We shall assume that the medium is a collection of  $N$  independent two-level atoms. In doing so, we therefore assume that only resonant or, at least, quasi-resonant, interactions take place. That is, the field frequency is close to the atomic frequency  $(E_2 - E_1)/\hbar$ . For each atom, the wave function is  $\Psi(x) = a_1\varphi_1(x) + a_2\varphi_2(x)$  and the Hamiltonian is  $H = H_0 + V = H_0 - exE_{tot}$  with the properties

$$i\hbar\frac{\partial\Psi}{\partial t} = H\Psi \quad (1.6)$$

$$\Psi = a_1\varphi_1 + a_2\varphi_2 \quad (1.7)$$

$$|a_1|^2 + |a_2|^2 = 1 \quad (1.8)$$

$$H_0\varphi_m = \hbar\omega_m\varphi_m, \quad m = 1, 2 \quad (1.9)$$

$$\int_V \varphi_m\varphi_n^* dx = \delta_{nm} \quad (1.10)$$

The polarization induced in each atom by the external electric field has its origin in the deformation of the electronic charge distribution induced by that electric field. It is given by

$$\begin{aligned} p &= \int_V \Psi^* ex\Psi dx \\ &= a_2a_1^* \int_V \varphi_1^* ex\varphi_2 dx + a_1a_2^* \int_V \varphi_2^* ex\varphi_1 dx \\ &\equiv ex_{12}\rho_{21} + ex_{21}\rho_{12} \end{aligned} \quad (1.11)$$

with the standard notation for the density matrix:  $\rho_{pq} = a_p a_q^*$ . The off-diagonal matrix elements of the density matrix are the atomic coherence, as opposed to the atomic polarization which is the product of the atomic coherence with the matrix element of the electric dipole moment. A coherence between two atomic levels  $p$  and  $q$  means that if the state of level  $p$  is modified, the level  $q$  will be affected even if the perturbation is applied only to the level  $p$ . In systems with more than two levels, this can happen even if the matrix element of the electric dipole between the two states vanishes (forbidden transition). This atomic coherence should not be confused with the so-called coherent states of the electromagnetic field.

From Schrödinger's equation, it follows that

$$\begin{aligned} i\hbar\frac{\partial a_1}{\partial t} &= \hbar\omega_1 a_1 + a_1 V_{11} + a_2 V_{12} \\ &= \hbar\omega_1 a_1 + a_2 V_{12} \\ &\simeq \hbar\omega_1 a_1 - a_2 \mu E_{tot} \end{aligned} \quad (1.12)$$

and similarly

$$i\hbar\frac{\partial a_2}{\partial t} \simeq \hbar\omega_2 a_2 - a_1\mu E_{tot} \quad (1.13)$$

To derive these two equations, we have made some assumptions:

1. The interaction Hamiltonian does not have diagonal matrix elements, i.e.,  $V_{11} = V_{22} = 0$  with  $\mathcal{O}_{nm} = \int_v \varphi_n^* \mathcal{O} \varphi_m dx$  for any operator  $\mathcal{O}$ .
2. The electric field  $E_{tot}(x, t)$  does not vary significantly over an atomic diameter. Therefore, it can be factored out in the off-diagonal matrix elements of  $V$  which can be written as  $V_{12} = -\mu E_{tot}$  where  $\mu = ex_{12}$  is the dipole matrix element of the atomic transition. This approximation is known as the *dipole approximation*.
3. To simplify the algebra, we have assumed without loss of generality that  $\mu = \mu^*$  since all physical quantities are functions of  $|\mu|^2$  which will appear as  $\mu^2$  in these notes.

From equations (1.12) and (1.13), it is easy to derive the pair of coupled equations for the bilinear functions of the coefficients  $a_p$ :

$$\frac{\partial}{\partial t} (a_2 a_1^*) = -i(\omega_2 - \omega_1) a_2 a_1^* + i\frac{\mu}{\hbar} E_{tot} (a_1 a_1^* - a_2 a_2^*) \quad (1.14)$$

$$\frac{\partial}{\partial t} (a_1 a_1^*) = i\frac{\mu}{\hbar} E_{tot} (a_2 a_1^* - a_1 a_2^*) \quad (1.15)$$

In the density matrix notation, these equations are written as

$$\frac{\partial \rho_{21}}{\partial t} = -i(\omega_2 - \omega_1) \rho_{21} + i\frac{\mu}{\hbar} E_{tot} (\rho_{11} - \rho_{22}) \quad (1.16)$$

$$\frac{\partial \rho_{11}}{\partial t} = -\frac{\partial \rho_{22}}{\partial t} = i\frac{\mu}{\hbar} E_{tot} (\rho_{21} - \rho_{21}^*) \quad (1.17)$$

The  $\rho_{pp}$  are associated with the atomic population in level  $p$ . Defining the population difference  $n = \rho_{11} - \rho_{22}$  and the atomic frequency  $\omega_a = \omega_2 - \omega_1 > 0$ , we can write the evolution equations for the density matrix elements as

$$\frac{\partial \rho_{21}}{\partial t} = -i\omega_a \rho_{21} + i\frac{\mu}{\hbar} E_{tot} n \quad (1.18)$$

$$\frac{\partial n}{\partial t} = 2i\frac{\mu}{\hbar} E_{tot} (\rho_{21} - \rho_{21}^*) \quad (1.19)$$

The closure relation we are looking for is

$$P_{tot} = Np \quad (1.20)$$

or equivalently  $P e^{i(k_f x - \omega_f t)} = \mu \rho_{21} \equiv \mu \sigma e^{i(k_f x - \omega_f t)}$ : the polarization  $P_{tot}$  which induces the electric field in Maxwell's equations is equal to the polarization induced by the electric field as derived from the Schrödinger equation. In doing so, we obtain a closed set of equations which couple the field and the material variables  $\{E_{tot}, \rho_{pq}\}$ . This formulation of the light-matter interaction leads to the so-called semiclassical description since the field is treated as classical while matter is fully quantized. Equation (1.20) results from the assumption that all atoms are identical. If the atoms differ by one or more variables,  $P_{tot}$  must be expressed as the mean value over that or these variables. For instance, in a gas, we must add to the energy of the atomic levels  $\hbar\omega_p$  the kinetic energy of the center of mass. The total polarization then becomes the average over the velocity distribution  $g(\mathbf{v})$  which is typically a gaussian or a lorentzian distribution:  $P_{tot} \sim \int g(\mathbf{v}) p(\mathbf{v}) d\mathbf{v}$ .

A last approximation is introduced now. This approximation is referred to as the *rotating wave approximation*. The left hand side of (1.18) is  $\partial\rho_{21}/\partial t \sim \exp[i(k_f x - \omega_f t)]$  while the right hand side of that equation is

$$\left\{ -i\omega_a \sigma + i\frac{\mu}{2\hbar} \left[ E + E^* e^{-2i(k_f x - \omega_f t)} \right] n \right\} e^{i(k_f x - \omega_f t)}. \quad (1.21)$$

Likewise, the left hand side of (1.19) is  $\partial n/\partial t$  while the right hand side of that equation is

$$i\frac{\mu}{\hbar} \left[ E^* \sigma - E \sigma^* + E \sigma e^{2i(k_f x - \omega_f t)} - E^* \sigma^* e^{-2i(k_f x - \omega_f t)} \right] \quad (1.22)$$

Since the field and the material variables  $E, \sigma,$  and  $n$  are slowly varying functions, we neglect fast oscillating terms proportional to  $\exp[\pm 2i(k_f x - \omega_f t)]$ , and obtain the coupled equations

$$(\partial_x + v^{-1}\partial_t) E = (iN\mu\omega_f/v\varepsilon'_0)\sigma \quad (1.23)$$

$$\frac{\partial\sigma}{\partial t} = -i\delta\sigma + i\frac{\mu}{2\hbar} E n \quad (1.24)$$

$$\frac{\partial n}{\partial t} = i\frac{\mu}{\hbar} (E^* \sigma - E \sigma^*) \quad (1.25)$$

with  $\delta \equiv \omega_a - \omega_f$ .

### 1.3 Phenomenology: incoherent pumping and decay

The description obtained sofar is incomplete. Equations (1.23)-(1.25) correctly describe the interaction process between *stable* atoms and a *lossless*

medium. However, the atomic levels are not stable. In addition, the two-level model of the medium accounts only for the quasi-resonant interaction with the field. Apart from that, there are nonresonant interactions (involving the other atomic levels of the active atoms and/or the passive host medium) which yield a linear, i.e., field-independent loss. The usual procedure is to add phenomenological constants to the evolution equations (1.23)-(1.25) in the following way. For the field equation, we add to the right hand side a term  $-\kappa E$

$$(\partial_x + v^{-1}\partial_t) E = -\kappa E + (iN\mu\omega_f/v\varepsilon'_0)\sigma \quad (1.26)$$

In the absence of interaction with the two-level medium, this leads, for instance, to a steady solution which decays according to the Beer-Lambert law:  $E(x) = E(0)\exp(-\kappa x)$ . The space-time dependent case in the linear approximation will be studied in the next section.

We now introduce phenomenological constants to account for the finite life-time of the two energy levels of the active medium. For the atomic polarization, we also add a linear damping term  $-\gamma_\perp\sigma$  while the population difference we add the damping  $-\gamma_\parallel n$ . However, we also have to take into account incoherent processes which populate the atomic levels at different rates. Let  $n^0$  be the population difference reached in steady state in the absence of interaction with the coherent field  $E_{tot}$ . Then we add a source term to the population inversion evolution equation and arrive at

$$\frac{\partial\sigma}{\partial t} = -(\gamma_\perp + i\delta)\sigma + i\frac{\mu}{2\hbar}En \quad (1.27)$$

$$\frac{\partial n}{\partial t} = \gamma_\parallel(n^0 - n) + i\frac{\mu}{\hbar}(E^*\sigma - E\sigma^*) \quad (1.28)$$

Equations (1.26)-(1.28) form the basis of our study of two-level atoms interacting with a monochromatic electric field<sup>1</sup>. The set of Eqs. (1.26)-(1.28) is widely known as the Maxwell-Bloch equations.

---

<sup>1</sup>In some areas, especially solid-state physics interacting with microwave radiation, the two relaxation times are written differently:  $T_2$  is used instead of  $1/\gamma_\perp$  and  $T_1$  is used instead of  $1/\gamma_\parallel$ .

# Chapter 2

## Propagation regimes

### 2.1 Linear propagation regime

As a first approach to Eqs. (1.26)-(1.28), we shall consider the linear regime of propagation, in which the problem is reduced to the pair of coupled linear equations for  $E$  and  $\sigma$

$$(\partial_x + v^{-1}\partial_t + \kappa) E = (iN\mu\omega_f/v\varepsilon'_0)\sigma \quad (2.1)$$

$$\frac{\partial\sigma}{\partial t} = -(\gamma_\perp + i\delta)\sigma + i\frac{\mu}{2\hbar}En \quad (2.2)$$

$$\frac{\partial n}{\partial t} = \gamma_\parallel(n^0 - n) \quad (2.3)$$

Indeed, equations (2.1)-(2.2) imply a linear relation  $\sigma \propto E$  while retaining the  $E$ -dependant term in (1.28) leads to nonlinear corrections to the relation  $\sigma \propto E$  and to  $n$ .

In the long time limit, we seek plane wave solutions

$$E = \mathcal{E}e^{i(kx-\omega t)}, \quad \sigma = se^{i(kx-\omega t)}, \quad n = n^0 \quad (2.4)$$

The frequency  $\omega$  and the wave number  $k$  which we have just introduced represent shifts of the unperturbed frequency  $\omega_f$  and wave number  $k_f$  of the field due to the atom-field interaction. Inserting (2.4) into the linearized equations (2.1)-(2.3) leads to

$$(ik - i\omega/v + \kappa)\mathcal{E} = \frac{iN\omega_f\mu}{\varepsilon'_0v}s \quad (2.5)$$

$$-i\omega s = -(\gamma_\perp + i\delta)s + \frac{i\mu}{2\hbar}n^0\mathcal{E} \quad (2.6)$$

These are two homogeneous equations for two variables  $a_1\mathcal{E} + b_1s = 0$  and  $a_2\mathcal{E} + b_2s = 0$ . The compatibility condition of this pair of homogeneous

equations is that the determinant of the coefficients vanishes:  $a_1 b_2 - a_2 b_1 = 0$ , otherwise only the trivial solution  $\mathcal{E} = s = 0$  exists. This leads to

$$(k - \omega/v - i\kappa)(\omega - \delta + i\gamma_\perp) + \frac{N\omega_f\mu^2 n^0}{2\hbar\varepsilon'_0 v} = 0 \quad (2.7)$$

This is the dispersion relation  $k = k(\omega)$  we were looking for. Its solution is

$$k = \frac{\omega}{v} + \frac{\omega - \delta}{\gamma_\perp} \alpha + i(\kappa - \alpha) \quad (2.8)$$

$$\alpha = -\frac{N\omega_f\mu^2 n^0}{2\hbar\varepsilon'_0 v \gamma_\perp [1 + (\omega - \delta)^2/\gamma_\perp^2]} \quad (2.9)$$

We have introduced the parameter  $\alpha \propto -n^0 \equiv \rho_{22}^0 - \rho_{11}^0$  which is the linear (or small signal) gain or loss, depending on whether it is positive or negative, respectively. The frequency detuning  $\omega - \delta = \omega - \omega_a + \omega_f$  is the difference between the effective field frequency  $\Omega_f = \omega_f + \omega$  and the atomic frequency  $\omega_a$ .

The stability properties of the plane wave are easily derived from (2.8), taking  $\omega$  real:

- $\alpha < \kappa$ : In this case,  $\text{Im } k > 0$  and the plane wave is attenuated in the linear regime since  $E, \sigma \sim \exp[-x \text{Im}(k)]$ .
- $\alpha > \kappa$ : In this case,  $\text{Im } k < 0$  and the plane wave is amplified in the linear regime.

Hence the plane wave solution is stable below the threshold  $\alpha = \kappa$  and unstable above the threshold. If  $\alpha > \kappa$ , there is a net gain and the linear theory is no longer able to describe correctly the system. The important property is that the gain condition  $\alpha > \kappa$  can be written as a condition for the population inversion as  $\rho_{22}^0 - \rho_{11}^0 > (\rho_{22}^0 - \rho_{11}^0)_{\text{threshold}} > 0$ . In other terms, an initial population inversion is necessary, though not sufficient, to ensure gain in the two-level medium. Note that the condition  $\alpha > \kappa$  can also be interpreted as a condition of strong light-matter interaction with  $\mu^2 > \mu_{\text{crit}}^2$ . These questions will be studied with more details in Chapter 4.

We can deduce from (2.6) the linearized eigensolution in the form of the ratio  $s/\mathcal{E}$ , from which we derive the expression

$$\frac{P}{E} = \frac{\mu s}{\mathcal{E}} = \frac{\mu^2 n^0}{2\hbar} \left[ \frac{\omega_a - \Omega_f}{\gamma_\perp^2 + (\omega_a - \Omega_f)^2} + \frac{i\gamma_\perp}{\gamma_\perp^2 + (\omega_a - \Omega_f)^2} \right] \equiv \chi_0(\Delta) \quad (2.10)$$

which defines the linear susceptibility  $\chi_0 = \chi'_0 + i\chi''_0$  with

$$\chi'_0(\Delta) = \frac{\mu^2 n^0}{2\hbar} \frac{\Delta}{\gamma_\perp^2 + \Delta^2} \quad (2.11)$$

$$\chi''_0(\Delta) = \frac{\mu^2 n^0}{2\hbar} \frac{\gamma_\perp}{\gamma_\perp^2 + \Delta^2} \quad (2.12)$$

and  $\Delta = \omega_a - \Omega_f$ . The real and imaginary parts of the susceptibility are related by the obvious property

$$\chi'_0(\Delta) = \frac{\Delta}{\gamma_\perp} \chi''_0(\Delta) \quad (2.13)$$

From (2.1) it follows that the imaginary part of the susceptibility describes the absorptive properties of the medium which affect the real amplitude of the field  $E$ . The linear gain is proportional to  $\chi''$ . A way to see this point is to decompose the field into amplitude and phase:  $E = |E| \exp(i\varphi)$ . Then it is easy to verify that  $\chi''$  contributes to the evolution of the amplitude  $|E|$  while  $\chi'$  contributes to the evolution of the phase  $\varphi$ :

$$(\partial_x + v^{-1}\partial_t + \kappa) |E| = -(N\omega_f/v\varepsilon'_0) |E| \chi'' \quad (2.14)$$

$$(\partial_x + v^{-1}\partial_t) \varphi = (N\omega_f/v\varepsilon'_0) \chi' \quad (2.15)$$

Another way to understand the susceptibility  $\chi$  is to introduce the relation  $P = \chi E$  into the definitions (1.3):

$$\begin{aligned} P_{tot} &= N \left[ \chi E e^{i(k_f x - \omega_f t)} + c.c. \right] \\ &= 2N\chi' E_{tot} + iN\chi'' \left[ E e^{i(k_f x - \omega_f t)} - c.c. \right] \\ &\equiv 2N\chi' E_{tot} + iN\chi'' E_{diss} \end{aligned} \quad (2.16)$$

Inserting this result in the Maxwell equation (1.2) leads to

$$\left( \partial_{xx}^2 - \frac{1}{v_{eff}^2} \partial_{tt}^2 \right) E_{tot} = \frac{iN\chi''}{\varepsilon'_0 v^2} \partial_{tt}^2 E_{diss} \quad (2.17)$$

corresponding to the propagation of a wave with velocity  $v_{eff} = v/n$  where  $n = \sqrt{1 + 2N\chi'/\varepsilon'_0}$  is the refractive index of the active medium. It is apparent on Eq.(2.17) that  $\chi'$  contributes to the phase evolution while  $\chi''$  contributes to dissipative processes since  $\chi'' \sim \gamma_\perp$ .

As a function of  $\delta - \omega = \omega_a - \Omega_f$ , the imaginary part  $\chi''(\omega_a - \Omega_f)$  is a Lorentzian peaked at  $\omega_a = \Omega_f$ . The real part of  $\chi_0$  describes the dispersive

properties of the medium which affect the phase of the complex field amplitude  $E$ . It vanishes for  $\omega_a = \Omega_f$ , where  $\chi_0''$  is maximum. It is a characteristic of linear systems that dispersion vanishes where absorption is maximum. The function  $g = \Delta / (\Delta^2 + \gamma_\perp^2)$  with  $\Delta = \omega_a - \Omega_f$  is associated with dispersion and has extrema at  $\Delta_\pm = \pm\gamma_\perp$  where its value is  $g_\pm = \pm 1/(2\gamma_\perp)$ . The function  $f = \gamma_\perp / (\Delta^2 + \gamma_\perp^2)$  which is associated with absorption has the property that  $f(\pm\gamma_\perp) = 1/(2\gamma_\perp)$  at the extrema of  $g$ . A graphical representation of the functions  $f$  and  $g$  versus  $\Delta$  is displayed in Fig.2.1.

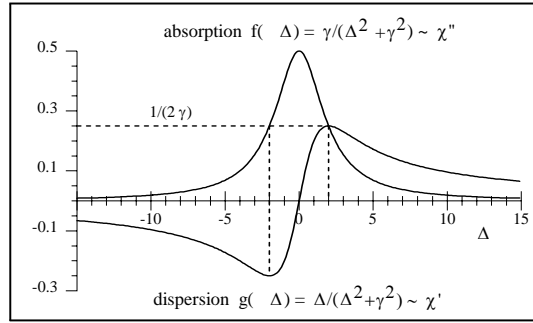


Figure 2.1: Linear dispersion and absorption.

In particular, it follows from this discussion that the *full width at half maximum* (FWHM) of the absorption curve  $f$  is  $2\gamma_\perp$  since the half maximum of  $f$  is reached at  $\Delta = \pm\gamma_\perp$ .

Another property which is important because its validity goes well beyond the linear regime is the relation, on resonance ( $\omega_a = \Omega_f$ ), between the imaginary part of the susceptibility and the slope of its real part:

$$\chi_0''(\Delta = 0) = \gamma_\perp \left. \frac{\partial \chi_0'(\Delta)}{\partial \Delta} \right|_{\Delta=0} \quad (2.18)$$

This relation, derived from (2.13), relates the linear gain to the dispersive properties of the medium at the resonance.

## 2.2 Nonlinear susceptibility

The nonlinear equations (1.26)-(1.28) admit *steady state* solutions of the form

$$dE/dx + \kappa E = (iN\mu\omega_f/v\varepsilon'_0)\sigma \quad (2.19)$$

$$\sigma = \frac{i\mu}{2\hbar} \frac{En}{\gamma_{\perp} + i\delta} \quad (2.20)$$

$$n = n^0 + \frac{i\mu}{\hbar\gamma_{\parallel}} (E^*\sigma - E\sigma^*) \quad (2.21)$$

From the last two equations we obtain an expression of the material variables in terms of the field intensity

$$n = n^0 \left\{ 1 + \frac{|\mu E|^2}{\hbar^2 \gamma_{\perp} \gamma_{\parallel} [1 + (\delta/\gamma_{\perp})^2]} \right\}^{-1} \quad (2.22)$$

$$\sigma = E \frac{\mu n^0}{2\hbar \gamma_{\perp}} \frac{i + \delta/\gamma_{\perp}}{1 + (\delta/\gamma_{\perp})^2} \left\{ 1 + \frac{|\mu E|^2}{\hbar^2 \gamma_{\perp} \gamma_{\parallel} [1 + (\delta/\gamma_{\perp})^2]} \right\}^{-1} \quad (2.23)$$

Note that in the strong field limit,  $|E| \rightarrow \infty$ , we have  $n \rightarrow 0$  and  $\sigma \rightarrow 0$ . Hence we obtain

$$|E| \rightarrow \infty: \quad \rho_{11} \rightarrow 1/2, \quad \rho_{22} \rightarrow 1/2, \quad \rho_{12} \rightarrow 0 \quad (2.24)$$

In other terms, a strong field bleaches the atomic system :  $n = \rho_{11} - \rho_{22} \rightarrow 0$  (which is independent of  $n^0$ ) but destroys the atomic coherence :  $\rho_{12} \rightarrow 0$ .

The susceptibility  $\chi$  is defined by  $P \equiv \chi E$ ; therefore the steady state susceptibility is

$$\chi_s = \chi'_s + i\chi''_s = \frac{\mu^2 n^0}{2\hbar \gamma_{\perp}} \frac{i + \delta/\gamma_{\perp}}{1 + (\delta/\gamma_{\perp})^2} \left\{ 1 + \frac{|\mu E|^2}{\hbar^2 \gamma_{\perp} \gamma_{\parallel} [1 + (\delta/\gamma_{\perp})^2]} \right\}^{-1} \quad (2.25)$$

We have the obvious relation between the real and imaginary parts of the susceptibility:

$$\chi' = (\delta/\gamma_{\perp})\chi'' \quad (2.26)$$

The linear susceptibility  $\chi_0$  derived in Section 2.1 is  $\omega$ -dependant but field-independent. It fully characterizes the linear response of the medium to the external electric field via the dispersion relation  $k = k(\omega)$  which originates from the atom-field interaction. On the contrary,  $\chi_s$  is the static ( $k = \omega = 0$ ) component of the susceptibility but it is field-dependent as no assumption has been made on the field amplitude. The susceptibility  $\chi_s$  neglects the back reaction of the medium on the propagation characteristics of the field:  $\Omega_f = \omega_f$ . Both expressions represent different approximations of a more

general function which depends on  $\omega$  and on the field. To make contact with the linearized susceptibility, we write the susceptibility  $\chi_s$  in the form

$$\chi'_s = \frac{\mu^2 n^0}{2\hbar} \frac{\Delta}{\tilde{\gamma}_\perp^2 + \Delta^2} = \frac{\mu^2 n^0}{2\hbar \gamma_\perp} \frac{\Delta/\gamma_\perp}{1 + K + (\Delta/\gamma_\perp)^2} \quad (2.27)$$

$$\chi''_s = \frac{\mu^2 n^0}{2\hbar \sqrt{1 + |\mu E|^2 / (\hbar^2 \gamma_\perp \gamma_\parallel)}} \frac{\tilde{\gamma}_\perp}{\tilde{\gamma}_\perp^2 + \Delta^2} = \frac{\mu^2 n^0}{2\hbar \gamma_\perp} \frac{1}{1 + K + (\Delta/\gamma_\perp)^2} \quad (2.28)$$

with

$$\tilde{\gamma}_\perp = \gamma_\perp \sqrt{1 + |\mu E|^2 / (\hbar^2 \gamma_\perp \gamma_\parallel)} \equiv \gamma_\perp \sqrt{1 + K} \quad (2.29)$$

and  $\Delta = \omega_a - \Omega_f$ . The real and imaginary parts of  $\chi_s 2\hbar \gamma_\perp / (\mu^2 n^0)$  are displayed in figure 2.2.

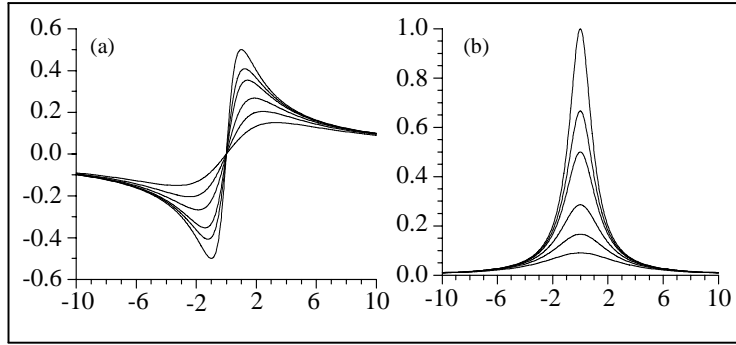


Figure 2.2: Nonlinear dispersion and absorption as a function of  $\Delta$ . (a)  $\chi' = \text{Re}(\chi) = \Delta / (1 + K + \Delta^2)$ . (b)  $\chi'' = \text{Im}(\chi) = 1 / (1 + K + \Delta^2)$ . Units of  $\chi$  are  $\mu^2 n^0 / (2\hbar \gamma_\perp)$ . From top to bottom,  $K = 0, 0.5, 1, 2.5, 5$  and  $10$ .

Note that Eq. (2.18) remains valid for the nonlinear susceptibility defined by Eqs. (2.27) and (2.28). The field dependence that appears in the static susceptibility (2.27) and (2.28) leads to an effect which is known as *power broadening*. For instance, the FWHM is

$$\text{FWHM} = 2\gamma_\perp \sqrt{1 + |\mu E|^2 / (\hbar^2 \gamma_\perp \gamma_\parallel)} \quad (2.30)$$

Another important effect is that the absorption, characterized by  $\chi''$ , is reduced by a factor  $\sqrt{1 + |\mu E|^2 / (\hbar^2 \gamma_\perp \gamma_\parallel)}$  from the low intensity limit: the

reduction of absorption with increasing intensity is known as saturation. It is interesting to note that absorption and dispersion expressed in terms of  $\tilde{\gamma}_\perp$  are not modified in the same way by the light-matter interaction. However, the relation (2.18) which relates the gain and the slope of the dispersion on resonance remains true in this nonlinear regime.

## 2.3 Nonlinear steady propagation

In this section, we assume that the system is below its amplification threshold ( $\alpha < \kappa$ ). From (2.19)-(2.21) it follows that the complex field amplitude in steady state is given by

$$dE/dx = -\kappa E - \bar{\alpha} E \frac{n}{n^0} (1 - i\delta/\gamma_\perp) \quad (2.31)$$

$$\bar{\alpha} \equiv \bar{\alpha}(x, \delta) = \frac{N\omega_f \mu^2 n^0(x)}{2\hbar\gamma_\perp \varepsilon'_0 v [1 + (\delta/\gamma_\perp)^2]} \quad (2.32)$$

We have seen in section 2.1 that  $n = n^0$  in the linear regime. Inserting this approximation in (2.31) and assuming that  $n^0$  is constant in space leads to the Beer-Lambert law

$$|E(x)|^2 = |E(0)|^2 e^{-\beta x} \quad (2.33)$$

$$\beta = 2(\kappa + \bar{\alpha}) \quad (2.34)$$

where  $\beta$  is the linear attenuation coefficient.

Coming back to the general equation (2.31), we introduce the polar decomposition of the field  $E = \bar{E}e^{i\phi}$  in terms of which the electric field real amplitude is the solution of

$$d\bar{E}/dx = -\kappa\bar{E} - \bar{\alpha}\bar{E}n/n^0 \quad (2.35)$$

The reduced intensity  $J$  defined by

$$J = \frac{|\mu E|^2}{\hbar^2 \gamma_\perp \gamma_\parallel [1 + (\delta/\gamma_\perp)^2]} \quad (2.36)$$

verifies the equation

$$dJ/dx = -2 \left( \kappa + \frac{\bar{\alpha}}{1 + J} \right) J \quad (2.37)$$

The difficulty with this equation is the space-dependence of  $\bar{\alpha}$ . Let us therefore consider the limit of negligible non resonant linear loss:  $\kappa \ll \bar{\alpha}$ . In that

limit, we obtain  $dJ/dx = -2\bar{\alpha}J/(1+J)$  which can be solved to give the implicit equation

$$J - J_0 + \ln(J/J_0) = -2 \int_0^x \bar{\alpha}(x') dx' \quad (2.38)$$

with  $J(0) = J_0$ . Let us define an extinction length  $x_{ext}$  as in the linear theory by the condition  $J(x_{ext}) \equiv J_0 e^{-1}$ . If the initial population difference  $n^0$  is space-independent,  $\bar{\alpha}$  is also space-independent and we find from (2.38)

$$x_{ext} = \frac{J_0(1 - 1/e) + 1}{2\bar{\alpha}} \quad (2.39)$$

In the weak field limit, we have of course  $x_{ext} \simeq 1/(2\bar{\alpha})$ . However, in the high intensity limit  $J_0 \gg 1$ , we obtain  $x_{ext} \simeq J_0(1 - 1/e)/2\bar{\alpha} \gg 1/(2\bar{\alpha})$ . Hence, the extinction length may be significantly increased in the high field limit because it saturates the atomic transition and tends to bleach the material medium.

## 2.4 Group and phase velocity

Let us consider again Maxwell equations for the electric field:

$$\left( \frac{\partial^2}{\partial x^2} - \frac{1}{v^2} \frac{\partial^2}{\partial t^2} \right) E = 0 \quad (2.40)$$

If the field propagates in vacuum,  $v = c$ . If the field propagates in a medium where the polarization is related to the electric field by the material relation  $P = \chi E$ , the velocity appearing in Eq. (2.40) is  $v = c/n = c/\sqrt{1 + \text{Re}(\chi)}$ , provided  $\chi$  is time-independent. In that case, we shall assume for simplicity in the following developments that  $\chi$  is real. The general solution of Eq. (2.40) is  $E = f(t - x/v)$  where the function  $f$  is determined either by the boundary or by the initial conditions. Thus, the plane  $t - x/v = \Pi$ , where  $\Pi$  is constant in space and time, is a plane where the electric field is constant. In other terms, a given value of the electric field propagates at the speed  $v$ . This speed is called the phase velocity, by reference to the simplest solution of Eq. (2.40), namely the running wave

$$g(t, x|k, \omega) = A \exp[i(kx - \omega t)] = A \exp[-i\omega(t - x/v)] \quad (2.41)$$

since  $k = \omega/v$ . Although the function  $g(x, t|k, \omega)$  verifies the Maxwell equation (2.40), it is not a physical solution since the electric field  $E$  must be real.

It is therefore at least the combination of two running waves  $g(x, t|k, \omega)$  and  $g^*(x, t|k, \omega) = g(x, t|-k, -\omega)$ .

In general, the amplitude  $A$  of the running wave in Eq. (2.41) is not a constant, but varies in space and time. Therefore, more general solutions are usually required. Their expression as a linear combination of running wave of the type (2.41) follows directly from the linearity of the equation and is the basis of the Fourier analysis of the Maxwell equations.

A less general representation is often adequate. Let us assume that, for a particular problem, the electric field can be written as a quasi-plane wave

$$E(x, t) = A(x, t)e^{i(\bar{k}x - \bar{\omega}t)} + c.c. \quad (2.42)$$

with

$$A(x, t) = \int_{\Delta\omega} a(\omega)e^{i[(k-\bar{k})x - (\omega-\bar{\omega})t]} d\omega \quad (2.43)$$

A quasi-plane wave is a solution for which  $a(\omega)$  is sharply peaked around the frequency  $\bar{\omega}$ . It corresponds to a wave packet with frequency spread  $\Delta\omega$  around  $\bar{\omega}$ . The corresponding wave number is  $\bar{k} = \bar{\omega}n(\bar{\omega}, \bar{k})/c$ . In the integral (2.43), we may expand the wave number  $k$  appearing in the exponential around  $\bar{k}$ :

$$\begin{aligned} k &= \bar{k} + (\omega - \bar{\omega}) \left. \frac{\partial k}{\partial \omega} \right|_{\omega=\bar{\omega}} + \mathcal{O}[(\omega - \bar{\omega})^2] \\ &\equiv \bar{k} + \frac{\omega - \bar{\omega}}{v_g} + \mathcal{O}[(\omega - \bar{\omega})^2] \end{aligned} \quad (2.44)$$

which defines the group velocity  $v_g$  of the wave packet. Therefore, the expression for the field amplitude becomes

$$\begin{aligned} A(x, t) &= \int_{\Delta\omega} a(\omega)e^{i[(k-\bar{k})x - (\omega-\bar{\omega})t]} d\omega \\ &\simeq \int_{\Delta\omega} a(\omega)e^{-i(\omega-\bar{\omega})(t-x/v_g)} d\omega \end{aligned} \quad (2.45)$$

The planes  $t - x/v_g = \Pi_g$ , where  $\Pi_g$  is constant in space and time, move at the group velocity  $v_g$ . On  $\Pi_g$  the amplitude of the field is constant: as a result of the interference among the running waves with a small spread in frequency, all of them propagating at the phase velocity  $v$ , there will be an envelope  $A(x, t)$ , corresponding to a space and time localization of electromagnetic energy, which propagates at the group velocity  $v_g$ .

An equation for the group velocity is easily obtained by differentiating with respect to  $k$  the dispersion relation  $kc = \omega n(\omega, k)$ :

$$\begin{aligned}
 c &= \frac{d\omega}{dk}n + \omega \frac{dn}{dk} \\
 &= n \frac{\partial \omega}{\partial k} + \omega \left( \frac{\partial n}{\partial k} + \frac{\partial n}{\partial \omega} \frac{\partial \omega}{\partial k} \right) \\
 &= v_g \left( n + \omega \frac{\partial n}{\partial \omega} \right) + \omega \frac{\partial n}{\partial k}
 \end{aligned} \tag{2.46}$$

which leads to the result

$$v_g \equiv \frac{\partial \omega}{\partial k} = \frac{c - \omega \frac{\partial n}{\partial k}}{n + \omega \frac{\partial n}{\partial \omega}} \tag{2.47}$$

Let us emphasize that this last result is not constrained by the linearity condition: it is valid for any nonlinear medium for which the refractive index is a scalar. If the medium is birefringent, the refractive index must be treated as a vector and the group velocity must be generalized accordingly.

There are two contributions to the group velocity: the first term  $c / (n + \omega \partial n / \partial \omega)$  is only due to the frequency dispersion of the medium. It results from the fact that the refractive index varies with frequency. The second term,  $-\omega (\partial n / \partial k) / (n + \omega \partial n / \partial \omega)$ , is proportional to the spatial dispersion of the medium. It results from the fact that the medium has a non-local response to a probe field, i.e., that the wave packet has a finite spatial extension. The denominator  $\partial (n\omega) / \partial \omega = n + \omega \partial n / \partial \omega \equiv n_g$  is also known as the group refractive index since  $v_g = c / n_g$ .

# Chapter 3

## Ultrashort pulse propagation

### 3.1 Introduction

In this chapter, we consider the propagation of short pulses in a nonlinear medium. We know that a field of low intensity  $I$  propagating in an absorbing medium is attenuated. Beer-Lambert's law quantifies this property in the linear regime by stating that the intensity varies along the propagation of the beam according to the law  $dI/dx = -CI$  where  $C$  is independent of  $I$  though it is frequency-dependent. This equation is discussed at the end of Chapter 2. In that chapter, we also derived equation (2.37) which generalizes Beer-Lambert's law for a beam of arbitrary initial intensity propagating in a nonlinear medium modelled as a two-level medium. In this chapter we shall see how this law is modified when it is a pulse that propagates in the same nonlinear medium. To concentrate on the essential, we consider only a short pulse. This means that the pulse duration is much shorter than any atomic characteristic time so that atoms can be treated as stable: the population difference and the atomic polarization vary only as a result of the resonant interaction with the light pulse.

### 3.2 Self-induced transparency

Let us consider the propagation equation (1.23) and the material equations (1.24)-(1.25)

$$(v\partial_x + \partial_t) E = (iN\mu\omega_c/\varepsilon'_0)\sigma \quad (3.1)$$

$$\frac{\partial\sigma}{\partial t} = -i(\omega_a - \omega_c)\sigma + \frac{i\mu}{2\hbar}En \quad (3.2)$$

$$\frac{\partial n}{\partial t} = i\frac{\mu}{\hbar}(E^*\sigma - E\sigma^*) \quad (3.3)$$

As a first step, we generalize these equations to account for the dispersion of the atomic frequency  $\omega_a$ . Let us assume that the medium is characterized by a distribution  $g(\omega_a)$  of atomic frequencies normalized to unity:  $\int_0^\infty g(\omega_a) d\omega_a = 1$ . Then Eqs. (3.1)-(3.3) become

$$(v\partial_x + \partial_t) E = (iN\mu\omega_c/\varepsilon'_0) \int_0^\infty g(\omega)\sigma(\omega)d\omega \quad (3.4)$$

$$\frac{\partial\sigma}{\partial t} = -i(\omega - \omega_c)\sigma + \frac{i\mu}{2\hbar}En \quad (3.5)$$

$$\frac{\partial n}{\partial t} = i\frac{\mu}{\hbar}(E^*\sigma - E\sigma^*) \quad (3.6)$$

where  $\sigma$  and  $n$  are of course functions of  $x, t$ , and  $\omega$ . We decompose the complex electric field and polarization into real and imaginary parts

$$E(x, t) = \mathcal{E}(x, t)e^{i\phi(x, t)} \quad (3.7)$$

$$\sigma(\omega, x, t) = \frac{1}{2}[\mathcal{Q}(\omega, x, t) - i\mathcal{P}(\omega, x, t)]e^{i\phi(x, t)} \quad (3.8)$$

Since  $e^{i\pi/2} = i$ ,  $\mathcal{P}$  is the quadrature of the atomic polarization which is out-of-phase with respect to the field, while  $\mathcal{Q}$  is the quadrature of the atomic polarization in phase with the electric field. This decomposition is physically relevant since we shall see that  $\mathcal{Q}$  contributes to the phase  $\phi$  of the field and is therefore associated with the material dispersion while  $\mathcal{P}$  is related to the variation of the field amplitude  $\mathcal{E}$  and is thus associated with absorption. It follows directly that the evolution equations are

$$(v\partial_x + \partial_t) \mathcal{E}(x, t) = \frac{N\mu\omega_c}{2\varepsilon'_0} \int_0^\infty \mathcal{P}(\omega, x, t)g(\omega)d\omega \quad (3.9)$$

$$\mathcal{E}(x, t) (v\partial_x + \partial_t) \phi(x, t) = \frac{N\mu\omega_c}{2\varepsilon'_0} \int_0^\infty \mathcal{Q}(\omega, x, t)g(\omega)d\omega \quad (3.10)$$

$$\partial_t \mathcal{Q}(\omega, x, t) = \{\omega_c - \omega - [\partial_t \phi(x, t)]\} \mathcal{P}(\omega, x, t) \quad (3.11)$$

$$\begin{aligned} \partial_t \mathcal{P}(\omega, x, t) &= -\{\omega_c - \omega - [\partial_t \phi(x, t)]\} \mathcal{Q}(\omega, x, t) \\ &\quad -(\mu/\hbar)n(\omega, x, t)\mathcal{E}(x, t) \end{aligned} \quad (3.12)$$

$$\partial_t n(\omega, x, t) = (\mu/\hbar)\mathcal{E}(x, t)\mathcal{P}(\omega, x, t) \quad (3.13)$$

We shall seek solutions of these equations assuming that:

- $\phi(x, -\infty) = 0$  (initial condition),
- the frequency distribution has a maximum at  $\omega_c$  and it is symmetric around that maximum  $g(\omega - \omega_c) = g(\omega_c - \omega)$ ,

- $\mathcal{Q}(\omega, x, t)$  is an odd function of  $\omega - \omega_c$ :  $\mathcal{Q}(\omega - \omega_c, x, t) = -\mathcal{Q}(\omega_c - \omega, x, t)$ . This property was verified in Chapter 2: since  $P = (\chi' + i\chi'') E \sim \sigma$ , it follows that  $\mathcal{Q}(\omega - \omega_c, x, t)$  has the symmetry properties of  $\chi'$ . In the linear theory, its expression (2.11) shows indeed that it is an anti-symmetric function of the frequency detuning. In the nonlinear theory,  $\chi'$  is also an antisymmetric function of the frequency as shown in Eqs. (2.25) and (2.26). Thus, what is assumed here is that this is a generic property of the susceptibility and not a mere coincidence for the model studied in Chapter 2.

Let us extend the lower bound of integration in the right hand side of Eq. (3.10) to  $-\infty$ . Since  $\omega_c$  is a huge number for the optical domain ( $\omega_c \sim 10^{14} - 10^{15}$  Hz), this addition is negligible. Making this assumption implies  $(v\partial_x + \partial_t)\phi = 0$  so that  $\phi = f(x - vt)$ . Assuming that the phase of the field vanishes initially determines that  $f(x - vt) = 0$  and therefore  $\mathcal{E}$  is real. Hence, we are left with the equations

$$(v\partial_x + \partial_t)\mathcal{E}(x, t) = \frac{N\mu\omega_c}{2\varepsilon_0'} \int_0^\infty \mathcal{P}(\omega, x, t)g(\omega)d\omega \quad (3.14)$$

$$\partial_t\mathcal{Q}(\omega, x, t) = (\omega_c - \omega)\mathcal{P}(\omega, x, t) \quad (3.15)$$

$$\partial_t\mathcal{P}(\omega, x, t) = -(\omega_c - \omega)\mathcal{Q}(\omega, x, t) - (\mu/\hbar)n(\omega, x, t)\mathcal{E}(x, t) \quad (3.16)$$

$$\partial_t n(\omega, x, t) = (\mu/\hbar)\mathcal{E}(x, t)\mathcal{P}(\omega, x, t) \quad (3.17)$$

The formal solution of the polarization equations (3.15)-(3.16) is

$$\begin{Bmatrix} \mathcal{P}(\omega, x, t) \\ \mathcal{Q}(\omega, x, t) \end{Bmatrix} = -(\mu/\hbar) \int_{-\infty}^t dt' n(\omega, x, t') \mathcal{E}(x, t') \begin{Bmatrix} \cos \\ \sin \end{Bmatrix} [(\omega - \omega_c)(t' - t)] \quad (3.18)$$

At this point, we must recognize that it is not possible to pursue significantly further this analysis. A useful strategy to follow in this case is to reduced the ambition of this calculation by studying a function that carries less information. For this purpose, let us define a field area function  $\theta$  through

$$\theta(x, t) = (\mu/\hbar) \int_{-\infty}^t \mathcal{E}(x, t') dt' \quad (3.19)$$

or equivalently  $\partial_t\theta(x, t) = (\mu/\hbar)\mathcal{E}(x, t)$  and a parameter

$$a = N |\mu|^2 \omega_c / (2\hbar\varepsilon_0'v) \quad (3.20)$$

The function  $\theta$  is the area under the pulse up to time  $t$ . It is a kind of partial average. This function plays a dominant role in this chapter because it is that function which verifies a simple propagation equation.

We integrate the field equation (3.14) with respect to  $t$  and multiply it by  $\mu/\hbar$  to get

$$(v\partial_x + \partial_t)\theta(x, t) = -av(\mu/\hbar) \int_0^\infty g(\omega)\psi(\omega, x, t)d\omega \quad (3.21)$$

$$\psi(\omega, x, t) = \int_{-\infty}^t dt' \int_{-\infty}^{t'} dt'' n(\omega, x, t'')\mathcal{E}(x, t'') \cos [(\omega - \omega_c)(t'' - t')] \quad (3.22)$$

This last equation can be transformed as follows

$$\begin{aligned} \psi(t) &= \int_{-\infty}^t dt' \int_{-\infty}^{t'} dt'' f(t'') \cos [(\omega - \omega_c)(t'' - t')] \\ &= \frac{1}{\omega_c - \omega} \int_{-\infty}^t dt' \int_{-\infty}^{t'} dt'' f(t'') \partial_{t'} \sin [(\omega - \omega_c)(t'' - t')] \\ &= \frac{1}{\omega_c - \omega} \int_{-\infty}^t dt' \partial_{t'} \int_{-\infty}^{t'} dt'' f(t'') \sin [(\omega - \omega_c)(t'' - t')] \\ &= \int_{-\infty}^t f(t') \frac{\sin [(\omega - \omega_c)(t - t')]}{\omega - \omega_c} dt' \end{aligned} \quad (3.23)$$

To progress one step further, we consider the long time limit  $t \rightarrow +\infty$  and use the property

$$\lim_{t \rightarrow +\infty} \frac{\sin(\alpha t)}{\alpha} = \pi\delta(\alpha) \quad (3.24)$$

to study the equation that determines the evolution of the total area under the pulse  $\theta(x) = \theta(x, +\infty)$

$$\begin{aligned} d\theta(x)/dx &= -a(\mu/\hbar) \int_0^\infty d\omega g(\omega) \int_{-\infty}^{+\infty} n(\omega, x, t)\mathcal{E}(x, t)\pi\delta(\omega - \omega_c)dt \\ &= -\pi a(\mu/\hbar)g(\omega_c) \int_{-\infty}^{+\infty} n(\omega_c, x, t)\mathcal{E}(x, t)dt \end{aligned} \quad (3.25)$$

Comparing equations (3.21) and (3.25), we conclude that *all atoms* of the medium contribute to the time evolution of the *partial* field envelope  $\theta(x, t)$  but that only the *resonant atoms*, for which  $\omega_a = \omega_c$ , contribute to the *total* field envelope. This remark has far reaching consequences. The atomic dynamics on resonance is governed by the pair of equations

$$\frac{\partial \mathcal{P}}{\partial t} = -(\mu/\hbar)\mathcal{E}n \quad (3.26)$$

$$\frac{\partial n}{\partial t} = (\mu/\hbar)\mathcal{E}\mathcal{P} \quad (3.27)$$

which is a conservative system since  $\partial_t(\mathcal{P}^2 + n^2) = 0$ . Hence,  $\mathcal{P}^2(x, t) + n^2(x, t) = n^2(x)$  where  $n(x)$  is the population difference before the pulse interacts with the medium. If the lower energy level of the medium is more populated than the upper energy level,  $n(x) > 0$  and the medium is an absorber. If the upper energy level of the medium is more populated than the lower energy level,  $n(x) < 0$  and the medium is an amplifier. The solution of (3.26)-(3.27) is

$$\mathcal{P}(x, t) = -n(x) \sin \theta(x, t) \quad (3.28)$$

$$n(x, t) = n(x) \cos \theta(x, t) \quad (3.29)$$

and therefore the equation for the total pulse area is

$$\begin{aligned} d\theta(x)/dx &= \pi a g(\omega_c) \int_{-\infty}^{+\infty} dt \partial_t \mathcal{P}(x, t) \\ &= -\pi a g(\omega_c) n(x) \sin \theta(x) \end{aligned} \quad (3.30)$$

Equation (3.30) is known as the McCall & Hahn theorem<sup>1</sup>. Its derivation and experimental verification was the subject of Sam McCall's Ph.D. thesis under the supervision of Hahn.

Let us analyze some properties of this equation which we rewrite in the form

$$d\theta(x)/dx = \alpha \sin \theta(x) \quad (3.31)$$

$$\alpha = -\frac{N\pi\mu^2\omega_c n}{2\hbar\varepsilon'_0 v} g(\omega_c) \quad (3.32)$$

In the low intensity limit,  $\theta \ll 1$ , we can approximate the sine function by its argument. This leads to the linear equation  $d\theta(x)/dx = \alpha\theta(x)$  which is a variation on Beer-Lambert's law, as should be. This limit also tells us that  $1/\alpha$  is the absorption length in the small signal limit.

The new features brought in by the nonlinear treatment of the light-matter interaction is the occurrence of non trivial stationary solutions. Indeed, it is clear that  $\theta = n\pi$  is a family of solutions of the McCall & Hahn equation (3.31). The existence of non trivial stationary solutions is not possible in the linear theory: in the low intensity regime, this family of solution is reduced to  $\theta = 0$  which is of little interest. However, at higher intensity, non trivial steady state solutions exist due to the nonlinear response of the medium to the field. This means that under suitable conditions, a medium

---

<sup>1</sup>S.L. McCall and E.L. Hahn, Phys. Rev. Lett. **18** (1967) 908; Phys. Rev. **183** (1969) 457; Phys. Rev. **A2** (1970) 861.

which is absorbing at low intensity<sup>2</sup> becomes transparent and the pulse propagates without attenuation. This phenomenon is called *self-induced transparency* (SIT) because it is the pulse itself which bleaches the medium. We shall elucidate in Section 3.3 the dynamical aspect of this unexpected property.

The existence of a solution  $\theta = n\pi$  does not guarantee its stability. Let us therefore consider infinitesimal deviations from the stationary solution:  $\theta_n = n\pi + \varepsilon\Theta_n(x) + \mathcal{O}(\varepsilon^2)$ . In the remainder of this chapter, we shall assume that  $n$ , and therefore  $\alpha$ , is constant in space. Inserting this solution into (3.31) and linearizing the resulting equation with respect to  $\varepsilon$  leads to  $d\Theta_n/dx = \Theta_n\alpha \cos(n\pi)$ . It follows that the solution  $\Theta_n$  is stable iff  $\alpha \cos(n\pi) < 0$ . We can therefore classify the stable solutions in two classes:

- for an attenuator ( $\alpha < 0$ ) the stable solutions are  $n = 0, 2, 4, \dots$
- for an amplifier ( $\alpha > 0$ ) the stable solutions are  $n = 1, 3, 5, \dots$

The general solution of equation (3.31) is

$$\tan \frac{\theta(x)}{2} = e^{\alpha x} \tan \frac{\theta(0)}{2} \quad (3.33)$$

Let us analyze this solution in more details. Let us consider an initial condition  $\theta(0)$ . There exists a non-negative integer  $n$  such that  $n\pi \leq \theta(0) \leq (n+1)\pi$ .

- For an attenuator, the pulse area  $\theta(x)$  decreases until it reaches the lower bound  $n\pi$  if  $n$  is even; it increases until it reaches the upper bound  $(n+1)\pi$  if  $n$  is odd. Practically, the bounds are reached after a few absorption lengths  $1/\alpha$ .
- For an amplifier, the pulse area  $\theta(x)$  decreases until it reaches the lower bound  $n\pi$  if  $n$  is odd; it increases until it reaches the upper bound  $(n+1)\pi$  if  $n$  is even.

---

<sup>2</sup>This absorption can be very strong, leading to a completely opaque medium at low intensity.

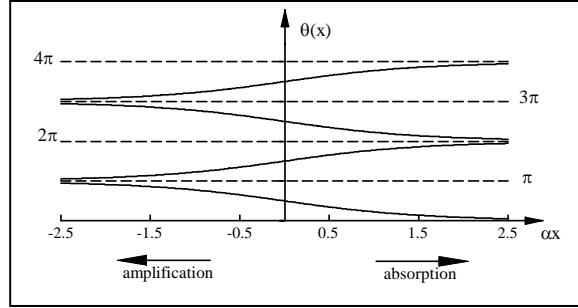


Figure 3.1: Steady state pulse area as a function of the propagation distance.

This discussion of the solutions is summarized in Fig. 3.1. When discussing the pulse propagation and reshaping, it should be borne in mind that the pulse envelope  $\theta(x, t)$  is not related in any simple way to the field energy and even less to energy conservation. In fact, multiplying equation (3.14) by  $\mathcal{E}$  and using equation (3.17) yields the law of energy variation

$$\partial_t \left( \mathcal{E}^2(x, t) - \frac{\hbar\omega_c}{\epsilon'_0} N \int_0^\infty g(\omega) n(\omega, x, t) d\omega \right) + v \partial_x \mathcal{E}^2(x, t) = 0 \quad (3.34)$$

Thus there is no inconsistency in the fact that a medium with all the atoms in the lower state cannot transfer any energy to the field and the fact that if the pulse is characterized by  $\theta(x = 0) = \pi + \epsilon$  with  $0 < \epsilon \ll 1$  it will reach  $\theta(x) = 2\pi$  for long distances.

### 3.3 Sine-Gordon equation

We have seen that in an inhomogeneous broadened medium (i.e., a medium in which there is a distribution of atomic frequencies  $g(\omega)$  which is not a delta function) the phenomenon of SIT may take place. In the previous section, we have provided a first analysis of this phenomenon by considering the spatial variation of the total field envelope. Although all atoms contribute to the field envelope  $\theta(x, t)$  given by equations (3.21)-(3.22), we have seen from equation (3.25) that only the resonant atoms ( $\delta = \omega - \omega_c = 0$ ) contribute to the total envelope  $\theta(x)$ . Therefore, we shall study in this section the dynamics of the light field interacting only with those atoms which are on resonance with the electric field optical carrier frequency  $\omega_c$ . This will describe the dynamics that leads, asymptotically, to the properties of  $\theta(x)$ .

Starting from equations (3.1)-(3.3) with  $\delta = 0$ , we may then assume that the polarization is purely imaginary and that  $\mu$  is real. Defining  $2i\sigma = s$ , we

write equations (3.1)-(3.3) in the form

$$(v\partial_x + \partial_t) E = (N\mu\omega_c/2\varepsilon'_0)s \quad (3.35)$$

$$\frac{\partial s}{\partial t} = -(\mu/\hbar) En \quad (3.36)$$

$$\frac{\partial n}{\partial t} = (\mu/\hbar) Es \quad (3.37)$$

As we have already noticed, there is an invariant  $s^2(x, t) + n^2(x, t) = C(x)$ . Let  $n(x)$  be the population difference in the absence of electric field (i.e., for  $t = -\infty$ ). The solution of the two material equations is given by (3.28) and (3.29). Using the property  $\partial\theta/\partial t = (\mu/\hbar) E$ , it is now easy to derive a closed equation for  $\theta$  :

$$\left(v\frac{\partial}{\partial x} + \frac{\partial}{\partial t}\right) \frac{\partial\theta}{\partial t} = -\frac{N\mu^2\omega_c n(x)}{2\varepsilon'_0\hbar} \sin\theta \quad (3.38)$$

To obtain one of the canonical forms of this equation, we introduce the change of variables

$$\xi = \Omega x/v, \quad \tau = \Omega(t - x/v), \quad \Omega^2 = N\mu^2\omega_c |n|/2\hbar\varepsilon'_0 \quad (3.39)$$

in terms of which equation (3.38) becomes

$$\frac{\partial^2\theta}{\partial\tau\partial\xi} = \pm \sin\theta \quad (3.40)$$

The minus sign corresponds to an attenuator ( $n > 0$ ), the plus sign corresponds to an amplifier ( $n < 0$ ). We have made the assumption that the medium is homogeneous ( $\partial n/\partial x = 0$ ) to simplify somewhat the analytic discussion which follows. Equation (3.40) is known as the sine-Gordon equation. It is a highly nonlinear equation describing the propagation of a short pulse in a nonlinear medium.

The sine-Gordon equation is not a newcomer in mathematics or physics. It was found at the end of the XIXth century by mathematicians working on differential geometry of surfaces with constant negative curvature such as the sphere. A good account of this aspect of the sine-Gordon is found in the classic book of Eisenhart<sup>3</sup>. It has also been derived in the context of dislocation theory, model field theories, and superconductivity<sup>4</sup>.

<sup>3</sup>L.P. Eisenhart, *A treatise on the differential geometry of curves and surfaces* (Dover, New York, 1960).

<sup>4</sup>See the review by G.L. Lamb, *Rev. Mod. Phys.* **43** (1971) 99 for further references on these topics.

A fascinating property of the sine-Gordon equation is that analytical solutions can be derived in a systematic way, though not all solutions are accessible analytically. For the simplest class of non trivial solutions, the  $2\pi$  solitons, only the Bäcklund theorem is needed to generate analytic solutions. For the higher order solutions, the Bianchi theorem is also needed. Its proof and applications are found in the complements to this chapter.

**Theorem 1** *The Bäcklund transformation.*

Let  $\theta_0$  and  $\theta_1$  be two functions which are related by the so-called Bäcklund transformations

$$\frac{\partial}{\partial \tau} \frac{\theta_1 - \theta_0}{2} = a \sin \frac{\theta_1 + \theta_0}{2} \quad (3.41)$$

$$\frac{\partial}{\partial \xi} \frac{\theta_1 + \theta_0}{2} = \pm \frac{1}{a} \sin \frac{\theta_1 - \theta_0}{2} \quad (3.42)$$

The Bäcklund theorem states that the functions  $\theta_0$  and  $\theta_1$  are solutions of the sine-Gordon equation.

**Proof.** The proof is elementary: deriving the first equation with respect to  $\xi$  and the second with respect to  $\tau$  leads to a pair of equations whose difference is the sine-Gordon equation for  $\theta_0$  and whose sum is the sine-Gordon equation for  $\theta_1$ . ■

The interest of this theorem is that it reduces the discussion of a second order PDE to a pair of first order PDE's: if a solution  $\theta_0$  is known, finding a second solution requires only two quadratures. The relevance of this theorem is that  $\theta_0 = 0$  generates via the Bäcklund transformations an infinite sequence of solutions.

### 3.4 $2\pi$ solitons

An obvious solution of the sine-Gordon is  $\theta_0 = 0$ . Using the Bäcklund transformation with the parameter  $a_1$  real, we find that, for an attenuator, a solution  $\theta_1$  is given by

$$\partial \theta_1 / \partial \tau = 2a \sin(\theta_1/2), \quad \partial \theta_1 / \partial \xi = -(2/a) \sin(\theta_1/2) \quad (3.43)$$

From these two equations it follows that  $\partial \theta_1 / \partial(a\tau) + \partial \theta_1 / \partial(\xi/a) = 0$  and therefore there exists a solution  $\theta_1$  which depends on a single variable  $\theta_1 = f(a\tau - \xi/a) \equiv f(\rho)$ . This solution is  $|\tan(\theta_1/4)| = \exp(\rho)$ . Hence, we have

$$(\mu/\hbar)E_1 = \partial_t \theta_1 = (2/w) \operatorname{sech}[(t - x/v_1)/w] \quad (3.44)$$

$$v_1 = v/(1 + 1/a^2), \quad w = 1/a\Omega \quad (3.45)$$

This solution describes a pulse which is a localized solution peaked at  $t = x/v_1$ , moving at the speed  $v_1$  which is always smaller than  $v$ , with a maximum of  $2/w$  and a full width at half maximum of  $2w \ln(2 + \sqrt{3}) \simeq 2.6339w \approx 8w/3$ . Indeed, the function  $f(z) = (2/\tau)\text{sech}(z/\tau)$  is maximum at  $z = 0$  where  $f(0) = 2/\tau$ . Hence at half maximum we have  $f(z^*) = 1/\tau = (2/\tau)\text{sech}(z^*/\tau)$  or  $1 = 4[\exp(z^*/\tau) + \exp(-z^*/\tau)]^{-1}$  and therefore  $y^2 - 4y + 1 = 0$  with  $y = \exp(z^*/\tau)$ . Thus, the one-parameter family of solutions  $f(z)$  has the property that the product of the maximum by the full width at half maximum is the constant  $4 \ln(2 + \sqrt{3})$ . In addition, the propagation speed is proportional to the width of the pulse: given two pulses verifying (3.44)-(3.45), the pulse with larger maximum will have the smaller width and the smaller velocity.

This solution is known as a  $2\pi$  soliton because the total area under the field envelope is  $2\pi$  :

$$\theta_1(x) = (\mu/\hbar) \int_{-\infty}^{+\infty} E_1(x, t) dt = 2\pi \quad (3.46)$$

In other terms, the soliton (3.44) we have just constructed corresponds to the  $2\pi$  solution of the McCall and Hahn (3.31).

No analytic expression is available for the stable solutions in an amplifier because the basic  $\pi$  solution verifies the third Painlevé transcendental equation, which is known only as an infinite series.

The physics of the  $2\pi$  soliton is easily understood in terms of the result  $n(x, t) = n(x) \cos \theta(x, t)$ :

1. The leading edge of the pulse interacts with the medium in such a way that the first quarter of the pulse, for which  $\theta(x, t_{\pi/2}) = \pi/2$ , leaves the system in the state  $n(x, t_{\pi/2}) = 0$ : there are exactly as many atoms in the upper and in the lower state and therefore the medium is transparent to the radiation.
2. The second quarter of the pulse inverts the medium since at  $t_\pi$  defined by  $\theta(x, t_\pi) = \pi$  we have  $n(x, t_\pi) = -n(x)$ .
3. The third quarter of the pulse restores transparency at  $t_{3\pi/2}$  since  $\theta(x, t_{3\pi/2}) = 3\pi/2$  implies  $n(x, t_{3\pi/2}) = 0$ .
4. Finally, the last quarter of the pulse brings the system back to its initial state  $n(x, t_{2\pi}) = n(x)$  with  $t_{2\pi}$  defined by  $\theta(x, t_{2\pi}) = 2\pi$ .

The interesting property is that this analysis holds irrespective of the initial population difference  $n(x)$ , provided  $n(x) \neq 0$ .

### 3.5 References

1. G.L. Lamb, *Elements of soliton theory* (Wiley, New York, 1960).
2. G. Eilenberger, *Solitons* (Springer, Heidelberg, 1981).
3. R.K. Dodd, J.C. Eilback, J.D. Gibbon, and M.C. Morris, *Solitons and nonlinear wave equations* (Academic Press, New York, 1982).
4. W. Eckhaus and A. van Harten, *The inverse scattering transformation and the theory of solitons* (North Holland, Amsterdam, 1983).
5. S. Novikov, S. Marakov, and L. Pitaevski, *Theory of solitons* (Consultant Bureau, New York, 1984).
6. M. Lakshmanan, *Solitons* (Springer, Heidelberg, 1988).
7. P.G. Drazin and R.S. Johnson, *Solitons: an introduction* (Cambridge University Press, 1989).
8. A. Hasegawa, *Optical solitons in fibers* (Springer, Heidelberg, 1989).
9. M. Remoissenet, *Waves called solitons* (Springer, Heidelberg, 1994).



## **Part II**

# **Cavity nonlinear optics**



# Chapter 4

## Laser theory

### 4.1 Introduction

In the previous chapters, we have described examples of light-matter interaction and nonlinear propagation. A completely different problem arises if the nonlinear medium is placed inside a resonant cavity. This was first realized in the microwave domain (typically cm wavelengths), developed for radar applications, where cavities having the dimensions of the wavelength to be amplified were easily constructed. The idea is to use a cavity in which the field can resonate. That is, if the cavity is a rectangular volume of sides  $L_x, L_y, L_z$  it supports modes  $\phi(x, y, z) = \phi(x)\phi(y)\phi(z)$  where  $\phi(r) = \sqrt{2} \sin(k_r r)$  with wave numbers  $k_r = \pm n_r \pi / L_r$ ,  $r$  being any of the three coordinates and  $n_r$  an integer. In maser cavities, this number is typically 1 or 2. Only modes of the field which are cavity eigenmodes would be amplified, the other modes being strongly damped. According to the results of Chapter 2, amplification requires an inversion of population of the two energy levels.

The extension of this technique to the optical domain was hampered by several problems, among which:

- in the optical domain such a cavity would have linear dimensions of the order of  $10^{-6}$  m and a precision of the order of 0.1% would mean a precision of  $10^{-9}$  m = 10 angstroms or about 10 atoms;
- in such a cavity, the amount of matter that can be inserted would make gain hardly possible;
- The spontaneous emission coefficient given by Einstein's  $A$  coefficient  $A = 2\omega_a^3 |\mu|^2 / (3h\epsilon_0' c^3)$  is generally larger in the optical domain than in the microwave domain because of the  $\omega^3$  factor. Is it possible to maintain a population inversion long enough to generate gain?

The solution was proposed simultaneously in Russia by Basov and Prokhorov and in the US by Schawlow and Townes. The trick is to use a Fabry-Perot interferometer as resonant cavity and exploit spontaneous emission to trigger the field amplification process as follows. The Fabry-Perot resonator is a volume limited longitudinally by two mirrors characterized by their reflectivity (which is a sensitive function of the optical frequency). In the case of lasers, it is customary not to have lateral reflecting boundaries. A nonlinear medium is selected because its spectrum has a pair of energy levels, between which a transition is allowed, and whose frequency difference matches an eigenfrequency of the Fabry-Perot. In addition, the upper of the two levels has to be metastable, i.e., as long lived as possible while the lowest of the two levels should be highly unstable, i.e., as short lived as possible. This is not the prevailing situation in spectroscopy but pairs of level matching these conditions can be found. The following sequence of processes takes place.

- An external source of energy, usually in the form of incoherent light or electric discharge, is used to create a population inversion between the two energy levels which have been selected. Alternative choices of incoherent sources being used are chemical reactions and inelastic collisions between gases.
- This leads to a field created by spontaneous emission associated to transitions from the upper to the lower levels. Its characteristics is to have a broad frequency distribution, typically a Lorentzian distribution, peaked around the atomic frequency and having a FWHM given by the inverse of the upper level atomic life time. In addition, the wave vectors are evenly distributed in all space directions.
- The cavity, which on purpose does not have reflecting lateral boundaries, selects in a purely geometric way wave vectors which are parallel to the resonator axis. Field components with other wave vectors quickly escape the cavity via the lateral boundaries. In addition, the cavity also selects photons whose frequency matches a cavity frequency.
- Stimulated emission now begins, in which a photon, whose frequency and wave vector have been selected by the cavity, interacts with the amplifying medium to produce a second photon *with the same phase and, in particular, the same frequency and wave vector*. In order to achieve amplification, the stimulated emission must compensate the inverse process, i.e., absorption. This requires that the stimulated gain  $\alpha$  defined by Eq. (2.9) be positive, which imposes that a population

inversion be created between the two levels involved in the atomic transition.

As a result of this sequence of processes, it appears that the spontaneous emission is essential to trigger the lasing process but it yields only a weak field. On the contrary, the stimulated field will have an intensity that grows proportionally to itself, i.e., an exponential growth which builds up from the weak spontaneous field. Hence the acronym laser which stands for **L**ight **A**mplification by **S**timulated **E**mission of **R**adiation. Finally, the balance between loss, gain, and saturation determines a finite intensity regime.

It is quite clear that the model for light-matter interaction which we have built in the first chapter fits nicely into the picture just described: it accounts for all the elements which have been described in the lasing process except for the spontaneous field because the field studied in Chapter 1 is not quantized. Since the spontaneous field is needed only in the short time limit to trigger stimulated amplification, we may use a model that neglects the quantum vacuum which produces the spontaneous emission and replace it by a *post-initial condition* which introduces that field into the picture. In doing so, we neglect the spontaneous contribution to the linewidth, which in any case is sharply reduced by the filtering action of the interferometer. As a result, we model the laser by means of the equations

$$(v\partial_x + \partial_t) E = -\kappa E + (iN\mu\omega_c/\varepsilon'_0)\sigma \quad (4.1)$$

$$\frac{\partial\sigma}{\partial t} = -(\gamma_\perp + i\delta)\sigma - i\frac{\mu}{2\hbar}En \quad (4.2)$$

$$\frac{\partial n}{\partial t} = \gamma_\parallel(n^0 - n) - i\frac{\mu}{\hbar}(E^*\sigma - E\sigma^*) \quad (4.3)$$

where  $n = n_2 - n_1$  is now the atomic population inversion and  $n^0 > 0$ . The frequency  $\omega_c$  is a cavity eigenfrequency. Given the definition (1.3) of the complex field and polarization amplitudes as coefficients of running waves, this model applies to a ring laser. It is a configuration in which the light follows a closed path, such as a triangular or a  $Z$  shape. There is an output mirror with reflectivity less than unity. All other mirrors are assumed to be fully reflecting. The damping rate  $\kappa$  can easily be expressed in terms of more accessible parameters of the laser. Let the material medium be characterized by an intensity absorption coefficient  $\alpha_{BL}$  (Beer-Lambert's law) and a refractive index  $n_r$ , while the cavity, of length  $L$ , is limited by a mirror of intensity reflectivity  $R < 1$ , the other mirrors being perfectly reflecting ( $R = 1$ ). In the absence of a nonlinear medium, Eq. (4.1) yields for the intensity loss per cavity round-trip

$$I(x, t + \tau)/I(x, t) = e^{-2\kappa L/v} = e^{-2\kappa n_r L/c} = Re^{-\alpha_{BL}L} \quad (4.4)$$

from which we obtain

$$\kappa = \frac{c}{2n_r} \left[ \alpha_{BL} + \frac{1}{L} \ln(1/R) \right] \quad (4.5)$$

This expression of the loss coefficient contains two parts:

- $c\alpha_{BL}/(2n_r)$  which accounts for the linear losses of any medium placed inside the cavity, such as the medium which serves as a support for the doping (i.e., active) atoms in a solid state laser, or the buffer gas in a gas laser, for instance.
- $[c/(2Ln_r)] \ln(1/R)$  which accounts for the losses due to the mirrors.

In the limit  $R \rightarrow 1$ , we obtain the expression

$$\kappa \simeq \frac{c}{2n_r} \left( \alpha_{BL} + \frac{1-R}{L} \right) \quad (4.6)$$

In some cases, mirrors may even be unnecessary. If the lasing medium is a crystal or a dopant embedded in a crystal, the difference between the refractive indices of the crystal and of the surrounding medium (usually air) provides a reflection coefficient which is given in the linear approximation by the Fresnel formula

$$R = \left( \frac{n_1 - n_2}{n_1 + n_2} \right)^2 \quad (4.7)$$

This expression is valid under normal incidence. For instance, InSb is a semiconductor at room temperature with a refractive index  $n = 4$  in the visible and near infrared. This leads to  $R = 0.36$  if we take  $n_1 = 1$  and  $n_2 = 4$ . Thus a crystal cut along crystallographic facets is a natural, poor but cheap, cavity. The crystal of YAG used in the Nd:YAG laser has a refractive index  $n_2 = 1.6$ . This yields  $R = 0.0533$ , which is too small. Hence, this laser will need external mirrors.

A cavity can easily support many modes. For instance the Nd ion in a YAG (yttrium aluminum garnet) matrix, which constitutes a standard solid state laser, has a set of allowed transitions between the  ${}^4F_{3/2}$  doublet and the  ${}^4I_{11/2}$  manifold. Widely used transitions around 1060nm are shown in Fig. 4.1. Cavity modes have frequencies given by  $\omega_{cav} = p\pi c/n_r L$  where  $p$  is an integer. Thus, two consecutive cavity modes are separated by  $\Delta\omega = \pi c/(n_r L)$ . Using the definition  $\lambda\omega = 2\pi v = 2\pi c/n_r$ , we find  $\Delta\omega = \omega_1 - \omega_2 = 2\pi c/(n_r \lambda_1) - 2\pi c/(n_r \lambda_2) = 2\pi c \Delta\lambda / (n_r \lambda_1 \lambda_2)$  where  $n_r$  is the Nd:YAG refractive index. This gives  $\Delta\lambda = \lambda_1 \lambda_2 / (2L) \simeq \lambda_1^2 / (2L)$ . Therefore  $\Delta\lambda \simeq$

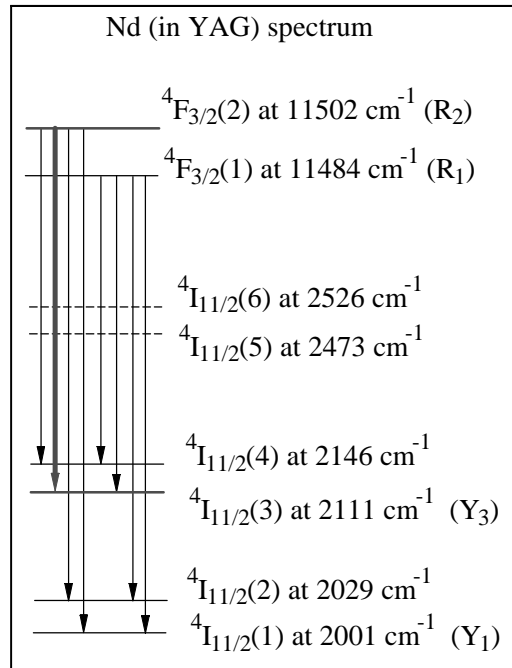


Figure 4.1: Allowed transitions visible on the fluorescence spectrum of the Nd:YAG between 1050 and 1080nm at  $300^\circ\text{C}$ . The  $R_2 - Y_3$  transition has the lowest lasing threshold at  $300^\circ\text{C}$ .

0.0532nm and  $\Delta\omega \simeq 9.4 \times 10^9 \text{ Hz}$  for the transition at 1064.14nm with a refractive index of 1.6 and a cavity of 1 cm. Since  $\gamma_\perp \simeq 10^{12} \text{ Hz}$  in this medium, up to 106 cavity modes could oscillate on each of these atomic transitions unless special care is taken to have the laser operating single mode. The usual solid state lasers have typical lengths of 1 to 10 cm and the cavity mode spacing will therefore be 1 to 10 times smaller so that 1 to 10 times more modes may oscillate simultaneously.

The selection of the lasing frequency strongly depends on the properties of the cavity mirrors and on the temperature. For instance, the usual setup for Nd:YAG lasers promotes lasing at 1064.14nm ( $R_2 \rightarrow Y_3$  transition), the most commonly used of the Nd lines at room temperature. At low temperature, it is the  $R_1 \rightarrow Y_1$  transition at 1061.52nm which has the lowest threshold. However, a different coating can easily be made which promotes the transition between the same  ${}^4F_{3/2}(2)$  upper level and a level of the  ${}^4I_{13/2}(2)$  manifold, with an atomic frequency at 1320.0nm ( $R_2 \rightarrow X_2$  transition). The following table gives the dominant transitions observed at room temperature in the fluorescence spectrum. The  $Y_n$  label the energy levels of the  ${}^4I_{11/2}$  manifold

while the  $X_n$  label the energy levels of the  ${}^4I_{13/2}$  manifold (from *Solid-State Laser Engineering* by Walter Koechner, Springer Verlag, 1996).

wavelength (nm)	transition	relative amplitude
1064.14	$R_2 \rightarrow Y_3$	100
1061.52	$R_1 \rightarrow Y_1$	92
1073.8	$R_1 \rightarrow Y_3$	65
1064.6	$R_1 \rightarrow Y_2$	$\sim 50$
1112.1	$R_2 \rightarrow Y_6$	49
1052.05	$R_2 \rightarrow Y_1$	46
1115.9	$R_1 \rightarrow Y_5$	46
1122.6	$R_1 \rightarrow Y_6$	40
1078.0	$R_1 \rightarrow Y_4$	34
1318.8	$R_2 \rightarrow X_1$	34
1338.2	$R_2 \rightarrow X_3$	24
1335.0	$R_1 \rightarrow X_2$	15
1356.4	$R_1 \rightarrow X_4$	14
1333.8	$R_1 \rightarrow X_1$	13
1320.0	$R_2 \rightarrow X_2$	9
1105.4	$R_2 \rightarrow Y_5$	9
1341.0	$R_2 \rightarrow X_4$	9

## 4.2 Single mode ring laser

In this section, we concentrate on the properties of a single mode laser in a ring geometry, that is, a resonator of length  $L$  where the mirrors (three of them at least) are placed such that light follows a closed path. This amounts to assume that the cavity eigenmodes are  $\phi(x) = L^{-1/2} \exp(ikx)$  where  $k = \pm 2n\pi/L$  and  $n$  is an integer. Equations (4.1)-(4.3) were derived for such a cavity. In the single mode regime, we may seek solutions with  $\partial E/\partial x = 0$ <sup>1</sup>. Another simplification comes from the assumption that one cavity frequency  $\omega_c$  matches the atomic frequency  $\omega_a$ . In that case,  $\delta = 0$  and we may seek solutions such that  $E$  is real and  $\sigma$  purely imaginary. Thus

$$\frac{dE}{dt} = -\kappa E + (iN\mu\omega_c/\varepsilon'_0)\sigma \quad (4.8)$$

$$\frac{d\sigma}{dt} = -\gamma_{\perp}\bar{\sigma} - i\frac{\mu}{2\hbar}En \quad (4.9)$$

---

<sup>1</sup>These are not the only single cavity mode solutions. Another class of solutions consists of a pulse train along the longitudinal cavity optical axis. See H. Risken and K. Nummedal, J. Appl. Phys. **39** (1968) 4662 and R. Graham and H. Haken, Z. Physik **213** (1968) 420.

$$\frac{dn}{dt} = \gamma_{\parallel}(n^0 - n) - i\frac{2\mu}{\hbar}E\sigma \quad (4.10)$$

Finally, the change of variables

$$E = \sqrt{\frac{\hbar^2\gamma_{\perp}\gamma_{\parallel}}{\mu^2}}\mathcal{E}, \quad \sigma = -i\frac{n^0}{2}\sqrt{\frac{\gamma_{\parallel}}{\gamma_{\perp}}}\mathcal{P}, \quad n = n^0\mathcal{D} \quad (4.11)$$

leads to the set of reduced equations

$$\frac{d\mathcal{E}}{d\bar{t}} = -\bar{\kappa}(\mathcal{E} - A\mathcal{P}) \quad (4.12)$$

$$\frac{d\mathcal{P}}{d\bar{t}} = -\mathcal{P} + \mathcal{E}\mathcal{D} \quad (4.13)$$

$$\frac{d\mathcal{D}}{d\bar{t}} = \bar{\gamma}(1 - \mathcal{D} - \mathcal{E}\mathcal{P}) \quad (4.14)$$

where we have introduced the dimensionless gain coefficient

$$A = \frac{Nn^0\mu^2\omega_c}{2\hbar\epsilon'_0\kappa\gamma_{\perp}} > 0 \quad (4.15)$$

and the reduced time and decay rates

$$\bar{t} \equiv \gamma_{\perp}t, \quad \bar{\gamma} = \gamma_{\parallel}/\gamma_{\perp}, \quad \bar{\kappa} = \kappa/\gamma_{\perp} \quad (4.16)$$

The definition of  $A$  is such that  $A > 0$  if there is population inversion. The parameter  $A$  is related to the linear gain  $\alpha$  defined in Chapter 2, equation (2.9), by the relation  $A = v\alpha/\kappa$ .

### 4.3 Steady states

Let us analyze the steady state properties of the laser. Since  $\Omega$  is the lasing frequency, the steady state field is  $d\mathcal{E}_s/dt = 0$ , corresponding to a constant intensity. From this it follows that  $\mathcal{P}$  and  $\mathcal{D}$  are also independent of time. The steady state properties of the laser are given by the solutions of the algebraic equations

$$\mathcal{E}_s - A\mathcal{P}_s = 0 \quad (4.17)$$

$$\mathcal{P}_s - \mathcal{E}_s\mathcal{D}_s = 0 \quad (4.18)$$

$$\mathcal{D}_s = 1 - \mathcal{E}_s\mathcal{P}_s \quad (4.19)$$

Eliminating the two material variables  $\mathcal{P}_s$  and  $\mathcal{D}_s$  from (4.18) and (4.19) leads to

$$\mathcal{D}_s = \frac{1}{1 + \mathcal{E}_s^2}, \quad \mathcal{P}_s = \frac{1}{1 + \mathcal{E}_s^2} \mathcal{E}_s \quad (4.20)$$

and the equation for the electric field becomes

$$\mathcal{E}_s \left( 1 - \frac{A}{1 + \mathcal{E}_s^2} \right) = 0 \quad (4.21)$$

There are two possible solutions:

1. The trivial solution  $\mathcal{E}_s = \mathcal{P}_s = \mathcal{D}_s - 1 = 0$ ;
2. The non-trivial solution  $\mathcal{E}_s \neq 0$  for which

$$\mathcal{E}_s^2 = A - 1, \quad \mathcal{P}_s = \mathcal{E}_s/A, \quad \mathcal{D}_s = 1/A \quad (4.22)$$

The lasing threshold condition is thus  $A = v\alpha/\kappa = 1$ . It is again a condition expressing a balance between gain ( $v\alpha$ ) and losses ( $\kappa$ ) as derived in Section (2.1) of the first chapter.

## 4.4 Rate equations

In most lasing materials, the atomic polarization is by far the fastest decaying process. This means  $\gamma_\perp \gg \gamma_\parallel$  and  $\gamma_\perp \gg \kappa$ . Let us show that in this limit the laser equations can be reduced to a simpler set of evolution equations. We begin with equations (4.12)-(4.14) and introduce a small parameter  $\varepsilon = \bar{\kappa} \equiv \kappa/\gamma_\perp$ . We also specify the ratio  $\gamma_\parallel/\gamma_\perp = \mathcal{O}(\varepsilon) = \varepsilon a_1 + \varepsilon^2 a_2 + \dots \equiv \varepsilon a(\varepsilon)$  with  $a_1 \neq 0$ . Note that  $a = \gamma_\parallel/(\varepsilon\gamma_\perp) = \gamma_\parallel/\kappa$ . The laser equations become

$$\frac{d\mathcal{E}}{dt} = -\varepsilon(\mathcal{E} - A\mathcal{P}) \quad (4.23)$$

$$\frac{d\mathcal{P}}{dt} = -\mathcal{P} + \mathcal{E}\mathcal{D} \quad (4.24)$$

$$\frac{d\mathcal{D}}{dt} = a\varepsilon(-\mathcal{D} + 1 - \mathcal{E}\mathcal{P}) \quad (4.25)$$

In the limit  $\varepsilon = 0$ , we have  $d\mathcal{E}/d\bar{t} = d\mathcal{D}/d\bar{t} = 0$  and  $d\mathcal{P}/d\bar{t} = -\mathcal{P} + \mathcal{E}\mathcal{D}$  which expresses the fact that on the time scale  $\bar{t} = \gamma_\perp t$  only the atomic polarization evolves while the field and the population inversion do not vary. This is not the information we seek, but it suggests that we rather look for a solution of

the laser equations (4.23)-(4.25) depending on the time scale  $\varepsilon\bar{t} = \kappa t \equiv t_\kappa$ . We easily obtain

$$\frac{d\mathcal{E}}{dt_\kappa} = -(\mathcal{E} - A\mathcal{P}) \quad (4.26)$$

$$-\mathcal{P} + \mathcal{E}\mathcal{D} = \varepsilon \frac{d\mathcal{P}}{dt_k} \simeq 0 \quad (4.27)$$

$$\frac{d\mathcal{D}}{dt_\kappa} = a(-\mathcal{D} + 1 - \mathcal{E}\mathcal{P}) \quad (4.28)$$

These equations express the dynamics of the slow variables  $\mathcal{E}$  and  $\mathcal{D}$  on the time scale  $t_\kappa$  and the relation between the atomic polarization and the slow variables at the same time:  $\mathcal{P}(t_\kappa) = \mathcal{E}(t_\kappa)\mathcal{D}(t_\kappa)$ . This algebraic relation neglects the fast transients that occur on the time scale  $\bar{t} = t_\kappa/\varepsilon$ . This property is illustrated in Fig. 4.2 where a qualitative representation of the deviation from steady state is plotted versus time. It should be stressed

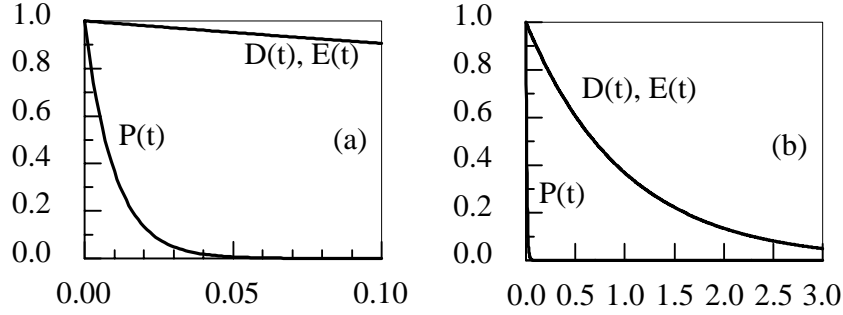


Figure 4.2: The functions  $\exp(-x)$  and  $\exp(-100x)$  are displayed using two different time scales to exemplify the difference between the time scales  $\bar{t}$  and  $t_\kappa$ .

that, by definition, the function  $\mathcal{D}(t_\kappa) \equiv \mathcal{P}(t_\kappa)/\mathcal{E}(t_\kappa)$  is also the nonlinear susceptibility of the medium. The dynamical equations are

$$\frac{d\mathcal{E}}{dt_\kappa} = \mathcal{E}(-1 + A\mathcal{D}) \quad (4.29)$$

$$\frac{d\mathcal{D}}{dt_\kappa} = a(-\mathcal{D} + 1 - \mathcal{D}\mathcal{E}^2) \quad (4.30)$$

From the field equation we easily derive an equation for the intensity  $\mathcal{E}^2$

$$\frac{d\mathcal{E}^2}{dt_\kappa} = 2\mathcal{E}^2(-1 + A\mathcal{D}) \quad (4.31)$$

Finally, defining the intensity  $I = \mathcal{E}^2$ , the pumping rate  $w = A$ , the ratio  $\tilde{\kappa} = \kappa/\gamma_{\parallel}$ , the scaled population inversion  $D = w\mathcal{D}$  and using the time  $\tilde{t} = at_{\kappa} = \gamma_{\parallel}t$ , the laser equations become

$$\frac{dI}{d\tilde{t}} = 2\tilde{\kappa}I(D - 1) \quad (4.32)$$

$$\frac{dD}{d\tilde{t}} = w - D(1 + I) \quad (4.33)$$

Equations that relate the population dynamics directly either to the electric field amplitude (as in Eqs. (4.29)-(4.30)) or to the electric field intensity (as in Eqs. (4.32)-(4.33)) are known as the *rate equations*. In the version (4.32)-(4.33), they describe the laser in terms of a “population dynamics” that couples the number of photons and the number of inverted atoms. A relevant property of the rate equations is that they do not allow for a Hopf bifurcation. More precisely, the value  $A_H$  of the pump parameter at which the Hopf appears moves to infinity in the rate equation limit. The source term  $w$  in the equation for the population inversion is known as the optical pump parameter. It models the balance of all the incoherent processes that lead to a population inversion in steady state and in the absence of interaction with the field. The lasing threshold occurs at  $w = 1$  and there is lasing for  $w > 1$ .

Let us stress that although the approach presented here is the usual procedure, known as the adiabatic elimination of the fast variables, an omission has been made which may constitute a serious mistake. To derive equations (4.23)-(4.25), we have assumed the existence of well-defined relations among the decay rates:  $\kappa/\gamma_{\perp} = \varepsilon$  and  $\gamma_{\parallel}/\gamma_{\perp} = \mathcal{O}(\varepsilon)$ . This is of course insufficient. To derive equations (4.23)-(4.25) we have to specify *all* the orders of magnitude: we have in fact assumed implicitly that the dynamical variables  $\mathcal{E}$ ,  $\mathcal{P}$ , and  $\mathcal{D}$  and the parameter  $A$  are  $\mathcal{O}(\varepsilon^0)$ . Under these conditions, equations (4.23)-(4.25) are indeed valid. A physical counterexample is the limit  $A = \mathcal{O}(1/\varepsilon)$  realized in the cryogenic hydrogen maser which is described by the laser equations<sup>2</sup>. It can be shown<sup>3</sup> that for this range of parameters, the steady state is not stable, but the intensity is a periodic function with a large amplitude maximum ( $\sim 1/\varepsilon$ ) of short duration separated by a long domain of vanishingly small intensity [ $\sim \exp(-1/\varepsilon)$ ]. In that situation, *two different scalings*, instead of one, are needed to describe the dynamical variables and

<sup>2</sup>A.C. Maan, H.T.C. Stoof, B.J. Verhaar and P. Mandel, Phys. Rev. Lett. **64** (1990) 2630; P. Mandel, A.C. Maan, B.J. Verhaar and H.T.C. Stoof, Phys. Rev. A **44** (1991) 608.

<sup>3</sup>K.A. Robbins, SIAM J. Appl. Math. **36** (1979) 457; A.C. Fowler and M.J. McGuinness, Physica **5D** (1982) 149.

the relevant time scales. This situation requires a more elaborate mathematical treatment. This periodic solution may undergo successive bifurcations leading to deterministic chaos.

The importance of the rate equations stems from the fact that generally they are the adequate level of description for many solid state lasers if the laser is subjected to an external constraint. Among the classic situations, let us mention the periodic modulation of either gain or cavity losses, the influence of an external feedback loop, the injected signal to mode- or phase-lock the laser.

## 4.5 Good cavity limit

There is a class of lasers, such as the  $\text{Ar}^+$  laser, for which a further simplification is possible. These lasers are characterized by the fact that the material variables, atomic polarization and population inversion, decay much faster than the field inside the cavity. That is, we have  $\gamma_{\perp} \simeq \gamma_{\parallel}$ , but  $\gamma_{\perp} \gg \kappa$  and  $\gamma_{\parallel} \gg \kappa$ . It turns out that the analysis of the previous section can be extended to cover the good cavity limit without much difficulty by simply taking the limit  $a = \gamma_{\parallel}/\kappa = \mathcal{O}(\varepsilon)$ . From equations (4.26)-(4.28) we obtain

$$\frac{d\mathcal{E}}{dt_{\kappa}} = -(\mathcal{E} - A\mathcal{P}) \quad (4.34)$$

$$0 = -\mathcal{P} + \mathcal{E}\mathcal{D} \quad (4.35)$$

$$0 = -\mathcal{D} + 1 - \mathcal{E}\mathcal{P} \quad (4.36)$$

Solving the last two equations to express  $\mathcal{P}$  and  $\mathcal{D}$  in terms of  $\mathcal{E}$  leads to a single equation for the complex field

$$\frac{d\mathcal{E}}{dt_{\kappa}} = \mathcal{E} \left( -1 + A \frac{1}{1 + \mathcal{E}^2} \right) \quad (4.37)$$

From this equation we derive an evolution equation for the field intensity  $I = \mathcal{E}^2$

$$\frac{dI}{d\tau} = I \left( -1 + \frac{A}{1 + I} \right) \quad (4.38)$$

where  $\tau = 2t_{\kappa} = 2\kappa t$ . Close to threshold, for  $I \ll 1$ , the so-called cubic approximation<sup>4</sup> may be used as well

$$\frac{dI}{d\tau} = I [-1 + A(1 - I)] \quad (4.39)$$

which can be solved exactly if the pump parameter  $A$  is a constant.

---

<sup>4</sup>The expression *cubic approximation* comes from early analyses of this equation which was expressed in terms of the field amplitude rather in terms of intensity.

## 4.6 References

### Books on resonators

1. G. Hernandez, *Fabry-Perot interferometers* (Cambridge University Press, 1986).
2. J.M. Vaughan, *The Fabry-Perot interferometer* (A. Hilger, Bristol, 1989).
3. N. Hodgson and H. Weber, *Optical resonators* (Springer, Heidelberg, 1997).

### Books on lasers

1. H. Haken, *Encyclopedia of physics* (V.XXV/2C) Genzel ed. (Springer, Heidelberg, 1970).
2. M. Sargent III, M.O. Scully, and W. Lamb Jr., *Laser physics* (Addison-Wesley, Reading 1974).
3. H. Haken, *Light* vol.1 & 2 (North-Holland, Amsterdam, 1981).
4. A.E. Siegman, *Lasers* (University Science Books, Mill Valley MA, 1986).
5. J. Hecht, *Understanding lasers* (IEEE Press, New York, 1988).
6. P.M. Milonni and J.H. Eberley, *Lasers* (Wiley, New York, 1988).
7. O. Svelto, *Principles of lasers* (Plenum, New York, 1989).
8. L. Mandel and E. Wolf, *Optical coherence and quantum optics* (Cambridge University press, 1995).
9. W.T. Silfast, *Laser fundamentals* (Cambridge University Press, 1996).
10. G. Grynberg, A. Aspect, and C. Fabre, *Introduction aux lasers et à l'optique quantique* (Editions Ellipses, Paris, 1997).
11. D. Dangoisse, D. Hennequin, and V. Zehnlé-Dhaoui, *Les lasers* (Dunod, Paris, 1998).

# Chapter 5

## Optical Bistability I

### 5.1 Introduction

In Chapter 4, we have studied properties of lasers, that is, nonlinear resonant cavities in which incoherent pumping induces a population inversion. In this chapter, we analyze a variant of this set-up by considering what happens if the nonlinear cavity is driven by a coherent source such as another laser and the nonlinear medium is not brought to a state of population inversion. Such a device is known under the generic name of optically bistable device and the associated phenomenon is known as optical bistability (OB) because for this class of devices the output intensity versus input intensity displays a hysteresis and therefore a domain of bistability. Most studies of OB have been motivated by applications to all-optical digital signal processing. Although this technology is not yet ripe for industrial applications, an intermediate step is the realization of electro-optical devices which are now close to industrial production. Device applications motivate the selection of topics in this chapter, but the last part will be devoted to more fundamental questions related to deterministic chaos.

The formulation of OB follows the pattern traced in the previous chapters. Starting for instance with Eqs. (4.12)-(4.14), we add a source term  $E_i$  to the field equation to account for the coherent driving of the nonlinear ring cavity. This leads to the set of coupled equations

$$\frac{dE}{dt} = -\bar{\kappa}(E + 2CP - E_i) \quad (5.1)$$

$$\frac{dP}{dt} = -P + ED \quad (5.2)$$

$$\frac{dD}{dt} = \bar{\gamma}(1 - D - EP) \quad (5.3)$$

where  $2C = Nn^0\mu^2\omega_c/(2\hbar\varepsilon'_0\kappa\gamma_\perp)$ ,  $n^0 = n_{11}^0 - n_{22}^0 > 0$ ,  $\omega_a = \omega_c = \omega_i$  where  $\omega_i$  is the frequency of the driving (or input) field. In the absence of a nonlinear medium and on resonance, the steady solution is  $E = E_i$  which gives  $E_i = \sqrt{T}E_{input}$  where  $E_{input}$  is the driving field outside the cavity and  $T$  is the field intensity transmission coefficient of the incoupling mirror. The output field is the fraction of the cavity field that escapes the cavity through the outcoupling mirror. It is a linear function of the cavity field amplitude. Because of this, the two fields are often not distinguished in physical discussions. Finally, the time and decay rate scaling is  $\bar{t} = \gamma_\perp t$ ,  $\bar{\kappa} = \kappa/\gamma_\perp$ , and  $\bar{\gamma} = \gamma_\parallel/\gamma_\perp$ .

## 5.2 Steady state solutions

Let us first consider the steady state solutions of equations (5.1)-(5.3)

$$D = 1/(1 + E^2) \quad (5.4)$$

$$P = E/(1 + E^2) \quad (5.5)$$

$$E_i = E + 2CE/(1 + E^2) \quad (5.6)$$

The electric field amplitude  $E$  is the solution of a cubic equation and there may be either one or three real solutions. The three classes of solutions are displayed in Fig. 5.1.

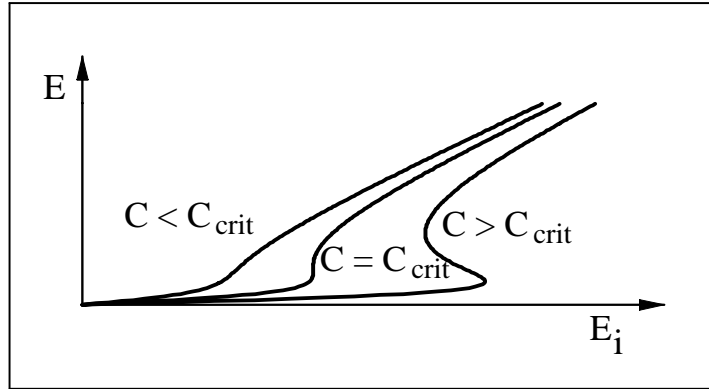


Figure 5.1: Cavity field amplitude *versus* input field amplitude.

We see that there is a critical value of  $C$  such that for  $C < C_{crit}$  the system is monostable, i.e., the cubic (5.6) has only one real root whereas for  $C > C_{crit}$  the system is bistable, i.e., the cubic (5.6) has a domain where the

three roots are real. For this reason the parameter  $C$  is usually referred to as the bistability parameter. Let us determine this critical value. From (5.6) it follows that

$$dE/dE_i = (1 + E^2) / (3E^2 - 2EE_i + 1 + 2C) \quad (5.7)$$

At the limit points, which exist only in the bistable domain, the derivative  $dE/dE_i$  is infinite, which implies  $3E^2 - 2EE_i + 1 + 2C = 0$ . The two solutions of this equation are

$$E_{\pm} = \frac{1}{3} \left( E_i \pm \sqrt{E_i^2 - 3(1 + 2C)} \right) \quad (5.8)$$

Thus the domain of existence for bistability is bounded by  $E_+ = E_- = E_{crit}$ , or equivalently  $3E_{crit} = E_{i,crit}$  and  $E_{i,crit}^2 = 3(1 + 2C_{crit})$ . Combining these relations with the steady state equation (5.6) leads to

$$C_{crit} = 4, \quad E_{crit} = \sqrt{3}, \quad E_{i,crit} = 3\sqrt{3} \quad (5.9)$$

At that point, there is a unique point with vertical slope. For  $C \lesssim C_{crit}$ , the device has the properties of an optical transistor and may be used as such. For  $C > C_{crit}$  the simultaneous solution of the steady state equation (5.6) and the condition for vertical slope  $2EE_i = 1 + 2C + 3E^2$  leads to  $E_{\pm}^4 + 2(1 - C)E_{\pm}^2 + 1 + 2C = 0$  whose solutions are

$$E_+^2 = C - 1 + \sqrt{C(C - 4)}, \quad E_-^2 = \frac{1 + 2C}{C - 1 + \sqrt{C(C - 4)}} \quad (5.10)$$

In the domain  $C > C_{crit}$ , there is an hysteresis which implies jump transitions between the two branches as the input field is varied across the limit points. This is displayed in Fig. 5.2.

### 5.3 Optical devices

The hysteresis displayed by the input/output characteristics of OB suggests to exploit the system as a binary memory. Consider the device being driven by an external field  $E_i = E_1$  in the bistable domain:  $E_- < E_1 < E_+$ . If the device has reached that state starting below the lower limit point  $E_-$  and increasing the driving field amplitude, the cavity field is on the lower branch, corresponding to a weak cavity field amplitude and to an even weaker transmitted or output field amplitude. If the driving field  $E_i$  is increased beyond the limit point  $E_-$ , the device will follow the bistable curve until  $E_-$  and

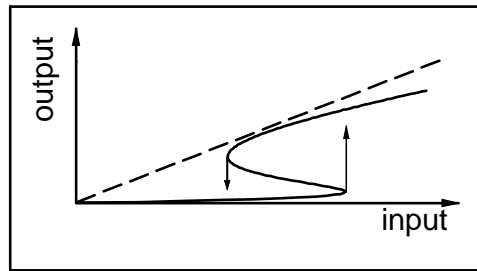


Figure 5.2: Switching between the two branches of the bistable system.

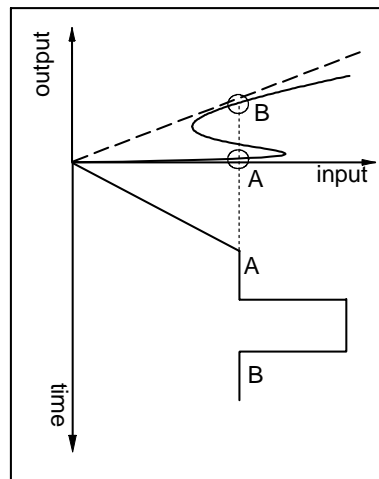


Figure 5.3: The use of a bistable device as binary memory.

then “jump” to the upper branch. Reducing  $E_i$  back to its initial value  $E_1$  leaves the device on the upper branch. Thus for the same value  $E_1$  of the input field, the device can be either on the upper or on the lower transmission branches of the input/output characteristics. This is the signature of a hysteresis and suggests that the device may be used as a binary memory. An illustration of this process is shown in Fig. 5.3.

A direct application of a bistable device is its function as a logic gate. Let us suppose that a holding beam prepares the device in the lower branch but in the bistable domain, as shown in Fig. 5.4. Figure 5.4 (a) displays a logical AND gate while Fig. 5.4 (b) displays a logical OR gate. In the case of an AND gate, both pulses A and B must arrive simultaneously to induce the switch to the upper branch, while each pulse, alone, cannot induce that

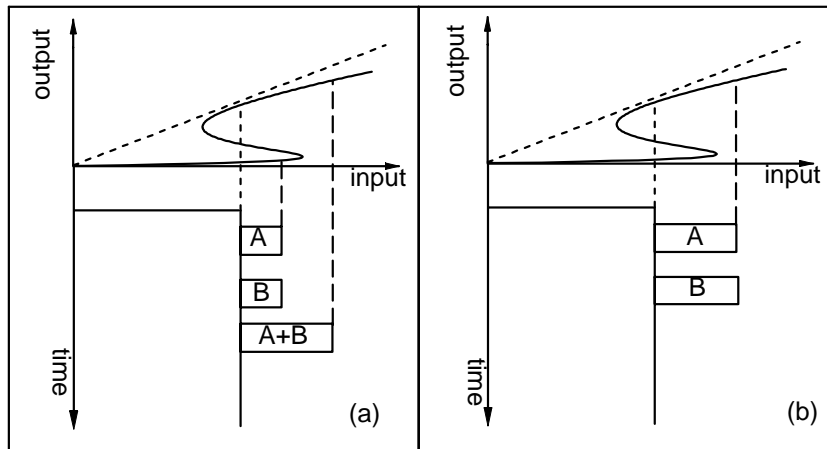


Figure 5.4: Example of logical gates using a bistable device. (a) Logical AND gate; (b) Logical OR gate.

switch. In the case of the logical OR gate, each pulse is able to induce the switch.

Another possible application of OB is the situation where  $C \simeq C_{crit}$ . In that case, the system has a characteristic similar to that of a transistor used to amplify an amplitude modulation. This is, in principle, also possible in optics as shown schematically in Fig. 5.5. It should be stressed that this figure, though a classic representation of a transistor action, is misleading. Indeed, the characteristic curve used here to support the intuition that amplification may occur is a steady state solution, while the input and output fields are time varying functions. There is no reason, *a priori*, to assume that the steady response curve describes adequately the temporal response of the device. More precisely, it may be that this representation is a good approximation of the dynamical response at low modulation frequency, but surely it fails to describe the response of the device at high frequencies.

## 5.4 Generic description

There exists a class of asymptotic models that can be described by a single dynamical equation  $dz/dt = f(z, E_i)$  where the scalar function  $f$  is a non-linear function of  $z$  such that  $f(z, E_i) = 0$  is the steady state hysteresis<sup>1</sup>.

<sup>1</sup>Not all models fall into this class. The rate equation limit, for instance, leads to a pair of dynamical equations. The fully developed hysteresis limit ( $C \rightarrow \infty$ ) produces a single

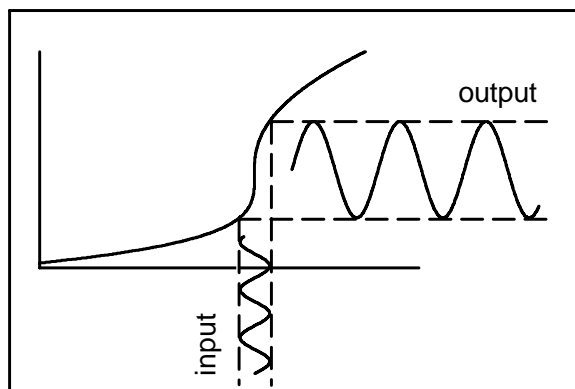


Figure 5.5: Use of an optical nonlinear device close to the bistable domain as an optical transistor.

Let us exclude from the following discussion the domain  $C \lesssim C_{crit}$  which is the optical transistor. Then the function  $f$  has two limit points and the vicinity of the limit point is unambiguously defined. In the vicinity of each limit point, the function  $f(z, E_i)$  may be approximated locally by a parabola which coincides with  $f(z, E_i)$  right at the limit point. We then make a change of variables such that the new coordinates of the limit point are  $(1, 1)$ . Let  $x$  be the rescaled dynamical variable (proportional to the cavity field, and therefore also proportional to the output field),  $\mu$  the rescaled input field and  $\tau$  the rescaled time. The orientation of the parabola is fixed by the further requirement that the coefficient of  $x^2$  be  $\pm 1$ . This procedure leads to generic equations, i.e., different physical processes and/or systems are described by the same equation. Figure 5.6 shows graphically this procedure.

The relevance of a reduced description is that in device applications based on switching between the two branches, one tries hard to prepare and maintain the device as close as possible to the limit point. The generic character of the local description around the limit points has been proved experimentally: the prediction of the generic equations have been confirmed by means of an electric circuit (Schmitt trigger), optically bistable devices (2 mm-thick interference filters and the 192m-long bistable device of Lille university) and bistability in Na vapor. The function  $f$  was different in each of these examples. The case of the Schmitt trigger is discussed in the Appendix to this chapter.

---

dynamical equation, but for a different variable near each limit point and the function  $f$  does not reduce to the full bistable curve in steady state.

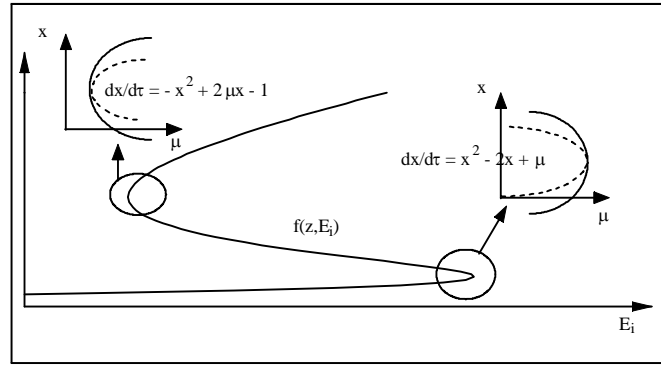


Figure 5.6: The full hysteresis  $f(z, E_i)$  and the local approximations at the limit points.

Close to the limit point which connects the lower and middle branches, the generic dynamical equation is

$$\frac{dx}{d\tau} = x^2 - 2x + \mu \quad (5.11)$$

Close to the limit point which connects the middle and the upper branches, the generic equation is

$$\frac{dx}{d\tau} = -x^2 + 2x\mu - 1 \quad (5.12)$$

The properties of these two equations are very similar and therefore only equation (5.11) will be studied in details.

## 5.5 Nonlinear stability

The steady state solutions of equation (5.11) are

$$x_{\pm} = 1 \pm \sqrt{1 - \mu} \quad (5.13)$$

Since the model is valid only in the vicinity of the limit point, we restrict our study to the first quadrant  $x \geq 0$  and  $\mu \geq 0$ .

A linear stability analysis of the steady states  $x_{\pm}$  is easily performed. Seeking a solutions of the form  $x_{\pm}(\tau) = x_{\pm} + \varepsilon y(\tau) + \mathcal{O}(\varepsilon^2)$  leads to the equation  $dy/d\tau = 2(x_{\pm} - 1)y$  and the solution of the linearized equation is

$$x_{\pm}(\tau) = x_{\pm} + \varepsilon e^{\pm 2\tau\sqrt{1-\mu}} + \mathcal{O}(\varepsilon^2) \quad (5.14)$$

Thus,  $x_+$  is linearly unstable and  $x_-$  is linearly stable. However, an exact solution of equation (5.11) is easily obtained by means of the nonlinear

transformation  $x = -u'/u$ , with  $u' \equiv du/d\tau$ , which transforms the nonlinear equation (5.11) into the linear equation  $u'' + 2u' + \mu u = 0$ . The general solution of that linear equation is

$$u(\tau) = C_1 e^{-\tau x_-} + C_2 e^{-\tau x_+} \quad (5.15)$$

Hence the solution for  $x(\tau)$  becomes

$$x(\tau) = \frac{x_- e^{-\tau x_-} + C x_+ e^{-\tau x_+}}{e^{-\tau x_-} + C e^{-\tau x_+}} \quad (5.16)$$

This solution depends on only one parameter,  $C = C_1/C_2$ , which is determined by the initial condition. The solution generated by the initial condition  $x(0) = x_+ + \beta$  for  $\mu < 1$  and  $\beta \leq 0$  is

$$x(t) = x_- + \frac{(x_+ - x_-)(x_+ - x_- + \beta)}{x_+ - x_- + \beta(1 - e^{2\tau\sqrt{1-\mu}})} \quad (5.17)$$

Since we have an exact solution, a complete stability analysis can be performed. It amounts to determine the basin of attraction of the steady state solutions, that is, to solve the initial value problem for Eq. (5.11).

There are four cases to be distinguished with  $\mu < 1$ :

1. If  $\beta < 0$  and  $|\beta| \rightarrow 0$  the long time limit of  $x(t)$  is  $x_- + \mathcal{O}(e^{-2\tau\sqrt{1-\mu}})$ . Thus for  $x(0) < x_+$  the lower branch solution  $x_-$  is an attractor. The domain of initial conditions  $0 < x(0) < x_+$  with  $\beta < 0$  and  $\mu < 1$  is the basin of attraction of the steady state (or fixed point)  $x_-$ .
2. If  $\beta = 0$ , the system is on a steady state solution  $x(t) = x(0) = x_+$  and, in the absence of perturbation (since  $\beta = 0$ ) the system remains in that state forever.
3. If  $\beta > 0$  and  $\beta \rightarrow 0$ , the solution diverges and becomes infinite in a finite time  $T$  given by  $x_+ - x_- + \beta = \beta \exp(2T\sqrt{1-\mu})$  i.e.,

$$T = \frac{\ln(x_+ - x_- + \beta) - \ln(\beta)}{2\sqrt{1-\mu}} \quad (5.18)$$

The fact that  $x(t)$  diverges in a *finite* time if  $1 - \mu = \mathcal{O}(1)$  is a signature of the nonlinearity. The infinite solution has a simple physical meaning: in the local description of the limit point, it is the upper branch of the function  $f(z, E_i)$  introduced in Section 5.4 and Fig. 5.6. Thus, the initial conditions lying above  $x_+$  belong to the basin of attraction of the upper branch of the function  $f(z, E_i)$ . This indicates

that the middle branch of the function  $f(z, E_i)$  is unstable close to the limit points. By continuity, we may infer the instability of the whole middle branch. Furthermore, if  $\mu$  is close to the limit point, the switching time  $T$  diverges as  $(1 - \mu)^{-1/2}$  or, in physical variables, as  $[(E_{i,\text{lim}} - E_i) / E_{i,\text{lim}}]^{-1/2}$ . This divergence near a limit point is known as *critical slowing down*. The same phenomenon occurs in the vicinity of the laser first threshold, for the same reason though with a different exponent. The difference in the exponent is related to the difference in the nature of the critical points: bifurcation for the laser and limit point in optical bistability.

4. If  $|\beta| \ll 1$  and  $1 - \mu = \mathcal{O}(1)$ , another singularity of the switching time appears

$$T = \frac{\ln(1/\beta)}{2\sqrt{1-\mu}} + \mathcal{O}(1) \quad (5.19)$$

This is another case of slowing down, known as *non critical slowing down*, characterized by a logarithmic divergence.

What is important to note here is that in both cases of slowing down, the divergence is related to a degeneracy: critical slowing down occurs near a limit point where two solutions of  $f(z, E_i)$  coincide, non critical slowing down occurs near the critical line or separatrix ( $x_+$ ) separating two basins of attraction, of  $x = x_-$  and of  $x = \infty$ . Critical slowing down can also be understood in the following way. The linear stability analysis yields the eigenvalue  $\lambda = 2\sqrt{1-\mu}$ . This defines a time scale  $\tau = 1/\lambda = 1/2\sqrt{1-\mu}$ . Close to the limit point,  $\lambda \rightarrow 0$  which implies that the characteristic relaxation time  $\tau \rightarrow \infty$ . Thus critical slowing down is associated with the degenerate situation that defines the limit point: two solutions of a single ordinary differential equation coincide at that point. This degeneracy induces the vanishing of at least one eigenvalue which, in turn, means the divergence of a characteristic time.

## 5.6 References

### Optical bistability

1. L.A. Lugiato, *Theory of optical bistability*, Progress in Optics vol. XXI, E. Wolf ed. (North Holland, Amsterdam, 1984), 71-216.
2. S.D. Smith, *Optical bistability, photonic logic and the optical computer*, Phil. Trans. R. Soc. London A **313** (1984) 187-451.

3. H.M. Gibbs, *Optical bistability: controlling light by light* (Academic Press, New York, 1985).

## 5.7 Appendix: The Schmitt trigger

The Schmitt trigger is an electronic circuit used in gating applications because it can display an hysteresis domain. It is described by the equation

$$\frac{dx}{dt} = y + Cx - \sinh(x) \quad (5.20)$$

where  $x$  and  $y$  are, respectively, the normalized output and input voltage. In the steady state regime, the equation for the slope of the characteristics is

$$\frac{dx}{dy} = \frac{1}{\cosh(x) - C} \quad (5.21)$$

Hence, there are limit points, and therefore bistability, iff  $C \geq 1$ . In that case, the two limit points are located at  $C = \cosh(x_M)$  and  $y_M = -Cx_M \pm \sqrt{C^2 - 1}$ . The steady state characteristics  $x = x(y)$  is shown in Fig. 5.7.

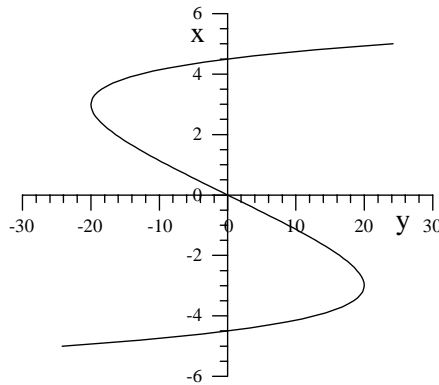


Figure 5.7: Steady state characteristic (output versus input voltage) of a Schmitt trigger for  $C = 10$ .

In the large hysteresis limit obtained for  $C \gg 1$ , the approximate coordinates of the limit points are

1.  $x > 0, C \gg 1$

Since  $C = \cosh(x_M) \simeq (1/2) \exp(x_M)$ , the coordinates of that limit point are

$$\begin{aligned} x_M &\simeq \ln(2C) > 0 \\ y_M &\simeq C[1 - \ln(2C)] < 0 \\ y_M + Cx_M &= +\sqrt{C^2 - 1} \end{aligned} \quad (5.22)$$

2.  $x < 0, C \gg 1$

Since  $C = \cosh(x_M) \simeq (1/2) \exp(-x_M)$ , the coordinates of that limit point are

$$\begin{aligned} x_M &\simeq -\ln(2C) < 0 \\ y_M &\simeq -C[1 - \ln(2C)] > 0 \\ y_M + Cx_M &= -\sqrt{C^2 - 1} \end{aligned} \quad (5.23)$$

Let us now consider the evolution equation in the vicinity of the limit point  $(x_M, y_M)$  with  $x_M < 0$  and  $y_M > 0$ :

$$\begin{aligned} \frac{dx}{dt} &= y + Cx - \left[ \sinh(x_M) + (x - x_M) \cosh(x_M) + \frac{(x - x_M)^2}{2} \sinh(x_M) + \dots \right] \\ &= y + Cx - \left[ -\sqrt{C^2 - 1} + (x - x_M)C - \frac{(x - x_M)^2}{2} \sqrt{C^2 - 1} + \dots \right] \\ &\simeq \frac{x^2}{2} \sqrt{C^2 - 1} - xx_M \sqrt{C^2 - 1} + \left( y - y_M + \frac{x_M^2}{2} \sqrt{C^2 - 1} \right) \end{aligned} \quad (5.24)$$

We define the parameters

$$\alpha = -|x_M|, \quad \beta = \frac{-2}{|x_M| \sqrt{C^2 - 1}} \quad (5.25)$$

and the scaled variables

$$x = \alpha z, \quad t = \beta \tau \quad (5.26)$$

Inserting these definitions in Eq. (5.24) leads to the canonical form

$$\frac{dz}{d\tau} = z^2 - 2z + \mu \quad (5.27)$$

where

$$\mu = 1 - \frac{2(y - y_M)}{x_M^2 \sqrt{C^2 - 1}} \leq 1 \quad (5.28)$$



# Chapter 6

## Optical Bistability II

Apart from its potential for applications in all-optical signal processing, optical bistability has also been a source of inspiration for studies in nonlinear dynamics. In this section, we develop this viewpoint which is based on the work of Ikeda *et al.*

### 6.1 Delay-differential equations

The starting point of this analysis is an alternative formulation of the cavity losses and boundary conditions in a resonant optically bistable cavity. Let us begin with equations (1.26)-(1.28) which we write as

$$\left(v \frac{\partial}{\partial x} + \frac{\partial}{\partial t}\right) \mathcal{E}_0 = (iN\mu\omega_i/\varepsilon'_0)\mathcal{P}_0 \quad (6.1)$$

$$\frac{\partial \mathcal{P}_0}{\partial t} = -[\gamma_{\perp} + i(\omega_a - \omega_i)]\mathcal{P}_0 + i\frac{\mu}{2\hbar}\mathcal{E}_0\mathcal{D}_0 \quad (6.2)$$

$$\frac{\partial \mathcal{D}_0}{\partial t} = \gamma_{\parallel}(\mathcal{D}_a - \mathcal{D}_0) + i\frac{\mu}{\hbar}(\mathcal{E}_0^*\mathcal{P}_0 - \mathcal{E}_0\mathcal{P}_0^*) \quad (6.3)$$

The effect of cavity losses has not been included in this formulation by means of a phenomenological constant. Rather, we formulate more consistently the boundary conditions by expressing the electric field  $E_{tot}(t, x=0)$  at the input mirror ( $x=0$ ) at time  $t$  as the sum of the input field transmitted through this mirror,  $\sqrt{T}E_i(t)$ , plus the cavity field that arrives at time  $t$  at the input mirror, having travelled the distance  $L-\ell$  in the cavity,  $RE_{tot}[t-(L-\ell)/v, x=\ell]$ , where  $R$  takes into account the reflection from the output and input mirrors. For simplicity, both mirrors have been assumed to have the same reflectivity. The cavity length is  $L$  and the nonlinear medium has a length  $\ell$ . Assuming also, for simplicity, that the

input and cavity fields can be written as quasi-plane waves  $E_{tot}(t, x) = \frac{1}{2} [\mathcal{E}_0(t, x)e^{i(kx - \omega t)} + c.c.]$  and  $E_i(t) = \frac{1}{2} [\mathcal{E}_i e^{-i\omega t} + c.c.]$  having the same frequency leads to the relation

$$\mathcal{E}_0(t, 0) = \sqrt{T}\mathcal{E}_i + R\mathcal{E}_0 [t - (L - \ell)/v, \ell] \quad (6.4)$$

for the complex field amplitudes since  $\omega L/v = 2\pi n$  with  $n$  integer.

In the rate equation limit and dispersive limit, a fairly intricate calculation leads from equations (6.1)-(6.4) to the reduced equation

$$\frac{1}{\gamma_{\parallel}\tau_r} \frac{d\varphi(\tau)}{d\tau} = -\varphi(\tau) + A^2 \{1 + 2B \cos [\varphi(\tau - 1) - \varphi(0)]\} \quad (6.5)$$

where the variable  $\varphi \sim \int_0^L \mathcal{D}_0(x, t) dx$  is the population difference averaged over the cavity length and  $\tau_r = L/v$  is the cavity round-trip time. This formulation of the Maxwell-Bloch equations incorporates quite naturally the finite velocity of light in the form of a delay: the field at time  $t$  depends explicitly on the field at time  $t - L/v$  and, through the differential equation for  $\varphi$ , it depends on the field at all intermediate times between  $t$  and  $t - L/v$ .

## 6.2 Discrete map equations

Equation (6.5) is a delay-differential equation, a class of equations on which rather little is known. Therefore some approximations will be introduced at this point. A first approximation is the singular limit  $\gamma_{\parallel}\tau_r \rightarrow \infty$  in which the evolution equations can be reduced to a discrete map. This is easily realized experimentally by a stroboscopic measure of the field intensity at the outcoupling mirror every  $\tau_r$ . Using this limit and the choice  $\varphi(0) = -\pi/2$  for the initial phase leads to the Ikeda map

$$\varphi(n + 1) = a - b \sin \varphi(n) \quad (6.6)$$

This map equation is a two-parameter map with a bounded nonlinearity. Another important equation obtained in the limit  $\gamma_{\parallel}\tau_r \rightarrow \infty$  is the equation for small amplitude solutions. We choose  $\varphi(0) = 0$  and expand the right hand side of equation (6.5) in powers of  $\varphi$ . Limiting the expansion to second order terms yields an equation which is easily transformed into its canonical form

$$x(n + 1) = \lambda x(n) [1 - x(n)] \quad (6.7)$$

where  $x(n)$  is defined on the fundamental interval  $[0, 1]$  and  $\lambda$  varies in the range  $[0, 4]$ . This is the simplest nonlinear discrete map, known as the

quadratic map. It was first derived in 1845 by the Belgian mathematician P.F. Verhulst to simulate the growth of a population constrained to a closed area. More recently, it was also introduced in economics to describe saving accounts with a self-limiting rate of interest, i.e., the rate of interest decreases proportionally to the deposit to avoid unbounded growth of a single deposit.

The most surprising feature of the map (6.7) is that the long time solutions, i.e.,  $\lim_{n \rightarrow \infty} x(n)$ , are not necessarily steady states. Depending on  $\lambda$ , the iterates of the map converge to a steady solution, a periodic solution or even a seemingly random solution. A sample of time-dependent solutions is shown in Fig. 6.1.

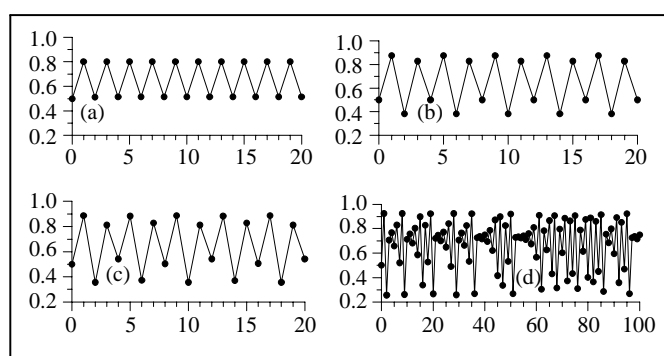


Figure 6.1: Iterates of the quadratic map  $x(n)$ , defined by Eq. (6.7), versus  $n$ . Initial condition:  $x(0) = 0.5$ . (a)  $\lambda = 3.2$ : period-2 solutions; (b)  $\lambda = 3.5$ : period-4 solutions; (c)  $\lambda = 3.55$ : period-8 solutions; (d)  $\lambda = 3.7$ : chaotic solutions. The solutions are the black dots at integer values of  $n$ ; the connecting lines are drawn as a visual help.

The fixed points (i.e., the steady states) of the map are given by the quadratic equation  $x = \lambda x(1 - x)$  whose solutions are

$$x_0 = 0, \quad x_1 = 1 - 1/\lambda \quad (6.8)$$

The stability of these solutions is easily assessed by means of a linear stability analysis. We seek solutions of the map (6.7) of the form  $x(n) = x_{0,1} + \varepsilon y(n) + \mathcal{O}(\varepsilon^2)$ . This leads to  $y(n+1) = \lambda(1 - 2x_{0,1})y(n)$ . The condition of stability is therefore  $|\lambda(1 - 2x_{0,1})| < 1$ . The trivial solution,  $x_0$ , is stable iff  $0 < \lambda < 1$ . The nontrivial solution is stable in the domain  $|2 - \lambda| < 1$  or  $1 < \lambda < 3$ . Thus steady state solutions of the quadratic map are stable only if  $0 < \lambda < 3$ .

Figure 6.1(a) gives an indication about happens close but above  $\lambda = 3$ : there appears periodic solutions. The simplest periodic solutions of the map

(6.7) should verify the equations

$$x_2 = f(\lambda, x_1), \quad x_1 = f(\lambda, x_2) \quad (6.9)$$

where  $f(\lambda, x) \equiv \lambda x(1 - x)$ . It is called a period-2 solution since the basic pattern which is repeated contains two points. Going back to the original variables, it means a solution with period  $2\tau_r = 2L/v$ : the basic field pattern is repeated every second round-trip time. Let us introduce the second iterate of the map  $f^{(2)}(\lambda, x) \equiv f(\lambda, f(\lambda, x))$ . It is obvious that the fixed points of the map are also fixed points of the second iterate of the map. However, the fixed points of  $f^{(2)}$  which are not fixed points of the map are period-2 solutions of the map. The fixed points of  $f^{(2)}$  verify the equation

$$x = f(\lambda, f(\lambda, x)) = \lambda f(\lambda, x) [1 - f(\lambda, x)] = \lambda^2 x(1 - x) (1 - \lambda x + \lambda x^2) \quad (6.10)$$

whose solutions are

$$x_0 = 0, \quad x_1 = 1 - 1/\lambda \quad (6.11)$$

$$x_{\pm} = \frac{\sqrt{\lambda + 1}}{2\lambda} \left( \sqrt{\lambda + 1} \pm \sqrt{\lambda - 3} \right) \quad (6.12)$$

The pair  $\{x_+, x_-\}$  is a periodic solution of the map (6.7) since it verifies the property  $x_+ = f(\lambda, x_-)$  and  $x_- = f(\lambda, x_+)$ . To test the linear stability of the solutions  $x_{\pm}$ , we consider them as fixed points of  $f^{(2)}$ . We seek solutions of the equation

$$x(\lambda, n + 2) = f(\lambda, f(\lambda, x(\lambda, n))) \quad (6.13)$$

which is equivalent to Eqs. (6.9), of the form  $x(\lambda, n) = x_{\pm} + \varepsilon x_1(\lambda, n) + \mathcal{O}(\varepsilon^2)$ . This leads directly to  $x_1(n + 2)/x_1(n) = 4 - \lambda(\lambda - 2)$ . The boundaries of stability are  $|4 - \lambda(\lambda - 2)| = 1$  whose solutions are  $\lambda = 3$  and  $\lambda = 1 + \sqrt{6} \simeq 3.4495$ . At this critical point, the period-2 solution loses its stability and now it should be clear that a new periodic solution will emerge, which is a period-4 solution of the map  $f(\lambda, x)$  or a fixed point of the fourth iterate  $f^{(4)}(\lambda, x) = f^{(2)}(\lambda, f^{(2)}(\lambda, x))$  which is not a fixed point of either  $f^{(2)}$  or  $f$ . Another property which is easy to verify is that the window in which the solution of period  $n$  is stable is bounded by  $|df^{(n)}/dx| = -1$  (lower bound) and  $|df^{(n)}/dx| = +1$  (upper bound). In each window, there is one particular solution, the super-cycle of period  $n$  for which  $df^{(n)}/dx = 0$ .

### 6.3 Deterministic chaos

By successive iterations, we construct the sequence of maps  $f^{(2^n)}$  and correspondingly the solutions of period  $2^n$ . This is visualized in Fig. 6.1 where

the first periodic solutions, of periods 2, 4, and 8, are drawn, and also an aperiodic solution. Another way to visualize this sequence is displayed in Fig. 6.2. To draw that figure, and Fig. 6.3 which displays two enlarged

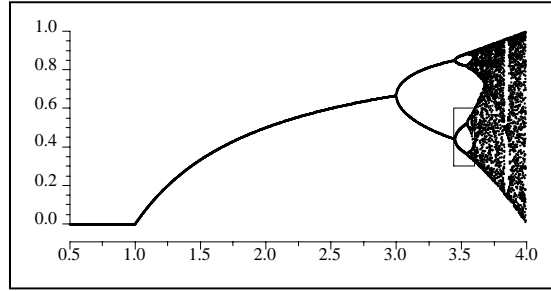


Figure 6.2: Solutions of the quadratic map *versus*  $\lambda$ . The rectangle is the area displayed in figure 6.3(a).

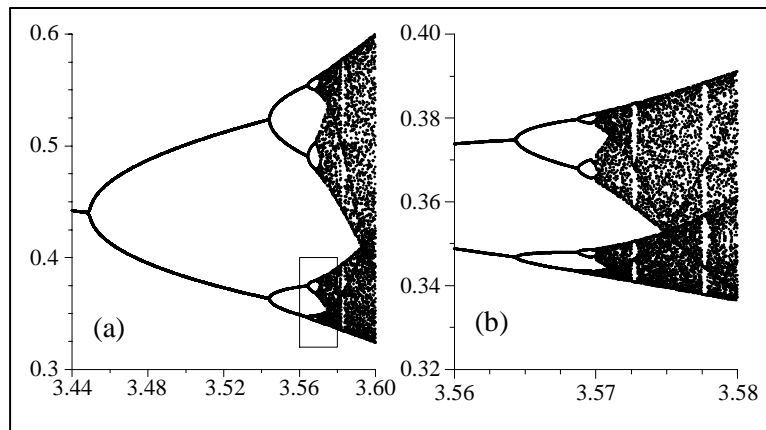


Figure 6.3: Two enlarged regions of Fig. 6.2. The rectangle in (a) is the area displayed in (b).

sections of Fig. 6.2, the quadratic map has been iterated  $10^3$  times for each value of  $\lambda$ , beginning with  $x(0) = 0.5$ . The next 32 iterates are displayed in the figure. Figures 6.2 and 6.3 indicate that something special happens if  $\lambda$  is close to 4. More precisely, unexpected properties appear at the limit of the period-doubling sequence. The first property which should be noticed is that there is an accumulation point,  $r_\infty$ , which is the limit of the sequence  $r_1, r_2, \dots$  where  $r_n$  is the lowest value of  $\mu$  where  $|df^{(n)}/dx| = 1$ . Likewise, the sequence  $R_1, R_2, \dots$  where  $R_n$  is the value of  $\mu$  where supercycles occur,

converges towards the same limit. Let  $d_n$  be the amplitude of the period- $2^n$  supercycle. The main result observed numerically and later proved analytically by Feigenbaum is that the cascade of period-doubling generated by the quadratic map is characterized by the scaling laws

$$\lim_{n \rightarrow \infty} \frac{r_{n+1} - r_n}{r_n - r_{n-1}} = \lim_{n \rightarrow \infty} \frac{R_{n+1} - R_n}{R_n - R_{n-1}} = \delta = 4.6692 \dots \quad (6.14)$$

$$\lim_{n \rightarrow \infty} \left| \frac{d_n}{d_{n+1}} \right| = \alpha = 2.5029 \dots \quad (6.15)$$

The constants  $\alpha$  and  $\beta$  are universal constants: they do not depend on any parameter. Thus the sequences  $\{r_n\}$  and  $\{R_n\}$  form a geometric progression. At the accumulation point  $r_\infty = R_\infty \equiv \lambda_\infty = 3.5699 \dots$ , the solution of the quadratic map is an aperiodic function. The range  $\lambda_\infty < \lambda < 4$  is the domain where the so-called deterministic chaos is found, except for small domains, called windows, in which the solutions are again periodic.

An example of chaotic solution is shown in figure 6.1(d). Although it is a bounded function, it has a positive Lyapunov exponent. The Lyapunov exponent  $\ell(x)$  is defined in terms of  $|f^{(n)}(x + \varepsilon) - f^{(n)}(x)| = \varepsilon \exp [n\ell(x; n, \varepsilon)]$  which yields

$$\begin{aligned} \ell(x) &= \lim_{n \rightarrow \infty} \lim_{\varepsilon \rightarrow 0} \ell(x; n, \varepsilon) \\ &= \lim_{n \rightarrow \infty} \lim_{\varepsilon \rightarrow 0} \frac{1}{n} \log \left| \frac{f^{(n)}(x + \varepsilon) - f^{(n)}(x)}{\varepsilon} \right| \\ &= \lim_{n \rightarrow \infty} \frac{1}{n} \log \left| \frac{df^{(n)}(x)}{dx} \right| \end{aligned} \quad (6.16)$$

A positive Lyapunov exponent means that if two initial conditions differ by an infinitesimal amount, the trajectories will diverge exponentially. A consequence of the positivity of  $\ell$  is that the solution of the quadratic map given by two different computers will be different since the round-off errors will be different, which amounts to introduce extremely small but uncontrolled differences in the two solutions. This is known as the sensitivity to initial conditions and is one of the main signatures of chaos. Because of this, it is important to find properties of the chaotic solutions which are independent of these aspects. One such property is the plot of the iterates in the  $(x(n+1), x(n))$  plane, that is, of one iterate versus the previous iterate, as shown in figure 6.4. In that figure, we have represented two of the periodic solutions of figure 6.1 and a chaotic solution. We first observe that the period- $2^n$  solutions leave only  $2^n$  points in that plane (figures 6.4(a) and (b) contain 500 points each, figure 6.4(c) contains  $10^4$  points!). For the chaotic

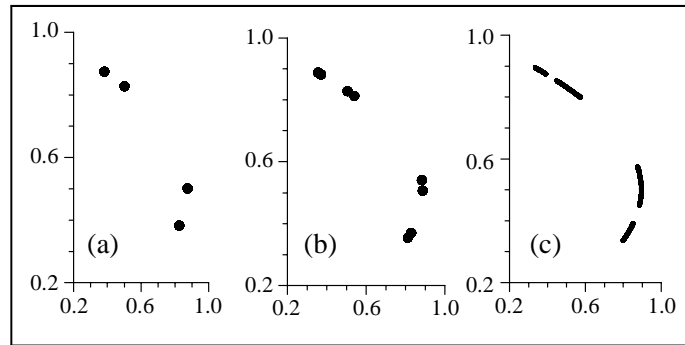


Figure 6.4: Plot of  $x(n + 1)$  versus  $x(n)$  for the quadratic map. Initial condition:  $x(0) = 0.5$ . The map is iterated  $10^3$  times before the next  $K$  iterations are recorded. (a)  $\lambda = 3.5$ : period-4 solution,  $K = 500$ , four different points; (b)  $\lambda = 3.55$ : period-8 solution,  $K = 500$ , eight different points; (c)  $\lambda = 3.58$ : chaotic solution,  $K = 10^4$  and  $10^4$  different points.

solution in figure 6.4(c), we also observe that points are not distributed at random in the plane, as would have been the case for a stochastic sequence of points. Thus the chaotic solution is far from being a random function. Two different chaotic solutions corresponding to the same  $\lambda$  but different  $x(0)$  will fill the same curve (made of disconnected segments) but following different time sequences. The curve generated by the chaotic solution is not always a continuous or a piecewise continuous curve: at the accumulation point  $\lambda_\infty$  of the quadratic map, it is a fractal. That is, it has a fractional dimension. At  $\lambda = \lambda_\infty$ , the Hausdorff dimension of the attractor is  $0.5388\dots$  and the Lyapunov exponent vanishes. There is an infinity of accumulation points, all of them corresponding to a fractal attractors and zero Lyapunov exponents. Apart from the accumulation points, the chaotic attractors have integer dimension but a positive Lyapunov exponent.

Other properties of the chaotic solutions are invariant. The Fourier transform of the quadratic map solutions also has such invariant properties with respect to the initial condition. In addition, the peak heights of the power spectrum for period- $2^n$  solutions display universal scaling laws.

Within the chaotic domain, windows of periodic solutions are found. The main windows are for the solutions of periods 3 and 5. These solutions period double and lead to chaos via the subharmonic bifurcation sequence  $p \cdot 2^n$ ,  $p = 3$  or  $5$ , with the scaling laws (6.14) and (6.15). Smaller windows with sequences  $p \cdot 2^n$  and  $p = 6, 7, \dots$  are also found in the chaotic domain. Finally, period tripling ( $p \cdot 3^n$ ), quadrupling ( $p \cdot 4^n$ ), and so on are also observed in windows embedded in the chaotic domain. These bifurcation sequences follow scaling

laws similar to (6.14) and (6.15) though with different numerical values for the corresponding universal constants. Each of these bifurcation sequences ends at an accumulation point where the attractor is fractal and the Lyapunov exponent vanishes.

## 6.4 References

### Ikeda delay-differential equations

#### Original papers:

1. K. Ikeda, Opt. Commun. **30** (1979) 257.
2. K. Ikeda, H. Daido, and O. Akimoto, Phys. Rev. Lett. **45** (1980) 709.
3. K. Ikeda and O. Akimoto, Phys. Rev. Lett. **48** (1982) 617.

#### Early observations of deterministic chaos in OB

##### (a) in hybrid electro-optic devices:

1. H.M. Gibbs, F.A. Hopf, D.L. Kaplan, and R.L. Shoemaker, Phys. Rev. Lett. **46** (1981) 474.
2. F.A. Hopf, D.L. Kaplan, H.M. Gibbs, and R.L. Shoemaker, Phys. Rev. A **25** (1982) 2172.
3. M.W. Derstine, H.M. Gibbs, F.A. Hopf, and D.L. Kaplan, Phys. Rev. A **26** (1982) 3720; *ibid.* **27** (1983) 3200.

##### (b) in pulsed pumped all-optical ring cavity:

1. H. Nakatsuka, S. Asaka, H. Itoh, K. Ikeda, and M. Matsuoka, Phys. Rev. Lett. **50** (1983) 109.

### Deterministic chaos

1. R.M. May, *Simple mathematical models with very complicated dynamics*, Nature **261** (1976) 459.
2. P. Collet and J.-P. Eckmann, *Iterated maps on the interval as dynamical systems* (Birkhäuser, Basel, 1981).
3. J.-P. Eckmann, *Roads to turbulence*, J. Math. Phys. **53** (1981) 643.
4. E. Ott, Rev. Mod. Phys. **53** (1981) 655.

5. H.G. Schuster, *Deterministic chaos* (Physik Verlag, Weinheim, 1984).
6. B.B. Mandelbrot, *The fractal geometry of nature* (Freeman, San Francisco, 1982).
7. P. Cvitanović, *Universality in chaos* (Adam Hilger, Bristol, 1984).



## **Part III**

# **Weakly nonlinear systems**



# Chapter 7

## Frequency mixing

With this chapter, we begin the study of systems that can be described by the fully nonlinear Maxwell equation

$$\Delta \vec{E} - \vec{\nabla} (\vec{\nabla} \cdot \vec{E}) - \frac{1}{c^2} \frac{\partial^2 \vec{E}}{\partial t^2} = \frac{1}{\epsilon_0 c^2} \frac{\partial^2}{\partial t^2} (\vec{P}_L + \vec{P}_{NL}) \quad (7.1)$$

where the total polarization has been split into linear and nonlinear parts. The nonlinear polarization will be assumed to be a bilinear function of the electric field components  $(E_x, E_y, E_z)$ . This is the lowest order possible nonlinear dependence on the electric field, but it requires special media since this dependence is ruled out by the two-level model which was developed and used in the first parts of these lecture notes.

### 7.1 Tensor $\rightarrow$ vector $\rightarrow$ scalar description

In principle, each of the three components of the polarization is a function of all three components of the electric field. We shall simplify our analysis by considering problems where the vectors  $\vec{P}$  and  $\vec{E}$  are parallel. With this restriction, the linear part of the polarization can be expressed quite generally as

$$\vec{P}_L(t) = \epsilon_0 \int_{-\infty}^t \chi^{(1)}(t - \tau) \vec{E}(\tau) d\tau \quad (7.2)$$

where the scalar linear susceptibility  $\chi^{(1)}(t)$  is independent of the electric field. Note that we must impose  $\chi^{(1)}(t) = 0$  if  $t < 0$  to guarantee causality:  $\vec{P}(t)$  cannot depend on the field  $\vec{E}(\tau)$  for  $\tau > t$ . Put in other words, causality means that the effect  $(\vec{P})$  depends on the cause  $(\vec{E})$  in the past and the present, but not in the future.

This leads to the Maxwell equation

$$\Delta \vec{E} - \vec{\nabla} (\vec{\nabla} \cdot \vec{E}) - \frac{1}{c^2} \frac{\partial^2 \vec{E}}{\partial t^2} - \frac{1}{c^2} \frac{\partial^2}{\partial t^2} \int_{-\infty}^t \chi^{(1)}(t - \tau) \vec{E}(\tau) d\tau = \frac{1}{\epsilon_0 c^2} \frac{\partial^2}{\partial t^2} \vec{P}_{NL} \quad (7.3)$$

The nonlinear medium will be characterized by a nonlinear atomic polarization which is a function of the electric field of higher order than linear. In this and the next chapters, we will assume that the vector character of the fields can be neglected and the problem reduced to a 1D problem. This means that  $\vec{P}_{NL}$  does not mix the Cartesian components of the electric field. In a linear isotropic medium where  $\vec{P}$  is a linear function of  $\vec{E}$ , the condition  $\vec{\nabla} \cdot \vec{D} = 0$  implies  $\vec{\nabla} \cdot \vec{E} = 0$ . This is no longer true in a nonlinear medium. However, in optics the correction is usually very small. In particular, in the slowly varying approximation which will be introduced in this chapter, it remains an excellent approximation. With this approximation, the nonlinear Maxwell equation reduces to

$$\frac{\partial^2 E}{\partial z^2} - \frac{1}{c^2} \frac{\partial^2 E}{\partial t^2} - \frac{1}{c^2} \frac{\partial^2}{\partial t^2} \int_{-\infty}^t \chi^{(1)}(t - \tau) E(\tau) d\tau = \frac{1}{\epsilon_0 c^2} \frac{\partial^2}{\partial t^2} P_{NL} \quad (7.4)$$

## 7.2 Multiple time-scales

In all the applications treated in this and the next chapter, we shall deal with optical fields. We wish to exploit the fact that they can be expressed as a fast optical oscillation modulated by an amplitude which varies on a much slower scale. Let us write  $E(t) = E(t, s) + c.c. = \mathcal{E}(s)e^{-i\omega t} + c.c.$  where  $t$  is the "fast time" and  $s$  the "slow time". More precisely, what is meant by fast and slow times is that the time  $t$  characterizes the fast oscillations and is typical of optical variations in vacuum while  $s$  characterizes the time variations of the atomic medium.

In the spirit of the multiple time-scale analysis, we treat functions of these two times as functions of two independent variables. The justification of this procedure can be found in textbooks on applied mathematics. The integral

in Eq. (7.4) becomes

$$\begin{aligned}
 J &= \int_{-\infty}^t \chi^{(1)}(t-\tau)E(\tau)d\tau = \int_0^{\infty} \chi^{(1)}(\bar{t})E(t-\bar{t})d\bar{t} \\
 &= \mathcal{E}(s)e^{-i\omega t} \int_0^{\infty} \chi^{(1)}(\bar{t})e^{i\omega\bar{t}}d\bar{t} + \mathcal{E}^*(s)e^{i\omega t} \int_0^{\infty} \chi^{(1)}(\bar{t})e^{-i\omega\bar{t}}d\bar{t} \\
 &\equiv E(t,s)\chi^{(1)}(\omega) + E^*(t,s)\chi^{(1)}(-\omega)
 \end{aligned} \tag{7.5}$$

where  $\chi^{(1)}(\omega)$  is the Fourier transform of  $\chi^{(1)}(t)$  since  $\chi^{(1)}(t) = 0$  if  $t < 0$ . By definition,  $\chi^{(1)}(-\omega)$  is the complex conjugate of  $\chi^{(1)}(\omega)$ . To simplify the following discussion, we assume that  $\chi^{(1)}(\omega)$  is real and therefore it is an even function of  $\omega$ :  $\chi^{(1)}(\omega) = \chi^{(1)}(-\omega)$ . This assumption is in agreement with the results obtained in Chapter 2. This means that in the linear regime, we consider only dispersion and not absorption.

Thus we arrive at the relation  $P_L(t) = \varepsilon_0 E(t)\chi^{(1)}(\omega)$  which can be viewed as an expression of the slowly varying envelope approximation and the absence of absorption. This leads to the electric field equation

$$\frac{\partial^2 E}{\partial z^2} - \frac{1 + \chi^{(1)}(\omega)}{c^2} \frac{\partial^2 E}{\partial t^2} = \frac{1}{\varepsilon_0 c^2} \frac{\partial^2}{\partial t^2} P_{NL} \tag{7.6}$$

We can introduce the refractive index  $n(\omega) = \sqrt{1 + \chi^{(1)}(\omega)}$  and write the electric field equation as

$$\frac{\partial^2 E}{\partial z^2} - \frac{n^2}{c^2} \frac{\partial^2 E}{\partial t^2} = \frac{1}{\varepsilon_0 c^2} \frac{\partial^2}{\partial t^2} P_{NL} \tag{7.7}$$

*Note: the atomic polarization defined in this Part III of the lecture notes differs by a factor  $i$  from the atomic polarization used in Parts I and II. Hence, there is also a permutation of the role of real and imaginary parts of the susceptibility between the two Parts.*

### 7.3 $\chi^{(2)}$ media

In this chapter, it will be assumed that the polarization of the nonlinear medium has a quadratic dependence in the field

$$P_{NL} = P^{(2)} = \chi^{(2)} E^2 \tag{7.8}$$

Note that if the nonlinear medium is invariant under the transformation  $z \rightarrow -z$ , then  $\chi^{(2)}$  must vanish identically because physically it is clear that

changing  $E$  into  $-E$  implies changing  $P$  into  $-P$ . To visualize this fact, let us remember that the microscopic polarization is a measure of the field-induced deformation of the electronic cloud surrounding the nucleus of an atom, while the macroscopic polarization  $P$  is the statistical average of the microscopic polarizations over the material sample. Thus, if the medium is invariant under the transformation  $z \rightarrow -z$ , a  $\pi$  phase change of the electric field will only induce a similar change in the microscopic and the macroscopic polarizations. However, if the medium is not symmetric under the transformation  $z \rightarrow -z$ , there is no reason why a change of sign of the electric field must induce the same change in the polarization. A general analysis of the relation between polarization and field leads to the conclusion that second harmonic generation and, more generally  $\chi^{(2n)}$  processes, can occur but only in media which lack the invariance under spatial reflection. This is the case, for instance, of noncentrosymmetric crystals such as ZnS, CdTe, GaAs, LiNbO<sub>3</sub>, and BaTiO<sub>3</sub>. Other examples are interfaces, such as the surface of any solid in contact with a medium having either a different periodicity or no periodicity at all, such as any gas, for instance.

Let us suppose first that a monochromatic optical field  $E = \mathcal{E}_1 e^{-i\omega_1 t} + c.c.$  is applied to such a nonlinear system. The induced polarization is

$$P = \chi^{(2)} (\mathcal{E}_1 e^{-i\omega_1 t} + c.c.)^2 = \chi^{(2)} (\mathcal{E}_1^2 e^{-2i\omega_1 t} + 2|\mathcal{E}_1|^2 + \mathcal{E}_1^{*2} e^{2i\omega_1 t}) \quad (7.9)$$

Hence there are two physical processes involved:

- *second harmonic generation* characterized by

$$P(2\omega) = \chi^{(2)} \mathcal{E}_1^2 e^{-2i\omega_1 t} \quad (7.10)$$

In this process, the nonlinear medium transforms the input electric field at frequency  $\omega$  into a polarization oscillating at twice that frequency. This component of the polarization will drive the Maxwell equation (7.4) and induce a field oscillating at the frequency  $2\omega$ . This process is routinely used to double a laser frequency with a conversion efficiency that can easily reach 80% today.

- *optical rectification* characterized by

$$P(0) = 2\chi^{(2)} |\mathcal{E}_1|^2 \quad (7.11)$$

In this process, a static electric field is induced inside the nonlinear medium.

One can model a  $\chi^{(2)}$  medium by means of a two-level medium by assuming that two-photon transitions coexist with single photon transitions. In that case, the process associated with  $P(2\omega)$  would be interpreted as the absorption of two photons at frequency  $\omega$  (hence the dependence on the square of the field amplitude) by an atom in its ground level, followed by the emission of a single photon at twice the frequency ( $2\omega$ ).

If two fields  $E = \mathcal{E}_1 e^{-i\omega_1 t} + \mathcal{E}_2 e^{-i\omega_2 t} + c.c.$  are applied to the nonlinear medium, there is a richer selection of possible processes since

$$\begin{aligned} P &= \chi^{(2)} (\mathcal{E}_1 e^{-i\omega_1 t} + \mathcal{E}_2 e^{-i\omega_2 t} + c.c.)^2 \\ &= \chi^{(2)} (\mathcal{E}_1^2 e^{-2i\omega_1 t} + c.c.) \\ &\quad + \chi^{(2)} (\mathcal{E}_2^2 e^{-2i\omega_2 t} + c.c.) \\ &\quad + 2\chi^{(2)} (\mathcal{E}_1 \mathcal{E}_2 e^{-i(\omega_1 + \omega_2)t} + c.c.) \\ &\quad + 2\chi^{(2)} (\mathcal{E}_1 \mathcal{E}_2^* e^{-i(\omega_1 - \omega_2)t} + c.c.) \end{aligned} \quad (7.12)$$

$$+ 2\chi^{(2)} (|\mathcal{E}_1|^2 + |\mathcal{E}_2|^2) \quad (7.13)$$

The five processes involved here are:

- *second harmonic generation*

$$P(2\omega_1) = \chi^{(2)} \mathcal{E}_1^2 e^{-2i\omega_1 t} \quad (7.14)$$

$$P(2\omega_2) = \chi^{(2)} \mathcal{E}_2^2 e^{-2i\omega_2 t} \quad (7.15)$$

- *sum frequency generation*

$$P(\omega_1 + \omega_2) = 2\chi^{(2)} \mathcal{E}_1 \mathcal{E}_2 e^{-i(\omega_1 + \omega_2)t} \quad (7.16)$$

- *difference frequency generation*

$$P(\omega_1 - \omega_2) = 2\chi^{(2)} \mathcal{E}_1 \mathcal{E}_2^* e^{-i(\omega_1 - \omega_2)t} \quad (7.17)$$

- *optical rectification*

$$P(0) = 2\chi^{(2)} (|\mathcal{E}_1|^2 + |\mathcal{E}_2|^2) \quad (7.18)$$

To each source term of the form  $P(\omega_p)$  there corresponds a field component at frequency  $\omega_p$ . The main fact that should be clear at this point is that a nonlinear medium with a  $\chi^{(2)}$  nonlinearity will invariably generate new frequencies. These are not small modifications of the injected frequency: apart from the zero frequency (optical rectification), the new frequencies can

be close to either half or twice the injected frequencies. These processes are of course limited by the energy-momentum conservation laws which will restrict the range of possible frequencies and will affect drastically the conversion efficiency via the so-called phase matching condition. The most important applications of  $\chi^{(2)}$  nonlinearities are second harmonic generation (SHG) with single input beam, sum and difference frequencies with two input beams (SFG and DFG). SHG will be studied in the next chapter, SFG and DFG will be developed in Chapter 9.

## 7.4 References

### The founding papers of nonlinear optics

1. J.A. Armstrong, N. Bloembergen, J. Ducuing, and P.S. Pershan, *Phys. Rev.* **127**, 171 (1962).
2. N. Bloembergen and P.S. Pershan, *Phys. Rev.* **128**, 193 (1962).
3. N. Bloembergen and Y.R. Shen, *Phys. Rev.* **133**, 210 (1964).

### Books on nonlinear optics

1. N. Bloembergen, *Nonlinear optics* (Benjamin, New York, 1965).
2. A. Yariv and P. Yeh, *Optical waves in crystals* (Wiley, New York, 1984).
3. Y.R. Shen, *The principles of nonlinear optics* (Wiley, New York, 1984).
4. P.N. Butcher and D. Cotter, *The elements of nonlinear optics* (Cambridge University Press, 1991).
5. R.W. Boyd, *Nonlinear Optics* (Academic Press, New York, 1992).
6. A.C. Newell and J.V. Moloney, *Nonlinear optics* (Addison-Wesley, Reading, 1992).
7. P. Mandel, *Theoretical problems in cavity nonlinear optics* (Cambridge University Press, 1997).

# Chapter 8

## Second harmonic generation

### 8.1 Formulation

In this section we consider the properties of an optical beam sent through a  $\chi^{(2)}$  nonlinear medium which generates the second harmonic of the injected field. Thus the total field inside the material sample is  $E = E_1 + E_2 = \mathcal{E}_1 \exp(-i\omega t) + \mathcal{E}_2 \exp(-2i\omega t) + c.c.$  Hence the associated polarization  $P = \chi^{(2)} E^2$  is

$$\begin{aligned} P &= \chi^{(2)} \left[ \begin{aligned} &\mathcal{E}_1^2 \exp(-2i\omega t) + \mathcal{E}_2^2 \exp(-4i\omega t) \\ &+ \mathcal{E}_1^{*2} \exp(2i\omega t) + \mathcal{E}_2^{*2} \exp(4i\omega t) \end{aligned} \right] \\ &+ 2\chi^{(2)} \left[ \begin{aligned} &\mathcal{E}_1 \mathcal{E}_2 \exp(-3i\omega t) + \mathcal{E}_1 \mathcal{E}_2^* \exp(-i\omega t) \\ &+ \mathcal{E}_1^* \mathcal{E}_2^* \exp(3i\omega t) + \mathcal{E}_1^* \mathcal{E}_2 \exp(i\omega t) \end{aligned} \right] \\ &+ 2\chi^{(2)} [|\mathcal{E}_1|^2 + |\mathcal{E}_2|^2] \\ &\equiv [P(2\omega) + P(4\omega) + c.c.] + [P(3\omega) + P(\omega) + c.c.] + P(0) \quad (8.1) \end{aligned}$$

Here we meet a problem related to the nonlinear nature of the medium. Assuming a field which oscillates at frequencies  $n\omega$  with  $n = 1$  and  $2$ , the polarization has components at frequencies  $n\omega$  with  $n = 0, 1, 2, 3, 4$ . Thus, we should add components oscillating at frequencies  $3\omega$  and  $4\omega$  to the electric field, in which case frequencies at  $n\omega$  with  $n = 0, 1, \dots, 8$  will be generated by the polarization. Continuing this process leads to a field generation at all integer multiple frequencies of the fundamental frequency  $\omega$ . In practice, however, the generation of harmonics higher than the second is negligible in  $\chi^{(2)}$  nonlinear media under usual operating conditions and can therefore be neglected in the analysis of the SHG process. This results from the fact that in the Maxwell equations for the field at frequency  $\omega$ , the  $\chi^{(2)}$  nonlinearity will induce a source oscillating at the same frequency  $\omega$  only via  $P(2\omega)$  whereas the other components of the atomic polarization will oscillate at a largely

different high frequency. Therefore, these other components will average to zero. This is another variant of the rotating wave approximation already introduced in Chapter 1.

In the same way that we have introduced a slowly varying electric field amplitude by  $E = E_1 + E_2 + c.c.$  with  $E_j = \mathcal{E}_j e^{-i\omega_j t}$ , we introduce a slowly varying polarization by  $P = \sum_n P(n\omega) = \sum_n [\mathcal{P}(n\omega) e^{-in\omega t} + c.c.]$ . Inserting these definitions into Maxwell equation (7.4) and using the property (7.5) for the linear polarization leads to an equation for the total electric field. Since we are dealing with optical fields, it is safe to assume that all the coefficients of a given oscillating exponential  $\exp(-in\omega t)$  must vanish identically. This leads to a pair of equations which we can write in compact form as

$$\frac{\partial^2 E_m}{\partial z^2} - \frac{n_m^2}{c^2} \frac{\partial^2 E_m}{\partial t^2} = \frac{1}{\varepsilon_0 c^2} \frac{\partial^2}{\partial t^2} P(m\omega) \quad (8.2)$$

where  $m = 1, 2$ . Assuming  $\text{Im} [\chi^{(1)}(m\omega)] = 0$ , the refractive index is defined as

$$n_m^2 = 1 + \chi^{(1)}(m\omega) \quad (8.3)$$

and

$$P(\omega) = \mathcal{P}(\omega) e^{-i\omega t} = 2\chi^{(2)} \mathcal{E}_1^* \mathcal{E}_2 e^{-i\omega t}, \quad (8.4)$$

$$P(2\omega) = \mathcal{P}(2\omega) e^{-2i\omega t} = \chi^{(2)} \mathcal{E}_1^2 e^{-2i\omega t} \quad (8.5)$$

As a last step, we extract the spatial variation on the optical scale

$$\mathcal{E}_m = A_m e^{ik_m z} \quad (8.6)$$

where

$$ck_m = n_m \omega_m \quad (8.7)$$

with  $\omega_m = m\omega$ . The amplitude  $A_m$  can still vary in space, but it will be assumed that this variation is slow compared with the optical variation with characteristic length  $1/k_m$ . Introducing these expressions into (8.2) leads without approximation to

$$\begin{aligned} & e^{ik_m z} \left[ \frac{\partial^2 A_m}{\partial z^2} + 2ik_m \frac{\partial A_m}{\partial z} - \frac{n_m^2}{c^2} \left( \frac{\partial^2 A_m}{\partial t^2} - 2i\omega_m \frac{\partial A_m}{\partial t} \right) \right] \\ &= \frac{1}{\varepsilon_0 c^2} \left[ \frac{\partial^2 \mathcal{P}(m\omega)}{\partial t^2} - 2i\omega_m \frac{\partial \mathcal{P}(m\omega)}{\partial t} - \omega_m^2 \mathcal{P}(m\omega) \right] \end{aligned} \quad (8.8)$$

We now invoke the slow variation in space and time of the electric field and polarization amplitudes to justify the approximations

$$\frac{\partial^2 A_m}{\partial z^2} + 2ik_m \frac{\partial A_m}{\partial z} \simeq 2ik_m \frac{\partial A_m}{\partial z} \quad (8.9)$$

$$\frac{\partial^2 A_m}{\partial t^2} - 2i\omega_m \frac{\partial A_m}{\partial t} \simeq -2i\omega_m \frac{\partial A_m}{\partial t} \quad (8.10)$$

$$\begin{aligned} \frac{\partial^2 \mathcal{P}(m\omega)}{\partial t^2} - 2i\omega_m \frac{\partial \mathcal{P}(m\omega)}{\partial t} - \omega_m^2 \mathcal{P}(m\omega) &\simeq -2i\omega_m \frac{\partial \mathcal{P}(m\omega)}{\partial t} - \omega_m^2 \mathcal{P}(m\omega) \\ &\approx -\omega_m^2 \mathcal{P}(m\omega) \end{aligned} \quad (8.11)$$

with which the coupled Maxwell equations (8.8) for the two field amplitudes become

$$\frac{\partial A_1}{\partial z} + \frac{n_1}{c} \frac{\partial A_1}{\partial t} = \frac{i\omega_1 \chi^{(2)}}{n_1 \varepsilon_0 c} A_1^* A_2 e^{-i(2k_1 - k_2)z} \quad (8.12)$$

$$\frac{\partial A_2}{\partial z} + \frac{n_2}{c} \frac{\partial A_2}{\partial t} = \frac{i\omega_2 \chi^{(2)}}{2n_2 \varepsilon_0 c} A_1^2 e^{i(2k_1 - k_2)z} \quad (8.13)$$

The quantity  $\Delta k = 2k_1 - k_2$  is the spatial phase matching whose consideration is of paramount importance in determining the efficiency of SHG.

## 8.2 Free running SHG

There are two typical situations which we shall consider: either the  $\chi^{(2)}$  medium stands alone or it is embedded in a cavity characterized by the reflectivity of its mirrors at the fundamental and harmonic frequencies. In this section, we consider the first situation, that of propagation in empty space before and after the field interacts with the nonlinear medium. We can therefore assume that the fields oscillate strictly at  $\omega_1$  and  $2\omega_1$ . This means that the amplitude functions  $A_m$  no longer depend on time. Thus, it is assumed that a regime has been reached, in which the complex amplitudes  $A_m$  are time-independent. This does not rule out "turbulent" regimes where the  $A_m$  would be space- and time-dependent. These turbulent regimes are not studied here.

The resulting propagation equations are

$$\frac{dA_1}{dz} = \frac{i\omega_1 \chi^{(2)}}{n_1 \varepsilon_0 c} A_1^* A_2 e^{-iz\Delta k} \quad (8.14)$$

$$\frac{dA_2}{dz} = \frac{i\omega_2 \chi^{(2)}}{n_2 \varepsilon_0 c} A_1^2 e^{iz\Delta k} \quad (8.15)$$

and  $\Delta k = 2k_1 - k_2$ . Note the property

$$\frac{d|A_1|^2}{dz} = \frac{i\omega_1 \chi^{(2)}}{n_1 \varepsilon_0 c} [A_1^* A_2 e^{-iz\Delta k} - A_1^2 A_2^* e^{iz\Delta k}] \quad (8.16)$$

$$\frac{d|A_2|^2}{dz} = \frac{i\omega_1\chi^{(2)}}{n_2\varepsilon_0c} [-A_1^{*2}A_2e^{-iz\Delta k} + A_1^2A_2^*e^{iz\Delta k}] \quad (8.17)$$

from which it follows that  $J \equiv n_1|A_1|^2 + n_2|A_2|^2$  is a constant of the motion. The invariance of  $J$  simply expresses the conservation of the power flow. This suggests that we use new variables defined by  $A_m = \sqrt{J/n_m}\rho_m \exp(i\phi_m)$  with real  $\rho_m$  and  $\phi_m$  and such that

$$\rho_1^2 + \rho_2^2 = 1 \quad (8.18)$$

Equations (8.14)-(8.15) become

$$\frac{d\rho_1}{dz} + i\rho_1\frac{d\phi_1}{dz} = \frac{i\omega_1\chi^{(2)}\sqrt{J}}{n_1\sqrt{n_2}\varepsilon_0c}\rho_1\rho_2e^{-i\theta} \quad (8.19)$$

$$\frac{d\rho_2}{dz} + i\rho_2\frac{d\phi_2}{dz} = \frac{i\omega_1\chi^{(2)}\sqrt{J}}{n_1\sqrt{n_2}\varepsilon_0c}\rho_1^2e^{i\theta} \quad (8.20)$$

with  $\theta = 2\phi_1 - \phi_2 + z\Delta k$ . A last change of variables is

$$\zeta = z\frac{\omega_1}{c}\frac{\chi^{(2)}}{\varepsilon_0}\frac{\sqrt{J}}{n_1\sqrt{n_2}} \equiv z/\ell \quad (8.21)$$

with the characteristic length  $\ell$  defined as

$$\ell = \frac{n_1\sqrt{n_2}\varepsilon_0c}{\omega_1\chi^{(2)}\sqrt{J}} \quad (8.22)$$

Note that  $\ell$  is a function of the field powers through  $J$ . Let us consider as an example, frequency doubling of the Nd:YAG output at 1064nm by a noncentrosymmetric crystal of KDP ( $\text{KH}_2\text{PO}_4$ ) which has a  $\bar{4}2m$  tetragonal symmetry. The Nd:YAG emits a field at  $\lambda = 1.06 \times 10^{-6}\text{m}$ . The KDP has an ordinary refractive index  $n_o(\omega) = 1.4939$  along which the input field is sent and an extraordinary index at the harmonic frequency  $n_e(2\omega) = 1.4706$  along which the frequency-doubled field propagates. The nonlinearity is characterized by  $\chi^{(2)}/\varepsilon_0 \simeq 1.5 \times 10^{-9}\text{esu}$  or  $1.5 \times 10^{-9} \times \frac{3}{4\pi} \times 10^4\text{m/V}$ . The incident field is of the order of  $10^2\text{esu}$ , i.e., an intensity of  $2.5\text{MW/cm}^2$ . Let us recall that a laser pulse of  $x$  mJ during  $y$  ms focused on an area of  $z \mu\text{m}^2$  corresponds to an intensity of  $x/(yz)10^{12}\text{W/m}^2 = x/(yz)10^2\text{MW/cm}^2$  and a field amplitude of  $4x/(yz)10^3\text{esu}$ . Assuming  $|A_2(0)| = 0$ , one easily finds  $\ell = 10^3|A_1(0)|^{-1}\text{cm}$  where the field amplitude of the Nd:YAG is expressed in esu. Thus, for the standard value  $|A_1(0)| \simeq 10^2\text{esu}$  the characteristic length is 10 cm.

Eventually, we obtain for the amplitudes the pair of equations

$$\frac{d\rho_1}{d\zeta} = \rho_1\rho_2 \sin \theta \quad (8.23)$$

$$\frac{d\rho_2}{d\zeta} = -\rho_1^2 \sin \theta \quad (8.24)$$

and for the phase mismatch

$$\begin{aligned} \frac{d\theta}{d\zeta} &= \ell\Delta k + 2\rho_2 \cos \theta - (\rho_1^2/\rho_2) \cos \theta \\ &= \ell\Delta k + \frac{\cos \theta}{\sin \theta} \frac{d}{d\zeta} \ln(\rho_1^2 \rho_2) \end{aligned} \quad (8.25)$$

In the case of perfect phase matching,  $\Delta k = 0$ , the phase equation (8.25) reduces to

$$\frac{d}{d\zeta} \ln(\rho_1^2 \rho_2) = \frac{\sin \theta}{\cos \theta} \frac{d\theta}{d\zeta} = -\frac{d \ln(\cos \theta)}{d\zeta} \quad (8.26)$$

and therefore  $d \ln(\cos \theta \rho_1^2 \rho_2) / d\zeta = 0$  which leads to a second invariant

$$\rho_1^2 \rho_2 \cos \theta = G \quad (8.27)$$

A special value is  $G = 0$  which can be fulfilled either if  $\rho_2$  vanishes at the entrance face of the nonlinear medium or if  $\cos \theta = 0$ . If  $\rho_2(\zeta = 0) = 0$ , the initial field  $\rho_1(\zeta = 0) = 1$  induces a growth of  $\rho_2$  if  $\sin \theta < 0$ . Otherwise,  $\rho_2$  becomes negative, which is not physical. If  $\cos \theta \neq 0$ , it must be the second harmonic field that vanishes at the entrance face of the medium because from (8.18) the vanishing of  $\rho_1$  implies  $\rho_2 = 1$ , which is not SHG.

With this result, it is easy to find the exact second invariant without the  $\Delta k = 0$  restriction

$$\begin{aligned} \frac{d}{d\zeta} \rho_1^2 \rho_2 \cos \theta &= -\rho_1^2 \rho_2 \ell \Delta k \sin \theta \\ &= \rho_2 \ell \Delta k \frac{d}{d\zeta} \rho_2 \\ &= \frac{d}{d\zeta} \frac{\ell \Delta k}{2} \rho_2^2 \end{aligned} \quad (8.28)$$

from where it follows that the function  $H$  defined through

$$H = \rho_1^2 \rho_2 \cos \theta - \frac{\ell \Delta k}{2} \rho_2^2 \quad (8.29)$$

is the constant of the motion we are looking for. Practically, the invariant is conveniently determined in terms of the input field characteristics. Thus, we can identify three situations which in order of increasing complexity are

- perfect phase matching  $\Delta k = 0$  and  $G = 0$
- perfect phase matching  $\Delta k = 0$  but  $G \neq 0$
- imperfect phase matching  $\Delta k \neq 0$ .

**Perfect matching and  $G = 0$** 

The condition  $G = 0$  implies  $\cos \theta = 0$  and therefore  $\theta = \pm\pi/2$ . We choose  $\theta = -\pi/2$  to have  $d\rho_2/dt > 0$ . Then the two amplitude equations (8.23)-(8.24) become

$$\frac{d\rho_1}{d\zeta} = -\rho_1\rho_2, \quad \frac{d\rho_2}{d\zeta} = \rho_1^2 \quad (8.30)$$

Using the property  $\rho_1^2 + \rho_2^2 = 1$ , the second equation yields  $d\rho_2/d\zeta = 1 - \rho_2^2$  whose solution is  $\rho_2 = \tanh(\zeta + \zeta_0)$  and therefore  $\rho_1 = \operatorname{sech}(\zeta + \zeta_0)$ . To fix the integration constant, we impose  $\rho_2(\zeta = 0) = 0$ . The solution then becomes

$$\rho_1 = \operatorname{sech}(\zeta), \quad \rho_2 = \tanh(\zeta) \quad (8.31)$$

where  $\zeta = z/\ell$  and the characteristic length is

$$\ell = \frac{\sqrt{n_1 n_2} \varepsilon_0 c}{\omega_1 \chi^{(2)} |A_1(0)|} \quad (8.32)$$

Thus, in the limit  $\zeta \rightarrow \infty$ , all the field at the fundamental frequency  $\omega_1$  will be converted into its second harmonic. It is clear now that the choice  $\theta = \pi/2$  leads to unacceptable negative amplitude solutions since it amounts to change  $\zeta \rightarrow -\zeta$  or  $(\rho_1, \rho_2) \rightarrow (\rho_1, -\rho_2)$ . The functions  $\rho_1$  and  $\rho_2$  given by (8.31) are displayed in figure 8.1.

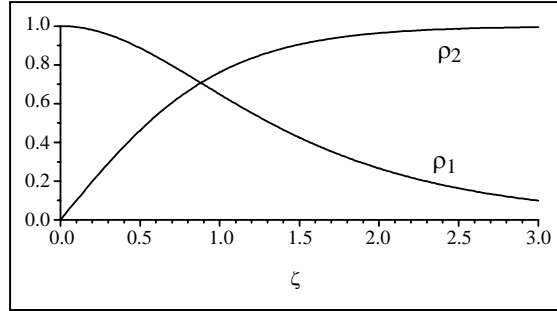


Figure 8.1: Field amplitude  $\rho_1 = \operatorname{sech}(\zeta)$  and  $\rho_2 = \tanh(\zeta)$  of the two fields as a function of the reduced distance  $\zeta = z/\ell$  in the case of perfect phase matching  $\Delta k = 0$ . The initial condition is  $\rho_1 = 1$  and  $\theta = -\pi/2$ .

One obvious consequence of the result (8.31) is that increasing the length of the crystal is not necessarily the best way to increase the conversion efficiency. Note also that reverting to the unscaled notation, we can express the

result  $\rho_2 = \tanh(\zeta)$  as

$$\eta = \frac{|A_2(z)|^2}{|A_1(0)|^2} = \frac{n_1}{n_2} \tanh^2(z/\ell) \quad (8.33)$$

In the numerical example discussed just after (8.22),  $\ell = 10$  cm and  $n_2/n_1 = 0.9844$ . The factor  $\eta$  measures the conversion rate into the SHG. The following table illustrates these properties:

$z/\ell$	0.2	0.4	0.6	0.8	1	1.5	2	2.5	3
$\rho_2$	0.197	0.380	0.537	0.664	0.762	0.905	0.964	0.987	0.995
$\eta$ (%)	3.82	14.21	28.39	43.40	57.15	80.62	91.48	95.90	97.46

### Perfect matching but $G \neq 0$

The constant  $G$  is not arbitrary. The maximum of  $G$  is determined as follows:

$$\max(G) = \max(\rho_1^2 \rho_2) = \max\left(\rho_1^2 \sqrt{1 - \rho_1^2}\right) = \sqrt{4/27} \quad (8.34)$$

and the maximum occurs for

$$\rho_1|_{\max(G)} = \sqrt{2/3} \quad \rho_2|_{\max(G)} = \sqrt{1/3} \quad (8.35)$$

Using the two constants of the motion  $\rho_1^2 + \rho_2^2 = 1$  and  $\rho_1^2 \rho_2 \cos \theta = G$  leads to  $\cos \theta = G / [\rho_2 (1 - \rho_2^2)]$ . Hence

$$\begin{aligned} \frac{d\rho_2^2}{d\zeta} &= -2\rho_2\rho_1^2 \sin \theta = \pm 2\rho_2 (1 - \rho_2^2) \sqrt{1 - \cos^2 \theta} \\ &= \pm 2\sqrt{\rho_2^2 (1 - \rho_2^2)^2 - G^2} \end{aligned} \quad (8.36)$$

This indicates that  $\rho_2^2$  can be expressed in terms of the Jacobi elliptic functions. The  $\pm$  sign in front of the square root appearing in Eq. (8.36) is determined by the sign of  $\sin \theta$  at the entrance face of the medium. The main point to stress here is that the field amplitudes  $\rho_1$  and  $\rho_2$  are periodic functions of  $\zeta$ . Since  $\rho_1^2 + \rho_2^2 = 1$ , the two fields exchange periodically energy as the medium length  $\zeta$  increases. This indicates that for each medium, there is a optimum sample length for harmonic conversion. Increasing slightly the medium length beyond this optimum length is in fact counterproductive since it reduces the conversion efficiency. The solution  $\rho_2^2$  obtained by numerical integration of equation (8.36) and  $\rho_1^2 = 1 - \rho_2^2$  are displayed in figure 8.2.

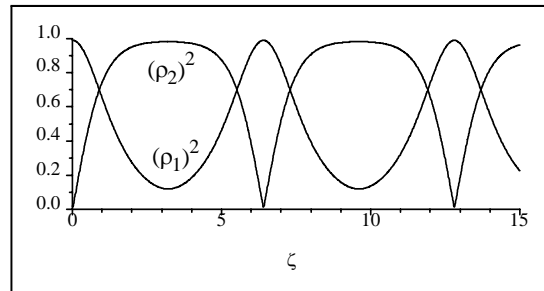


Figure 8.2: Reduced intensities  $\rho_1^2$  and  $\rho_2^2$  obtained from the numerical simulation of equation (8.36) as a function of the reduced distance  $\zeta = z/\ell$  in the case of perfect phase matching  $\Delta k = 0$ . The initial condition is  $\rho_1^2 = 0.99$  and  $\theta = \pi/4$ .

It is important to determine the length for maximum conversion or at least to have an estimate of it. One quantity which is easily determined is the period of the field intensities  $\rho_p^2$ . Using the theory of elliptic functions, one derives the equation for the period as

$$\Pi = \int_{x_a}^{x_b} \frac{dx}{\sqrt{x(1-x)^2 - G^2}} \quad (8.37)$$

where  $x_a$  and  $x_b$  are the two lowest positive roots of the cubic  $x(1-x)^2 = G^2$  with  $x_a \leq x_b$ . The main feature of this result is that the period depends on the initial conditions  $\rho_1(0)$ ,  $\rho_2(0)$  and  $\theta(0)$  via the invariant  $G$ . Figure 8.3, which represents the second harmonic intensity  $\rho_2^2$  as a function of  $\zeta$ , is designed to illustrate the results of this section. In figure 8.3(a),  $\theta$  is constant and  $\rho_1^2$  varies. In figure 8.3b,  $\rho_1^2$  is constant and  $\theta$  varies.

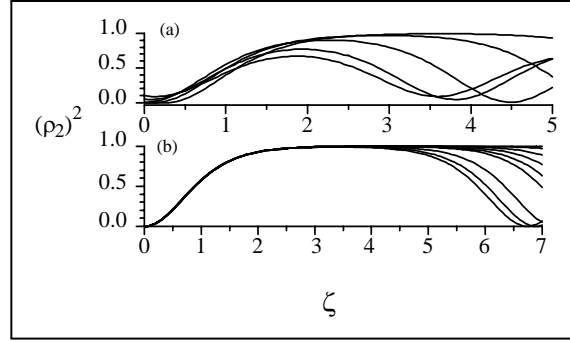


Figure 8.3: Reduced intensity of the second harmonic  $\rho_2^2$  as a function of the reduced distance  $\zeta = z/\ell$  in the case of perfect phase matching  $\Delta k = 0$ . (a) The initial condition is  $\theta = \pi/4$ . The intensity of the fundamental field at  $\zeta = 0$  is  $\rho_1^2 = 0.9, 0.95, 0.99, 0.999, \text{ and } 0.9999$  from left to right. (b) The initial condition is  $\rho_1^2 = 0.9999$  and  $\theta = \pi/10, 2\pi/10, 3\pi/10, 4\pi/10, 4.2\pi/10, 4.4\pi/10, 4.6\pi/10, 4.8\pi/10, \text{ and } \pi/2$  from left to right.

### Imperfect phase matching

It is a simple matter to verify that using the constants of the motion  $\rho_1^2 + \rho_2^2 = 1$  and  $H$ , Eq. (8.36) is generalized into

$$\begin{aligned} \frac{d\rho_2^2}{d\zeta} &= \pm 2\rho_2(1 - \rho_2^2) \sqrt{1 - \cos^2 \theta} \\ &= \pm 2\sqrt{\rho_2^2(1 - \rho_2^2)^2 - \left(H + \frac{\ell\Delta k}{2}\rho_2^2\right)^2} \end{aligned} \quad (8.38)$$

Though the form of this equation is more complex, it is clear that we are again dealing with an elliptic function, which means that  $\rho_2^2$  is a periodic function of space. Examples of the intensity variation versus propagation length is displayed in figure 8.4. The initial condition is  $\rho_1^2 = 0.99$  and  $\theta = \pi/4$ . Each curve is labelled by  $\Delta s = \ell\Delta k$ .

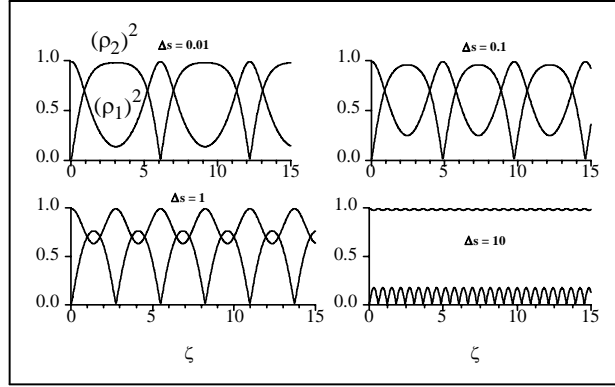


Figure 8.4: Field intensities  $\rho_1^2$  and  $\rho_2^2$  as a function of the reduced distance  $\zeta = z/\ell$  for different values of the phase mismatch. The initial condition is  $\rho_1^2 = 0.99$  and  $\theta = \pi/4$ . Each curve is labelled by  $\Delta s = \ell\Delta k$ .

### Phase matching

The phase matching condition plays a fundamental role in SHG. To gain some further understanding into this question, let us consider the limit of weak depletion of the pump field  $A_1$ . That is, we assume a  $\chi^{(2)}$  medium such that we may neglect, in first approximation, the spatial variation of the pump field. Assuming  $A_1$  to be constant leads from (8.15) to the result

$$A_2(z) = \frac{\omega_1 \chi^{(2)}}{n_2 \varepsilon_0 c} A_1^2 \frac{e^{iz\Delta k} - 1}{\Delta k} \quad (8.39)$$

and from there we can evaluate the intensity of the second harmonic to be

$$I_2(z) = |A_2(z)|^2 = \left( \frac{z\omega_1 \chi^{(2)}}{n_2 \varepsilon_0 c} \right)^2 |A_1|^4 \frac{\sin^2(z\Delta k/2)}{(z\Delta k/2)^2} \quad (8.40)$$

or equivalently

$$I_2(z, \Delta k) = [\max I_2(z, \Delta k)] \text{sinc}^2(z\Delta k/2) \quad (8.41)$$

where the cardinal sine function is defined by  $\text{sinc}(x) \equiv \sin(x)/x$ . The function  $\text{sinc}^2(x)$  is displayed in figure 8.5.

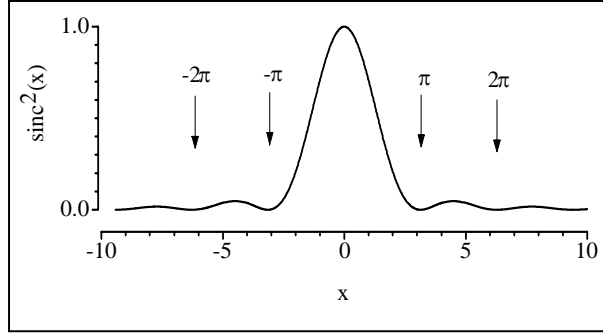


Figure 8.5: Efficiency of the conversion into the second harmonic as a function of  $x = z\Delta k/2$ .

The minima of  $\text{sinc}^2(x)$  occur for  $\sin(x) = 0$  and  $x \neq 0$ , i.e., for  $\Delta k = \pm 2n\pi/z$  with  $n$  integer and there is one maximum at the origin  $x = 0$ . The function  $\text{sinc}(x)$  has a characteristic length which is the distance between two consecutive minima. It is called the coherence length  $L_c$  and given by  $|\Delta k| = 2\pi/L_c$ :

$$L_c = \frac{2\pi}{|\Delta k|} = \frac{2\pi}{|k(2\omega) - 2k(\omega)|} = \frac{\pi c}{\omega |n(2\omega) - n(\omega)|} = \frac{\lambda}{2 |n(2\omega) - n(\omega)|} \quad (8.42)$$

where  $\lambda$  is the wavelength of the input field. Using the numerical values  $\lambda = 1.06 \times 10^{-6}\text{m}$ ,  $n_o(\omega) = 1.4939$  and  $n_e(2\omega) = 1.4706$  discussed after (8.22) leads to  $L_c \simeq 23 \times 10^{-6}\text{ m}$  or about 22 wavelengths.

It follows from (8.40) that the efficiency in the weak pump depletion limit is given by

$$\eta = \frac{|A_2(z)|^2}{|A_1(0)|^2} = \left( \frac{z\omega_1\chi^{(2)} |A_1(0)|}{n_2\epsilon_0 c} \right)^2 \text{sinc}^2(z\Delta k/2) \quad (8.43)$$

which reduces to the result (8.33) if  $\Delta k = 0$  and  $z \rightarrow 0$  so that  $\tanh(z/\ell) \simeq z/\ell$  and  $\text{sinc}^2(z\Delta k/2) \simeq 1$ .

The importance of achieving phase matching is clear from the previous discussions. To realize phase matching means to verify the momentum conservation law  $2k_1 = k_2$ . But  $ck_m = n_m\omega_m$  and the energy conservation law requires  $\omega_1 = 2\omega_2$ . Hence, perfect phase matching requires  $n(\omega_1) = n(\omega_2)$ . This is, in general, not possible because the rule is that the refractive index  $n(\omega)$  increases monotonically with frequency. However, many crystals display birefringence, a property by which the refractive index depends on the electric field polarization. This leads to the introduction, in linear optics, of the ordinary and extraordinary polarizations and the corresponding

refractive indices  $n_o$  and  $n_e$ . In such a case, one can choose to phase match two fields propagating with different polarizations; the matching condition becomes  $n_o(\omega_1) = n_e(\omega_2)$  or  $n_e(\omega_1) = n_o(\omega_2)$ . Still another possibility is to exploit the dependence of  $n_e(\omega, \theta)$  on the angle  $\theta$  between the so-called optic axis and the  $\mathbf{k}$  vector (angle tuning).

Recently, a new method has appeared which is called *quasi-phase matching*. It amounts to exploit the modern techniques of material engineering to modulate periodically the nonlinearity:  $\chi^{(2)} \sim \exp(iz\Delta k)$  where  $\Delta k$  is the phase mismatch which is produced in the medium with a constant  $\chi^{(2)}$ . The grating at  $\Delta k$  which is created in the medium is a powerful tool since it is entirely controlled at the fabrication stage and does not depend on the medium characteristics. In particular, it is possible in this way to enhance conversion processes with a large  $\chi^{(2)}$  which would otherwise be impossible because their mismatch is too large. Typical gain enhancements obtained experimentally in this way have reached 20.

#### Papers on quasi-phase matching

1. M.M. Fejer, G.A. Magel, D.H. Jundt and R.L. Byer, IEEE J. Quantum Electron. **28**, 2631 (1992).
2. L.E. Myers, R.C. Eckardt, M.M. Fejer, R.L. Byer, W.R. Bosenberg and J.W. Pierce, J. Opt. Soc. Am. B **12**, 2102 (1995).

### 8.3 Intracavity SHG

A fairly different situation is realized if the nonlinear medium is placed inside a resonant cavity. Figure 8.6 is a schematic representation of the set-up we shall analyze: a  $\chi^{(2)}$  nonlinear medium is placed in a resonant cavity. The cavity is resonant at frequencies  $\omega$  and  $2\omega$ . This type of configuration is called a doubly resonant cavity. In the singly resonant cavity, only one field is resonant with the cavity. A plane wave  $E(\omega)$  at the fundamental frequency  $\omega$  is injected into the cavity. The nonlinear medium generates the second harmonic and part of both fields escapes the cavity through the outcoupling mirror.

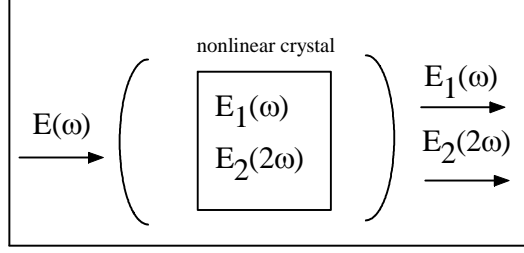


Figure 8.6: Configuration for intracavity SHG.

We start again with equations (8.2) for the two fields. A simple model is obtained by assuming the decomposition  $\mathcal{E}_m(z, t) = A_m(t)u_m(z)$  where  $u_m(z)$  is a cavity eigenmode verifying the conditions  $\int_0^L u_m^*(z)u_n(z)dz = \delta_{mn}$ . Typically, we have  $u_m(z) = \sqrt{1/L} \exp(ikz)$  for a ring cavity and  $u_m(z) = \sqrt{2/L} \sin(kz)$  for a Fabry-Perot cavity. Note the difference with Eq. (8.6): in this case, we assume that the amplitude  $A_m$  is space-independent because  $u_m$  is a cavity eigenmode and we consider a monomode oscillation, i.e., only one mode of the cavity is excited by the field at  $m\omega$ .

Using the slowly varying envelope approximation (8.9)-(8.11) are replaced by the more general equations

$$u_1 \frac{dA_1}{dt} = i \frac{\chi^{(2)}\omega_1}{\varepsilon_0 n_1^2} u_1^* u_2 A_1^* A_2 \quad (8.44)$$

$$u_2 \frac{dA_2}{dt} = i \frac{\chi^{(2)}\omega_1}{\varepsilon_0 n_2^2} u_1^2 A_1^2 \quad (8.45)$$

We multiply the equation for  $A_p$  by  $u_p^*$  and integrate the resulting equations over the cavity length. This leads to

$$\frac{dA_1}{dt} = i \frac{\chi^{(2)}\omega_1}{\varepsilon_0 n_1^2} f A_1^* A_2 \quad (8.46)$$

$$\frac{dA_2}{dt} = i \frac{\chi^{(2)}\omega_1}{\varepsilon_0 n_2^2} f^* A_1^2 \quad (8.47)$$

where  $f = \int_0^L (u_1^*)^2 u_2 dz$ . Two cases may occur:

**Case I:**  $u_1 = \sqrt{1/L} \exp(ik_1 z)$  and  $u_2 = \sqrt{1/L} \exp(ik_2 z)$ . Then

$$f = \frac{e^{-iL\Delta k/2}}{\sqrt{L}} \text{sinc}(L\Delta k/2) \quad (8.48)$$

**Case II:**  $u_1 = \sqrt{2/L} \sin(k_1 z)$  and  $u_2 = \sqrt{2/L} \sin(k_2 z)$ . Then

$$f = \frac{1}{\sqrt{2L}} \sin(L\Delta k/2) \operatorname{sinc}(L\Delta k/2) \quad (8.49)$$

To derive this result, an approximation has been introduced: only oscillations in space at the wave number  $\Delta k = 2k_1 - k_2$  have been retained. Oscillations at  $2k_1 + k_2$  or at  $\pm k_2$  have been neglected because they will average to zero compared with the slow oscillations at  $\Delta k$ .

We now add two ingredients: (i) the dynamical equation for the field oscillating at  $\omega$  is driven by the external monochromatic field. Only the fraction  $A$  of that driving field amplitude is transferred inside the cavity through the incoupling mirror. (ii) The cavity is lossy at both frequencies  $\omega$  and  $2\omega$ . Hence we have to add a loss term  $-\kappa_m A_m$  to the equation for  $A_m$ . The resulting equations are

$$\frac{dA_1}{dt} = -\kappa_1 A_1 + \frac{i\chi^{(2)}\omega}{\varepsilon_0 n_1^2} f A_1^* A_2 + A \quad (8.50)$$

$$\frac{dA_2}{dt} = -\kappa_2 A_2 + \frac{i\chi^{(2)}\omega}{\varepsilon_0 n_2^2} f^* A_1^2 \quad (8.51)$$

We fix the arbitrary reference phase of  $A_1$  and  $A_2$  by requiring that  $A$  be real and positive.

Let us introduce dimensionless fields  $\mathcal{E}_p$  and  $\mathcal{E}$  through the definitions  $A_p = \alpha_p \mathcal{E}_p$ ,  $A = \alpha_1 \kappa_2 \mathcal{E}$ , and the parameters

$$\alpha_1 = \frac{\varepsilon_0 \kappa_2 n_1 n_2}{\chi^{(2)} \omega_1 f} \quad \alpha_2 = -i \frac{\varepsilon_0 \kappa_2 n_1^2 f^*}{\chi^{(2)} \omega_1 f^2} \quad \gamma = \kappa_1 / \kappa_2 \quad (8.52)$$

where  $\Phi = \psi$  for a ring cavity and  $\Phi = 0$  for a Fabry-Perot cavity. Therefore, the dynamical equations become

$$\frac{d\mathcal{E}_1}{d\tau} = -\gamma \mathcal{E}_1 + \mathcal{E}_1^* \mathcal{E}_2 + \mathcal{E} \quad (8.53)$$

$$\frac{d\mathcal{E}_2}{d\tau} = -\mathcal{E}_2 - \mathcal{E}_1^2 \quad (8.54)$$

and the reduced time is  $\tau = \kappa_2 t$ . In this way, we see that in both cases, the ring cavity with  $\psi \neq 0$  and the Fabry-Perot cavity with  $\psi = 0$ , the intrinsic dynamics of intracavity SHG expressed in terms of the dimensionless fields  $\mathcal{E}_1$ ,  $\mathcal{E}_2$  and  $\mathcal{E}$  is the same, the difference being only in the actual values of the physical fields  $A_1$ ,  $A_2$  and  $A$  for which special features occur. For instance, we shall see that an instability is reached for  $\mathcal{E}_{th} = 1$ . The nature and the

properties of this instability are the same in both cases, the difference being in the value of the driving field intensity  $|A_{th}|^2$ . If  $A_{th}$  is sufficiently large, we need not be worried by an instability since it will not hamper the stable steady regime of the device. However, if  $A_{th}$  is sufficiently small, the threshold may be reached and cause problems.

To simplify the discussion, we consider the limit of perfect conversion in which  $\gamma = 0$ . In other terms, the field at frequency  $\omega$  is trapped in the cavity and the outcoupling mirror is assumed to be perfectly reflecting at that frequency. Hence the dynamical equations for intracavity second harmonic (ISHG) reduce to

$$\frac{d\mathcal{E}_1}{d\tau} = \mathcal{E}_1^* \mathcal{E}_2 + \mathcal{E}, \quad \frac{d\mathcal{E}_2}{d\tau} = -\mathcal{E}_2 - \mathcal{E}_1^2 \quad (8.55)$$

The simplest solutions of these equations are the steady states. It directly follows from Eq. (8.55) that in steady state  $|\mathcal{E}_1|^2 \mathcal{E}_1 = \mathcal{E}$ . If we choose the arbitrary phase of  $A$  such that  $\mathcal{E}$  is real and positive, it follows that  $\mathcal{E}_1$  must also be real and positive. Hence, the steady state solutions are

$$\mathcal{E}_1 = \mathcal{E}^{1/3}, \quad \mathcal{E}_2 = -\mathcal{E}^{2/3} = \mathcal{E}^{2/3} e^{i\pi} \quad (8.56)$$

This result shows that the two fields  $\mathcal{E}_1$  and  $\mathcal{E}_2$  are dephased by half a period.

To test the stability of these solutions against fluctuations, we proceed in two steps. First, since the steady state solutions are real, we shall assume real perturbations, i.e., amplitude fluctuations with constant phases. This means that we seek solutions of equations (8.55) of the form  $\mathcal{E}_1 = \mathcal{E}^{1/3} + \eta e_1(\tau) + \mathcal{O}(\eta^2)$  and  $\mathcal{E}_2 = -\mathcal{E}^{2/3} + \eta e_2(\tau) + \mathcal{O}(\eta^2)$  with  $0 < \eta \ll 1$ . We introduce this solution into equations (8.55) and linearize them with respect to  $\eta$ . This leads to a pair of linear equations for the deviations  $e_1$  and  $e_2$  from steady state whose solutions are  $e_m(\tau) = c_{m,1} \exp(\lambda_1 \tau) + c_{m,2} \exp(\lambda_2 \tau)$  with the characteristic roots

$$\lambda_{1,2} = \frac{1}{2} \left( -1 - \mathcal{E}^{2/3} \pm \sqrt{\mathcal{E}^{4/3} - 10\mathcal{E}^{2/3} + 1} \right) \quad (8.57)$$

The function  $x^2 - 10x + 1$  is negative in the range  $[5 - \sqrt{24}, 5 + \sqrt{24}] \simeq [0.101, 9.899]$  and positive otherwise. Hence the two roots  $\lambda_{1,2}$  are real and negative for  $0 < \mathcal{E}^{2/3} < 5 - \sqrt{24}$  and  $5 + \sqrt{24} < \mathcal{E}^{2/3} < \infty$  while they are complex conjugates with negative real parts in the range  $5 - \sqrt{24} < \mathcal{E}^{2/3} < 5 + \sqrt{24}$ . Thus, the steady state (8.56) is always stable.

This result is in fact grossly incomplete because we have restricted the solutions to be real. If this restriction is relaxed, a new feature appears. Let

us introduce the general decomposition  $\mathcal{E}_1 = X + iU$  and  $\mathcal{E}_2 = Y + iV$ . The four components of the fields verify the equations

$$\begin{aligned} dX/d\tau &= XY + UV + \mathcal{E} \\ dY/d\tau &= -Y - X^2 + U^2 \\ dU/d\tau &= XV - UY \\ dV/d\tau &= -V - 2UX \end{aligned} \quad (8.58)$$

The steady state solutions are  $X = \mathcal{E}^{1/3}, Y = -\mathcal{E}^{2/3}, U = 0, V = 0$ . We seek time-dependent solutions of the form  $X(\tau) = \mathcal{E}^{1/3} + \eta x_1(\tau) + \mathcal{O}(\eta^2), Y = -\mathcal{E}^{2/3} + \eta y_1 + \mathcal{O}(\eta^2), U = \eta u_1 + \mathcal{O}(\eta^3), V = \eta v_1 + \mathcal{O}(\eta^3)$ . This leads to four linearized equations and therefore to four characteristic roots. Two of them are the roots  $\lambda_{1,2}$  already analyzed. These roots are associated with amplitude fluctuations. The two new roots are associated with phase fluctuations and are given by

$$\lambda_{3,4} = \frac{1}{2} \left( -1 + \mathcal{E}^{2/3} \pm \sqrt{1 + \mathcal{E}^{4/3} - 6\mathcal{E}^{2/3}} \right) \quad (8.59)$$

These roots have a behavior which is very different from  $\lambda_{1,2}$ :

- real and negative in the range  $0 < \mathcal{E} < (3 - 2\sqrt{2})^{3/2} \simeq 0.0711$ ;
- complex conjugates in the range  $(3 - 2\sqrt{2})^{3/2} < \mathcal{E} < (3 + 2\sqrt{2})^{3/2} \simeq 14.0711$ .
- real with opposite signs for  $\mathcal{E} > (3 + 2\sqrt{2})^{3/2}$ ;
- A special point is reached if  $\mathcal{E} = 1$  where  $\lambda_{3,4} = \pm i$  : for  $0 < \mathcal{E} < 1$ , the real part of the roots is negative while above the critical threshold  $\mathcal{E} = 1$  at least one of the real parts is positive.

Thus the point  $\mathcal{E} = 1$  is a critical point beyond which the steady state solutions are unstable. At the critical point, the solutions are  $Z(\tau) = \bar{Z} + \eta [z_1 \exp(\lambda_1 \tau) + z_2 \exp(-\lambda_2 \tau) + z_3 \exp(i\tau) + z_4 \exp(-i\tau)] + \mathcal{O}(\eta^2)$  where  $Z$  is any of the four variables  $X, Y, U, V$  and  $\bar{Z}$  is the steady state solution. Thus we have time-periodic solutions and the critical point  $\mathcal{E} = 1$  is a *Hopf bifurcation* also known as a selfpulsing threshold. The Hopf bifurcation is a critical point where a branch of periodic solutions emerges from a steady state. Beyond this bifurcation point, the field intensities are periodic in time (AM and FM self modulations). The difficulty is to assess the stability of this periodic solution.

It can be shown, analytically, that close but above this Hopf bifurcation, periodic solutions are stable. Numerically, it has been found that for  $\mathcal{E} > 1$ , the stable solutions are periodic solutions with a domain of bistability. This conclusion is not modified if  $\gamma \neq 0$ . However, if frequency detunings are allowed so that  $\omega_1 \neq \omega$  and  $\omega_2 \neq 2\omega$  where  $\omega$  is the driving field frequency, the whole spectrum of complex solutions may appear, including deterministic chaotic solutions.



# Chapter 9

## Sum & difference frequency generation

### 9.1 Sum frequency generation

#### 9.1.1 Formulation

Sum frequency generation is a natural generalization of SHG. In this process, two fields oscillating at frequencies  $\omega_1$  and  $\omega_2$  interact in the  $\chi^{(2)}$  medium to generate a field at the sum frequency  $\omega_3 = \omega_1 + \omega_2$ . This process is useful, for instance, to convert an infrared signal/image into the visible. The total field in the medium is  $E = \mathcal{E}_1 e^{-i\omega_1 t} + \mathcal{E}_2 e^{-i\omega_2 t} + \mathcal{E}_3 e^{-i\omega_3 t} + c.c.$  Hence the polarization induced by this field is

$$\begin{aligned} P &= \chi^{(2)} E^2 = \chi^{(2)} (\mathcal{E}_1^2 e^{-2i\omega_1 t} + \mathcal{E}_2^2 e^{-2i\omega_2 t} + \mathcal{E}_3^2 e^{-2i\omega_3 t} + c.c.) \\ &\quad + 2\chi^{(2)} (\mathcal{E}_1 \mathcal{E}_2 e^{-i(\omega_1 + \omega_2)t} + \mathcal{E}_3 \mathcal{E}_1^* e^{-i(\omega_3 - \omega_1)t} + \mathcal{E}_3 \mathcal{E}_2^* e^{-i(\omega_3 - \omega_2)t} + c.c.) \\ &\quad + 2\chi^{(2)} (\mathcal{E}_1 \mathcal{E}_2^* e^{-i(\omega_1 - \omega_2)t} + \mathcal{E}_3 \mathcal{E}_1 e^{-i(\omega_3 + \omega_1)t} + \mathcal{E}_3 \mathcal{E}_2 e^{-i(\omega_3 + \omega_2)t} + c.c.) \\ &\quad + 2\chi^{(2)} (|\mathcal{E}_1|^2 + |\mathcal{E}_2|^2 + |\mathcal{E}_3|^2) \end{aligned}$$

From this point on, we proceed exactly as in Chapter 8. Using the energy conservation law  $\omega_3 = \omega_1 + \omega_2$ , we derive evolution equations for the field components at  $\omega_n$  from Maxwell equation

$$\frac{\partial^2 E_m}{\partial z^2} - \frac{n_m^2}{c^2} \frac{\partial^2 E_m}{\partial t^2} = \frac{1}{\varepsilon_0 c^2} \frac{\partial^2}{\partial t^2} P(\omega_m) \quad (9.1)$$

with  $P(\omega_1) = 2\chi^{(2)} (\mathcal{E}_2^* \mathcal{E}_3 e^{-i\omega_1 t} + c.c.)$ ,  $P(\omega_2) = 2\chi^{(2)} (\mathcal{E}_1^* \mathcal{E}_3 e^{-i\omega_2 t} + c.c.)$ , and  $P(\omega_3) = 2\chi^{(2)} (\mathcal{E}_1 \mathcal{E}_2 e^{-i\omega_3 t} + c.c.)$  as the source for the electromagnetic field oscillating at the frequency  $\omega_m$ . The other contributions to the atomic polarization will give a negligible contribution because they oscillate at a much

higher frequency. This is yet another form of the rotating wave approximation introduced in Chapter 1.

Defining slowly varying complex amplitudes  $E_m = A_m \exp(ik_m z - i\omega_m t)$ , we arrive at the set of coupled equations

$$\frac{\partial A_1}{\partial z} + \frac{n_1}{c} \frac{\partial A_1}{\partial t} = \frac{i\omega_1 \chi^{(2)}}{\varepsilon_0 c n_1} A_2^* A_3 e^{iz\Delta k} \quad (9.2)$$

$$\frac{\partial A_2}{\partial z} + \frac{n_2}{c} \frac{\partial A_2}{\partial t} = \frac{i\omega_2 \chi^{(2)}}{\varepsilon_0 c n_2} A_1^* A_3 e^{iz\Delta k} \quad (9.3)$$

$$\frac{\partial A_3}{\partial z} + \frac{n_3}{c} \frac{\partial A_3}{\partial t} = \frac{i\omega_3 \chi^{(2)}}{\varepsilon_0 c n_3} A_1 A_2 e^{-iz\Delta k} \quad (9.4)$$

with  $\Delta k = k_3 - k_2 - k_1$ .

## 9.1.2 Free running SFG

### Invariants of the motion

In the free running case, we may set  $\partial A_m / \partial t = 0$ , as done in Chapter 8, leading to the simpler equations

$$\frac{dA_1}{dz} = \frac{i\omega_1 \chi^{(2)}}{\varepsilon_0 c n_1} A_2^* A_3 e^{iz\Delta k} \quad (9.5)$$

$$\frac{dA_2}{dz} = \frac{i\omega_2 \chi^{(2)}}{\varepsilon_0 c n_2} A_1^* A_3 e^{iz\Delta k} \quad (9.6)$$

$$\frac{dA_3}{dz} = \frac{i\omega_3 \chi^{(2)}}{\varepsilon_0 c n_3} A_1 A_2 e^{-iz\Delta k} \quad (9.7)$$

From these equations we obtain

$$n_1 \frac{d|A_1|^2}{dz} = \omega_1 \varphi, \quad n_2 \frac{d|A_2|^2}{dz} = \omega_2 \varphi, \quad n_3 \frac{d|A_3|^2}{dz} = -\omega_3 \varphi \quad (9.8)$$

and

$$\varphi = i \frac{\chi^{(2)}}{\varepsilon_0 c} (A_1^* A_2^* A_3 e^{iz\Delta k} - A_1 A_2 A_3^* e^{-iz\Delta k}) \quad (9.9)$$

Using the energy conservation law  $\omega_3 = \omega_1 + \omega_2$  leads to a first invariant

$$J \equiv n_1 |A_1|^2 + n_2 |A_2|^2 + n_3 |A_3|^2, \quad \frac{dJ}{dz} = 0 \quad (9.10)$$

However, it is also interesting to use equations (9.8) to build three new invariants

$$J_1 = \frac{n_1}{\omega_1} |A_1|^2 - \frac{n_2}{\omega_2} |A_2|^2, \quad \frac{dJ_1}{dz} = 0 \quad (9.11)$$

$$J_2 = \frac{n_2}{\omega_2} |A_2|^2 + \frac{n_3}{\omega_3} |A_3|^2, \quad \frac{dJ_2}{dz} = 0 \quad (9.12)$$

$$J_3 = \frac{n_3}{\omega_3} |A_3|^2 + \frac{n_1}{\omega_1} |A_1|^2, \quad \frac{dJ_3}{dz} = 0 \quad (9.13)$$

The existence of the invariant  $J$  suggests that we introduce the new variables

$$A_m = \sqrt{J \frac{\omega_m}{n_m}} \rho_m e^{i\phi_m} \quad (9.14)$$

in terms of which the dynamical equations for the field amplitudes are

$$\frac{d\rho_1}{d\zeta} = -\rho_2\rho_3 \sin \theta \quad (9.15)$$

$$\frac{d\rho_2}{d\zeta} = -\rho_3\rho_1 \sin \theta \quad (9.16)$$

$$\frac{d\rho_3}{d\zeta} = \rho_1\rho_2 \sin \theta \quad (9.17)$$

with the reduced variable:

$$\zeta = \frac{\chi^{(2)}}{\varepsilon_0 c} \sqrt{J \frac{\omega_1 \omega_2 \omega_3}{n_1 n_2 n_3}} z \quad (9.18)$$

and the phase variable  $\theta$  defined by

$$\theta = \phi_3 - \phi_1 - \phi_2 + z\Delta k$$

Note that although this change of variables is convenient to integrate the equations, the variables  $\rho$  and  $\zeta$  are not dimensionless! The invariance properties of the  $J_m$  defined in (9.11)-(9.13) imply the invariance of the three combinations

$$\rho_1^2 - \rho_2^2 = J_1/J, \quad \rho_1^2 + \rho_3^2 = J_3/J, \quad \rho_2^2 + \rho_3^2 = J_2/J \quad (9.19)$$

The phase  $\theta$  verifies the equation

$$\frac{d\theta}{d\zeta} = \ell\Delta k + \left( \frac{\rho_1\rho_2}{\rho_3} - \frac{\rho_1\rho_3}{\rho_2} - \frac{\rho_3\rho_2}{\rho_1} \right) \cos \theta \quad (9.20)$$

It is easy to verify that this equation can be written as  $d\theta/d\zeta = \ell\Delta k + (\cot\theta) d\ln(\rho_1\rho_2\rho_3)/d\zeta$ . If  $\Delta k = 0$ , this equation is easily integrated to give  $\rho_1\rho_2\rho_3 \cos\theta = G$ . The function  $G$  is a constant if there is perfect phase matching  $\Delta k = 0$ . Otherwise, it is no problem to verify that  $dG/d\zeta = -\rho_1\rho_2\rho_3\ell\Delta k \sin\theta = (\ell\Delta k/2) d\rho_1^2/d\zeta$  so that the general expression for the second invariant is

$$H = \rho_1\rho_2\rho_3 \cos\theta - \frac{\ell\Delta k}{2}\rho_1^2 \quad (9.21)$$

Using this result to express  $\sin\theta$  as a function of the three field amplitudes leads to

$$\frac{d\rho_1^2}{d\zeta} = \frac{d\rho_2^2}{d\zeta} = -\frac{d\rho_3^2}{d\zeta} = \pm 2\sqrt{\rho_1^2\rho_2^2\rho_3^2 - \left(H + \frac{\ell\Delta k}{2}\rho_1^2\right)^2} \quad (9.22)$$

Finally, using the invariants (9.19) we arrive at a closed equation for  $\rho_1^2$

$$\frac{d\rho_1^2}{d\zeta} = \pm 2\sqrt{\rho_1^2(\rho_1^2 - J_1/J)(J_3/J - \rho_1^2) - \left(H + \frac{\ell\Delta k}{2}\rho_1^2\right)^2} \quad (9.23)$$

which is a standard elliptic differential equation. This establishes again that the field amplitudes  $\rho_m$  are periodic in space.

To gain further insight into this problem, we continue this analysis of SFG by considering a number of limiting situations. In the subsections that follow, we consider perfect phase matching

$$\Delta k = 0, \quad \theta = \pm\pi/2, \quad \rho_3(0) = 0 \quad (9.24)$$

so that  $G = H = 0$ .

### Up-frequency conversion of a weak signal

We consider a situation in which a weak signal at frequency  $\omega_2$  is transformed into a signal at frequency  $\omega_3$  by interaction with a strong field at frequency  $\omega_1$ . The signal can be, for instance, an infrared image which is to be converted into a visible image. An equation for  $\rho_3$  is easily derived

$$\frac{d^2\rho_3}{d\zeta^2} + (\rho_1^2 + \rho_2^2)\rho_3 = 0 \quad (9.25)$$

In the limit of a strong field at  $\omega_1$  and a weak field at  $\omega_2$ , we can introduce the approximations  $\rho_1^2(\zeta) + \rho_2^2(\zeta) \simeq \rho_1^2(\zeta) \simeq \rho_1^2(0)$  in addition to the condition  $\rho_3(0) = 0$ . Hence the solution of (9.25) is  $\rho_3(\zeta) = A \sin[\zeta\rho_1(0)]$ . Using (9.17)

at  $\zeta = 0$  determines the constant  $A = \rho_2(0) \sin \theta = \pm \rho_2(0)$  and leads to the solution

$$\rho_3^2(\zeta) = \rho_2^2(0) \sin^2 [\zeta \rho_1(0)] \quad (9.26)$$

The invariance of  $\rho_2^2(\zeta) + \rho_3^2(\zeta)$  yields  $\rho_2^2(\zeta) = \rho_2^2(0) - \rho_3^2(\zeta)$  and therefore

$$\rho_2^2(\zeta) = \rho_2^2(0) \cos^2 [\zeta \rho_1(0)] \quad (9.27)$$

while

$$\rho_1(\zeta) = \rho_1(0) \quad (9.28)$$

This solution describes a periodic transfer of energy from frequency  $\omega_2$  to frequency  $\omega_3$  as shown in figure 9.1.

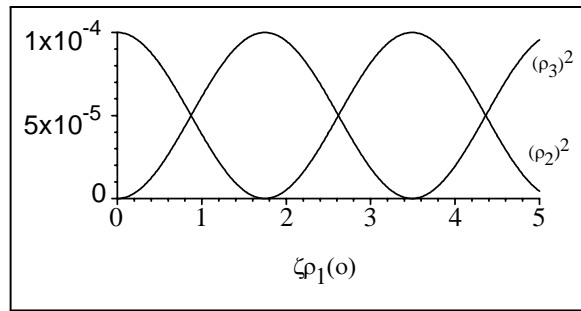


Figure 9.1: Up-conversion of a weak signal from frequency  $\omega_2$  to frequency  $\omega_3$  in the presence of a strong field at  $\omega_1$  by means of sum-frequency generation. Eqs. (9.26) and (9.27) are used with  $\rho_2(0) = 0.01$  and  $\rho_1 = 0.9$ .

As usual in this class of problems, this means that there is an optimum crystal length  $\ell$  for maximum conversion. As in the SHG case, the periodicity of the energy transfer is controlled, among other factors, by the input field at  $\omega_1$ . This is quite a convenient way to tune the effective length of the medium.

### Identical field amplitudes

Another special case arises if the normalized field amplitudes of the two input fields are equal:  $\rho_1(0) = \rho_2(0) \neq 0$ . These equalities lead to

$$\frac{d\rho_1}{d\zeta} = -\rho_1\rho_3, \quad \frac{d\rho_3}{d\zeta} = \rho_1^2 \quad (9.29)$$

which are the equations (8.30) derived in SHG. The solution of these equations is

$$\rho_1^2(\zeta) = \rho_2^2(\zeta) = \rho_1^2(0) \operatorname{sech}^2 [\zeta \rho_1(0)] \quad (9.30)$$

$$\rho_3^2(\zeta) = \rho_1^2(0) \tanh^2[\zeta \rho_1(0)] \quad (9.31)$$

As in the special case of SHG with perfect matching and  $G = 0$ , we find a solution which is not periodic: the transfer of energy from the input fields at frequencies  $\omega_1$  and  $\omega_2$  to the output field at  $\omega_3$  increases with the medium length.

### Weak conversion limit

Finally, in the weak conversion limit,  $\rho_1(\zeta) \simeq \rho_1(0)$  and  $\rho_2(\zeta) \simeq \rho_2(0)$ , a direct integration of Eq. (9.7) leads to a variation of the intensity  $|A_3|^2$  at  $\omega_3$  which is similar to the  $\text{sinc}^2$  law derived in (8.41).

## 9.2 Difference frequency generation

Let us now study the process of difference frequency generation. Usually, the expression *difference frequency generation* (DFG) is reserved to the situation in which two monochromatic input fields interact in a  $\chi^{(2)}$  medium to generate a field oscillating at the difference between the two input field frequencies, while *parametric amplification* is reserved to describe processes in which a single monochromatic input field is sent into the  $\chi^{(2)}$  medium and two monochromatic fields are generated with frequencies  $(\omega_1, \omega_2)$  and wave vectors  $(\mathbf{k}_1, \mathbf{k}_2)$  verifying the conservation law  $\omega_{input} = \omega_1 + \omega_2$  and  $\mathbf{k}_{input} \simeq \mathbf{k}_1 + \mathbf{k}_2$ . Both configurations are displayed in figure 9.2.

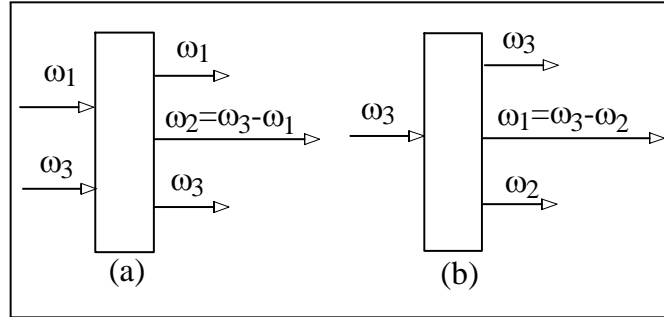


Figure 9.2: Standard configuration for (a) difference frequency generation. and (b) parametric amplification.

The notation used in this chapter and in the figure 9.2 is such that we can still use equations (9.2)-(9.4). Formally, the equations describing DFG and OPA (optical parametric amplification) are similar to the sum frequency

generation equations, the obvious difference being in the initial condition. This is completely true for propagation in bulk materials. However, if the nonlinear medium is placed in a resonant cavity, the resulting problem is substantially different from its SFG counterpart. The reason is linked to the fact that intracavity SHG is a thresholdless process whereas the intracavity DFG and OPA have a lasing threshold.

In this section, we focus on three-wave mixing processes with two input fields and three output fields, such that the new field oscillates at the difference between the two input field frequencies. To formulate this problem, we use the equations (9.5)-(9.7) to describe free running sum frequency generation

$$\frac{dA_1}{dz} = \frac{i\omega_1\chi^{(2)}}{\varepsilon_0cn_1}A_2^*A_3e^{iz\Delta k} \quad (9.32)$$

$$\frac{dA_2}{dz} = \frac{i\omega_2\chi^{(2)}}{\varepsilon_0cn_2}A_1^*A_3e^{iz\Delta k} \quad (9.33)$$

$$\frac{dA_3}{dz} = \frac{i\omega_3\chi^{(2)}}{\varepsilon_0cn_3}A_1A_2e^{-iz\Delta k} \quad (9.34)$$

with  $\omega_1 + \omega_2 = \omega_3$  and  $\Delta k = k_3 - k_2 - k_1$ . The input fields are  $A_1$  and  $A_3$ .

### 9.2.1 Two intense input fields

If both input fields are intense and depletion by transfer of energy to the field  $A_2$  created at the difference frequency can be neglected in first approximation, the process is described in first approximation by equation (9.33) with  $A_1$  and  $A_3$  constant:

$$\frac{dA_1}{dz} = 0, \quad \frac{dA_3}{dz} = 0, \quad (9.35)$$

$$\frac{dA_2}{dz} = \frac{i\omega_2\chi^{(2)}}{\varepsilon_0cn_2}A_1^*A_3e^{iz\Delta k} \quad (9.36)$$

Integration over  $z$  leads to

$$A_2(z) = \frac{\omega_2\chi^{(2)}}{\varepsilon_0cn_2}A_1^*A_3\frac{e^{iz\Delta k} - 1}{\Delta k} \quad (9.37)$$

and therefore

$$\begin{aligned} |A_2(L)|^2 &= \left(\frac{L\omega_2\chi^{(2)}}{\varepsilon_0cn_2}\right)^2 |A_3|^2 |A_1|^2 \text{sinc}^2(L\Delta k/2) \\ &= [\max |A_2(L)|^2] \text{sinc}^2(L\Delta k/2) \end{aligned} \quad (9.38)$$

This result shows a rather general property of DFG: the conversion efficiency increases with the frequency of the generated field. Thus conversion in the infrared is less favorable than conversion in the visible. Another point which is made clear by this result is the trade-off between crystal length and phase-matching. One way to increase field conversion is to use a longer crystal since  $|A_2(L)|^2$  increases with the square of the crystal length  $L$ . However, the product  $L\Delta k$  must also remain close to 0, which means that the longer the crystal, the smaller  $\Delta k$  must be. In practical devices, it is the phase matching condition which limits the crystal length.

### 9.2.2 One intense input field

More often, only one input field is intense and can be treated as a constant. The second input field serves as a "catalyst" to induce the required frequency  $\omega_2$ . Let  $\omega_3$  be the frequency of the intense field and  $\omega_1$  the frequency of the weak input field. This situation is described by the set of coupled linear equations

$$\frac{dA_1}{dz} = \frac{i\omega_1\chi^{(2)}}{\varepsilon_0cn_1}A_2^*A_3e^{iz\Delta k} \quad (9.39)$$

$$\frac{dA_2^*}{dz} = -\frac{i\omega_2\chi^{(2)}}{\varepsilon_0cn_2}A_1A_3^*e^{-iz\Delta k} \quad (9.40)$$

with  $A_3$  constant. Defining  $A_p = \mathcal{A}_pe^{iz\Delta k/2}$  leads to

$$\frac{d\mathcal{A}_1}{dz} = -i\frac{\Delta k}{2}\mathcal{A}_1 + iK_1\mathcal{A}_2^*\mathcal{A}_3 \quad (9.41)$$

$$\frac{d\mathcal{A}_2^*}{dz} = i\frac{\Delta k}{2}\mathcal{A}_2^* - iK_2\mathcal{A}_1\mathcal{A}_3^* \quad (9.42)$$

with

$$K_p = \frac{\omega_p\chi^{(2)}}{\varepsilon_0cn_p} \quad (9.43)$$

A simple way to solve equations (9.41)-(9.42) is to derive each of them with respect to  $z$ :

$$\frac{d^2\mathcal{A}_p}{dz^2} - K^2\mathcal{A}_p = 0 \quad (9.44)$$

for  $p = 1, 2$  and

$$K = \sqrt{K_1K_2|A_3|^2 - (\Delta k/2)^2} \quad (9.45)$$

We see clearly that if  $K$  is real,  $K^2 > 0$  and the fundamental solutions of Eq. (9.44) are the functions  $\exp(\pm Kz)$ , leading to the possibility of amplification

since  $\exp(Kz)$  is unbounded. If  $K$  is imaginary,  $K^2 < 0$  and the fundamental solutions of Eq. (9.44) are the bounded periodic functions  $\exp(\pm i|K|z)$  which cannot lead to amplification.

In the limit of intense pump field  $A_3$  which is defined more precisely by the inequality  $K_1 K_2 |A_3|^2 \gg (\Delta k/2)^2$ , the parameter  $K$  is real and can be interpreted as a gain per unit length. Therefore the solutions are of the form  $\mathcal{A}_1(z) = a_1 \exp(Kz) + a_2 \exp(-Kz)$  and  $\mathcal{A}_2(z) = b_1 \exp(Kz) + b_2 \exp(-Kz)$ . The boundary conditions for DFG are  $\mathcal{A}_1(0) = \mathcal{A}_1$  and  $\mathcal{A}_2(0) = 0$ , which imply from (9.41)-(9.42)  $d\mathcal{A}_1/dz|_{z=0} = -i(\Delta k/2)\mathcal{A}_1$  and  $d\mathcal{A}_2/dz|_{z=0} = -iK_2 A_3^* \mathcal{A}_1$ . Hence the solution of equations (9.41)-(9.42) is

$$\begin{aligned} \mathcal{A}_1(z) &= \frac{\mathcal{A}_1}{2} \left[ \left(1 - i\frac{\Delta k}{2K}\right) e^{Kz} + \left(1 + i\frac{\Delta k}{2K}\right) e^{-Kz} \right] \\ &= \mathcal{A}_1 \left[ \cosh(Kz) - i\frac{\Delta k}{2K} \sinh(Kz) \right] \end{aligned} \quad (9.46)$$

$$\mathcal{A}_2(z) = \frac{iK_2 A_3^* \mathcal{A}_1}{K} \sinh(Kz) \quad (9.47)$$

In terms of field intensities, we have

$$|A_1(z)|^2 = |A_1|^2 \left[ \cosh^2(Kz) + \left(\frac{\Delta k}{2K}\right)^2 \sinh^2(Kz) \right] \quad (9.48)$$

$$|A_2(z)|^2 = \left(\frac{K_2}{K}\right)^2 |A_3|^2 |A_1|^2 \sinh^2(Kz) \quad (9.49)$$

In the large  $z$  limit, that is for  $Kz \gg 1$ , we have the result

$$\frac{|A_1(z)|^2}{|A_1(0)|^2} = \left[ 1 + \left(\frac{\Delta k}{2K}\right)^2 \right] \frac{e^{2Kz}}{4} \quad (9.50)$$

$$|A_2(z)|^2 = \left(\frac{K_2}{K}\right)^2 |A_3|^2 |A_1|^2 \frac{e^{2Kz}}{4} \quad (9.51)$$

so that  $2K$  is a fair measure of the intensity gain. Note that in the limit  $Kz \gg 1$ , both fields  $A_1(z)$  and  $A_2(z)$  grow exponentially and at the same rate. For  $\text{LiNbO}_4$  we have  $\chi^{(2)}/\varepsilon_0 = 2.7 \times 10^{-8} \text{esu}$  and  $n_1 \simeq n_2 = 2.23$  at  $\lambda_1 \simeq \lambda_2 = 1.06 \times 10^{-6} \text{m}$ . Hence for our usual choice of the strong field  $|A_3| = 10^2 \text{esu}$ , the maximum gain (i.e., for exact phase matching) is  $K = 1.14 \text{cm}^{-1}$  which is quite poor.

It is quite easy to assess the influence of phase matching in the case of an intense and a weak input fields. If  $(\Delta k)^2 > 4K_1 K_2 |A_3|^2$ , we define the real characteristic wave number

$$k_c = [(\Delta k/2)^2 - K_1 K_2 |A_3|^2]^{-1/2} \quad (9.52)$$

in terms of which the solution (9.48) and (9.49) becomes

$$A_1(z) = A_1 \left[ \cos(k_c z) - \frac{i\Delta k}{2k_c} \sin(k_c z) \right] \quad (9.53)$$

$$A_2(z) = \frac{K_2}{k_c} A_3^* A_1 \sin(k_c z) \quad (9.54)$$

In these expressions, amplification is absent and replaced by a periodic and bounded variation of the fields as a function of the propagation distance.

# Chapter 10

## Optical parametric oscillator

### 10.1 Formulation

We have seen in the previous chapter that the yield of parametric conversion is fairly small in free space. Still, it is worth trying to improve the operating conditions because this process is potentially a versatile source of tunable radiation in the infrared. Therefore much development has taken place to improve the situation and today the optical parametric oscillator (OPO) is the most widely tunable laser source used in the IR.

The typical setup consists of a resonant cavity pumped by the field  $\mathcal{E}_3$ . The  $\chi^{(2)}$  medium is in the cavity and generates the two fields  $\mathcal{E}_1$  and  $\mathcal{E}_2$  whose frequencies add up to the frequency of the input field. We assume that the fields interact in a resonant cavity so that the basic modes are either running waves  $u_p = \sqrt{1/L}e^{ik_p z}$  or standing waves  $u_p = \sqrt{2/L}\sin(k_p z)$ . The main assumption is that each of the three fields can be associated with one – and only one – cavity mode. The basic evolution equations (8.2) derived in Chapter 8 become

$$u_1 \frac{dA_1}{dt} = \frac{i\omega_1 \chi^{(2)}}{\varepsilon_0 n_1^2} u_2^* u_3 A_2^* A_3 - \gamma_1 u_1 A_1 \quad (10.1)$$

$$u_2 \frac{dA_2}{dt} = \frac{i\omega_2 \chi^{(2)}}{\varepsilon_0 n_2^2} u_1^* u_3 A_1^* A_3 - \gamma_2 u_2 A_2 \quad (10.2)$$

$$u_3 \frac{dA_3}{dt} = \frac{i\omega_3 \chi^{(2)}}{\varepsilon_0 n_3^2} u_1 u_2 A_1 A_2 - \gamma_3 u_3 (A_3 - A) \quad (10.3)$$

and  $\int_0^L u_p^* u_q dz = \delta_{pq}$ . For running waves, these equations could also be derived from Eqs. (9.2)-(9.4), apart from the damping and pumping terms which are anyway added phenomenologically. We have added to each equation a damping term  $-\gamma_p u_p A_p$  to account for the cavity losses suffered by

each field. In addition, the equation for  $A_3$  contains a source term to account for the external pumping: in the absence of a nonlinear medium, the cavity field at  $\omega_3$  becomes in the long time limit  $A_3 = A$ . These equations already contain a simplifying assumption since there is no trace of the optical frequency: the assumption is that the driving field frequency  $\omega_e$  and the cavity field frequency  $\omega_3$  are sufficiently close that their difference can be neglected. We multiply the equation for  $A_p$  by  $u_p^*$  and integrate over the cavity length to obtain

$$\frac{dA_1}{dt} = \frac{i\omega_1\chi^{(2)}}{\varepsilon_0 n_1^2} f A_2^* A_3 - \gamma_1 A_1 \quad (10.4)$$

$$\frac{dA_2}{dt} = \frac{i\omega_2\chi^{(2)}}{\varepsilon_0 n_2^2} f A_1^* A_3 - \gamma_2 A_2 \quad (10.5)$$

$$\frac{dA_3}{dt} = \frac{i\omega_3\chi^{(2)}}{\varepsilon_0 n_3^2} f^* A_1 A_2 - \gamma_3 (A_3 - A) \quad (10.6)$$

where

$$f = \int_0^L u_1^* u_2^* u_3 dz \equiv \varphi e^{i\phi} \quad (10.7)$$

## 10.2 Threshold condition

Let us first perform a change of variables. Defining

$$\phi_p = \frac{\omega_p}{\gamma_p n_p^2} \frac{\chi^{(2)}}{\varepsilon_0} \varphi \quad (10.8)$$

we introduce the change of variables

$$A_1 = -\frac{ie^{i\phi} E_1}{\sqrt{\phi_2 \phi_3}}, \quad A_2 = \frac{E_2}{\sqrt{\phi_1 \phi_3}} \quad (10.9)$$

$$A_3 = -\frac{E_3}{\sqrt{\phi_1 \phi_2}}, \quad A = -\frac{E}{\sqrt{\phi_1 \phi_2}} \quad (10.10)$$

which leads to the evolution equations

$$\frac{dE_1}{dt} = \gamma_1 (-E_1 + E_2^* E_3) \quad (10.11)$$

$$\frac{dE_2}{dt} = \gamma_2 (-E_2 + E_1^* E_3) \quad (10.12)$$

$$\frac{dE_3}{dt} = \gamma_3 (-E_3 - E_1 E_2 + E) \quad (10.13)$$

This result simply means that once the right scaling of the fields is introduced, the intrinsic nonlinear dynamics of the optical system is the same for any cavity provided the assumption that each lasing mode is a cavity eigenmode is correct. What changes is the expression of the threshold at which the new fields appear.

In steady state, these equations lead to  $E = E_3 (1 + |E_1|^2) = E_3 (1 + |E_2|^2)$ . Therefore

$$|E_1|^2 = |E_2|^2 \quad (10.14)$$

and  $E_3$  is real since  $E$  is real. There are two steady state solutions to these equations: the one-field solution

$$E_1 = E_2 = 0, \quad E_3 = E \quad (10.15)$$

and the three-field solution  $E_1 = E_2^* E_3$  and  $E_2 = E_1^* E_3$  which implies  $E_1 = E_2^* E_3 = E_2^* E_3^{-1}$  so that

$$|E_1|^2 = |E_2|^2 = E - 1, \quad E_3 = 1 \quad (10.16)$$

The important fact to notice is the occurrence of a threshold  $E = E_{th}$  with

$$E_{th} = 1 \quad (10.17)$$

which means  $|A_{th}|^2 = (\phi_1 \phi_2)^{-1}$  for the driving field and such that:

- below threshold, there is no intracavity parametric process and the driving field is simply reduced linearly by the finite reflectivity of the mirrors;
- above threshold, the field amplitude at the driving frequency  $\omega_3$  remains constant while two fields are generated by parametric amplification and grow with the driving field amplitude.

This is completely different from the thresholdless operation of intracavity SHG.

### 10.3 Degenerate OPO

A particular configuration can be realized in which  $\omega_1 = \omega_2 = \omega_3/2$ . In this case, the problem is referred to as the degenerate optical parametric oscillator (DOPO) and it is described by the two coupled equations

$$\frac{dE_1}{dt} = \gamma_1 (-E_1 + E_1^* E_3) \quad (10.18)$$

$$\frac{dE_3}{dt} = \gamma_3 (-E_3 - E_1^2 + E) \quad (10.19)$$

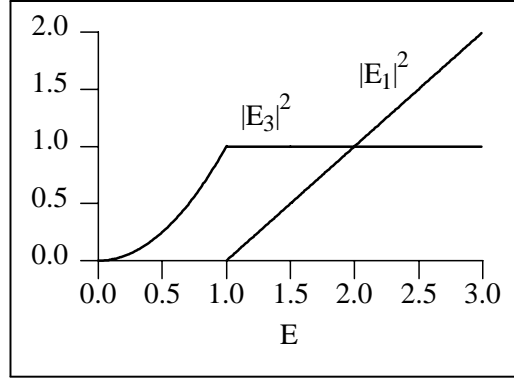


Figure 10.1: Steady state solutions of Eqs. (10.11)-(10.13).

These equations are very similar to Eqs. (8.53)-(8.54) of ISHG studied in chapter 7, except for the driving field: in ISHG, the driving field oscillates at  $\omega_1$  (in the notations of this chapter) and generates the field at  $\omega_3 = 2\omega_1$  while in the DOPO it is the driving field at  $\omega_3$  that generates the field at  $\omega_1 = \omega_3/2$ . This model can easily be generalized to include both driving fields and produces an interesting phase diagram with a tricritical point.

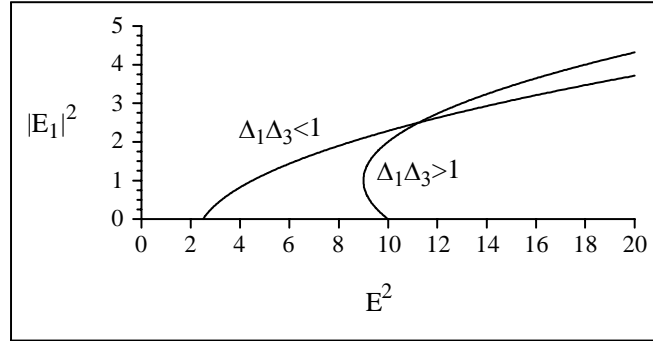


Figure 10.2: Intensity  $|E_1|^2$  as a function of the driving field intensity  $E^2$  for  $\Delta_1 = 1$ ,  $\Delta_3 = 1/2$  and 2 in the case of a DOPO.

Let us use the simplified model of the DOPO to assess the influence of detuning. If the driving field is not oscillating exactly at a resonance frequency of the cavity, we have to generalize equations (10.18) and (10.19) as follows

$$\frac{dE_1}{dt} = \gamma_1 [-(1 + i\Delta_1) E_1 + E_1^* E_3] \quad (10.20)$$

$$\frac{dE_3}{dt} = \gamma_3 [-(1 + i\Delta_3) E_3 - E_1^2 + E] \quad (10.21)$$

where

$$\Delta_1 = (\omega_1 - \omega_e/2)/\gamma_1, \quad \Delta_3 = (\omega_3 - \omega_e)/\gamma_3 \quad (10.22)$$

The frequency of the driving field is  $\omega_e$  while  $\omega_3$  and  $\omega_1$  are the cavity frequencies closest to  $\omega_e$  and  $\omega_e/2$ , respectively. Again, there are two possible steady state solutions, namely the one-field solution

$$E_1 = 0, \quad |E_3|^2 = \frac{E^2}{1 + \Delta_3^2} \quad (10.23)$$

and the two-field solutions

$$|E_3|^2 = 1 + \Delta_1^2 \quad (10.24)$$

$$0 = |E_1|^4 + 2|E_1|^2(1 - \Delta_1\Delta_3) - E^2 + (1 + \Delta_1^2)(1 + \Delta_3^2) \quad (10.25)$$

The solutions of (10.25) are

$$|E_1|^2 = \Delta_1\Delta_3 - 1 \pm \sqrt{E^2 - (\Delta_1 + \Delta_3)^2} \quad (10.26)$$

The threshold which separates the one-field and two-field solutions is

$$E_{th} = \sqrt{(1 + \Delta_1^2)(1 + \Delta_3^2)} = |\Delta_1 + \Delta_3| \quad (10.27)$$

$$1 = \Delta_1\Delta_3 \quad (10.28)$$

We notice first that the detuning increases the threshold field, which means that it acts as an additional loss.

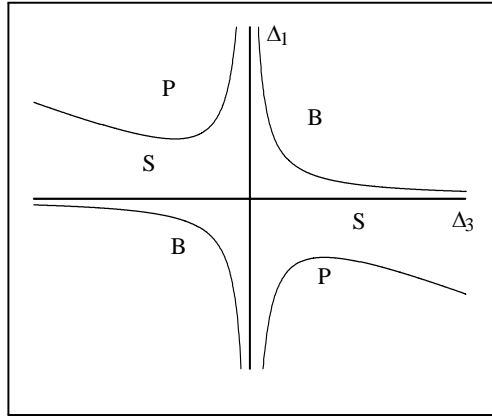


Figure 10.3: Stability boundaries for the detuned DOPO. The finite intensity steady state solution is stable in domain  $S$ , bistable in domain  $B$ , and unstable via a Hopf bifurcation in domain  $P$ . The boundary between  $S$  and  $B$  is  $\Delta_1\Delta_3 = 1$ . The boundary between  $S$  and  $P$  is  $\Delta_3(\gamma\Delta_3 + 2\Delta_1) = -\gamma - 2$ .

This is only a quantitative modification. Much more important is the qualitative change induced by the detunings on the nature and stability of the solutions above threshold:

- If  $E > E_{th}$ , the quadratic equation (10.25) for  $|E_1|^2$  has one real root if  $\Delta_1\Delta_3 < 1$  and two real roots if  $\Delta_1\Delta_3 > 1$ . Thus if both detunings have the same sign and their product is larger than unity, there is a domain of bistability. Figure 10.2 displays the two types of steady solutions.
- A linear stability analysis shows that in the monostable regime ( $\Delta_1\Delta_3 < 1$ ), there can be a Hopf or selfpulsing instability of the steady state at a finite distance from the threshold. Out of this selfpulsing instability, a branch of periodic solution emerges, whose stability is subjected to further constraints on the detunings. The existence condition for the Hopf bifurcation is

$$\Delta_3(\gamma\Delta_3 + 2\Delta_1) < -(\gamma + 2) \quad (10.29)$$

and the field intensity at the Hopf bifurcation is

$$|E_{1,H}|^2 = -\frac{\gamma^2(1 + \Delta_3^2)[\gamma^2\Delta_3^2 + (\gamma + 2)^2]}{2(\gamma + 1)^2(\gamma\Delta_3^2 + 2\Delta_3\Delta_1 + \gamma + 2)} \quad (10.30)$$

where  $\gamma = \gamma_3/\gamma_1$ . At that point, the two fields begin to oscillate with the frequency

$$\Omega_H^2 = \gamma_1^2 \left( 2|E_{1,H}|^2 + \gamma^2 \frac{1 + \Delta_3^2}{1 + \gamma} \right) \quad (10.31)$$

This discussion is summarized in figure 10.3 which shows how the inclusion of simple physical parameters may lead to a wealth of new features in the output fields.

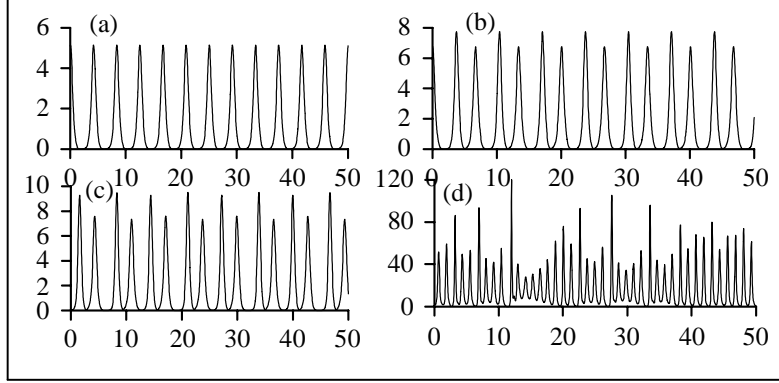


Figure 10.4: Intensity  $|E_1|^2$  of the subharmonic field as a function of the scaled time  $\tau = \gamma_1 t$  obtained by numerical simulation of the DOPO equations (10.20)-(10.21) for  $\gamma = 1$ ,  $\Delta_1 = 1$  and  $\Delta_3 = -3$ . (a)  $E = 6$ : period-1 solution; (b)  $E = 6.5$ : period-2 solution ; (c)  $E = 6.8$ : period-4 solution; (d)  $E = 20$ : chaotic solution.

In figure 10.4 we display periodic and chaotic solutions of the DOPO equations (10.20)-(10.21).

## 10.4 Ring and Fabry-Perot cavities

Using the ring cavity running wave eigenfunctions  $u_p = \sqrt{1/L} \exp(ik_p z)$  leads to

$$f = \frac{1}{\sqrt{L}} e^{iL\Delta k/2} \text{sinc}(L\Delta k/2) \quad (10.32)$$

The relation  $|A_{th}|^2 = (\phi_1 \phi_2)^{-1} \sim [\text{sinc}(L\Delta k/2)]^{-2}$  indicates that a good control of the phase matching is essential to build a ring cavity device which has a threshold power as low as possible.

With standing wave as cavity modes  $u_p(z) = \sqrt{2/L} \sin(k_p z)$ , the function  $f$  is

$$\begin{aligned} f &= \left(\frac{2}{L}\right)^{3/2} \frac{1}{(2i)^3} \int_0^L (e^{ik_1 z} - e^{-ik_1 z}) (e^{ik_2 z} - e^{-ik_2 z}) (e^{ik_3 z} - e^{-ik_3 z}) dz \\ &\simeq \left(\frac{2}{L}\right)^{3/2} \frac{1}{(2i)^3} \int_0^L (e^{iz\Delta k} - e^{-iz\Delta k}) dz \\ &\simeq -\frac{\Delta k}{2} \sqrt{\frac{L}{2}} \text{sinc}^2(L\Delta k/2) \end{aligned} \quad (10.33)$$

In deriving this result, we have neglected terms oscillating fast in space, typically with wave numbers  $k_1 \pm k_2 \pm k_3 \neq \Delta k$ , compared with the two terms oscillating at  $\Delta k$ . This configuration is known as triply resonant since all three modes are close to a cavity eigenmode.

For the ring laser we have

$$|A_{th}|^2 = \left( \frac{\varepsilon_0}{\chi^{(2)}} \right)^2 \frac{n_1^2 \gamma_1}{\omega_1} \frac{n_2^2 \gamma_2}{\omega_2} \frac{L}{\text{sinc}^2(L\Delta k/2)} \quad (10.34)$$

while for the Fabry-Perot we have

$$|A_{th}|^2 = \frac{2}{\sin^2(L\Delta k/2)} \left\{ \left( \frac{\varepsilon_0}{\chi^{(2)}} \right)^2 \frac{n_1^2 \gamma_1}{\omega_1} \frac{n_2^2 \gamma_2}{\omega_2} \frac{L}{\text{sinc}^2(L\Delta k/2)} \right\} \quad (10.35)$$

Thus the Fabry-Perot cavity is even more sensitive to the phase matching condition than the ring cavity.

Let us stress that for the two OPO cavity configurations which have been analyzed in this chapter, it was assumed that all three modes are resonants. This configuration is called the triply resonant configuration. Similarly, there can be doubly and singly resonant settings in which only two fields or one field, respectively, are resonant with the cavity. The non-resonant fields simply propagate through the  $\chi^{(2)}$  medium but do not feel the presence of the cavity. The description of these configurations is vastly more difficult than the triply resonant cavity unless the non-resonant fields are so intense that they can be assumed to remain constant, in which case the problem is trivial since it reduces to a single or a pair of linear differential equations. The difficulty of the general situation is that the resonant fields certainly vary in time and the non-resonant fields certainly vary in space. Therefore the  $\chi^{(2)}$  coupling leads to a space-time variation for all fields. Only approximate models have been used in analyzing these situations.

## 10.5 References

1.  $\chi^{(2)}$  second order nonlinear optics: from fundamentals to applications, C. Fabre and J.-P. Pocholle eds., Quantum & Semiclass. Optics **9** (1997) 131-295.

**Part IV**

**Quantum interference**



# Chapter 11

## Coherence and atomic interference

### 11.1 Atomic interference

The simplest situation in which atomic interference occurs is the interaction of a three-level medium with a bichromatic field. Let the field be given by

$$E_{tot} = E_a \cos(\omega_a t) + E_b \cos(\omega_b t) \quad (11.1)$$

The three atomic wave functions are  $\varphi_j$  and the corresponding energies are  $\hbar\omega_j$ . The interaction Hamiltonian is  $-erE_{tot}$ . This electric field interacts with a three-level medium as shown in Fig. 11.1. This configuration is usually

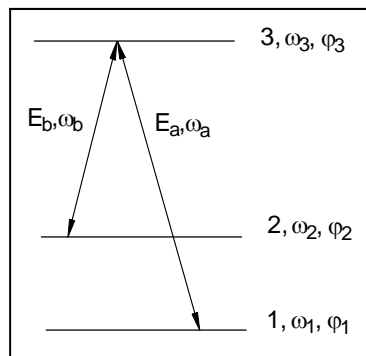


Figure 11.1: Configuration and notations for the three-level medium interacting with two monochromatic fields.

referred to as the  $\Lambda$  configuration. The other two possibilities are:

- The  $V$  configuration where the monochromatic fields connect levels 1 to 2 and levels 1 to 3;
- The ladder configurations where the monochromatic fields connect levels 1 to 2 and levels 2 to 3.

The main point is that in the  $\Lambda$  configuration, an atom in state 3 may decay EITHER through the channel 3 – 1 OR through the channel 3 – 2. In the case of two levels, the probability that the atom decays from the upper state 3 to the lower state 1 is of the form  $P(3 \rightarrow 1) = |C_{31}|^2$  where the complex coefficient  $C_{31}$  is related to the expansion of the total wave function on the basis of the atomic wave functions. When two decay channels are available, the probability is of the form  $P(3) = |C_{31} + C_{32}|^2$  which is the sum of two complex functions, each one associated with one of the decay channels. Hence the total transition probability is not be the sum of the partial transition probabilities:  $P(3) \neq P(3 \rightarrow 1) + P(3 \rightarrow 2)$ : there are interference terms which need not be positive. We shall see that these interference terms may compensate, partially or completely, the partial transition probabilities, therefore reducing the decay probability from level 3.

As a practical example, let us consider a three-level system interacting with the bichromatic field (11.1). We still have to specify the selection rules. Let them be given by

$$\langle j | erE_a | 3 \rangle = \mu E \delta_{j1} \quad \langle j | erE_b | 3 \rangle = \mu E \delta_{j2} \quad (11.2)$$

with all other matrix elements being zero. This corresponds to the interaction scheme of Fig. 11.1. The matrix elements are defined as usual by  $\langle j | \mathcal{O} | k \rangle = \int_V \varphi_j^*(\mathbf{r}) \mathcal{O}(\mathbf{r}) \varphi_k(\mathbf{r}) d\mathbf{r}$  for an operator  $\mathcal{O} \equiv \mathcal{O}(\mathbf{r})$ . To simplify the algebra of this example, we have assumed that the matrix elements are identical when they do not vanish. This simplification is without influence on the qualitative physical results described in this section.

Let us now assume that a superposition state  $\Phi(\mathbf{r}, t) = C_1(t)\varphi_1(\mathbf{r}) + C_2(t)\varphi_2(\mathbf{r})$  can be created. Then the probability of transition from state 3 to that superposition state is given by

$$\begin{aligned} W_1 &= \left| \langle C_1\varphi_1 e^{-i\omega_1 t} + C_2\varphi_2 e^{-i\omega_2 t} | -erE_{tot} | e^{-i\omega_3 t} \varphi_3 \rangle \right|^2 \\ &= \frac{|\mu E|^2}{4} \left| C_1 e^{i(\omega_{31} - \omega_a)t} + C_2 e^{i(\omega_{32} - \omega_b)t} \right|^2 \end{aligned} \quad (11.3)$$

where  $\omega_{jk} \equiv \omega_j - \omega_k$ . The case  $\omega_{31} - \omega_a = \omega_{32} - \omega_b$  is of special interest. If this condition is verified, that is, if the detuning between the field  $E_a$  and the atomic energy difference  $\omega_{31}$  equals the detuning between the field  $E_b$

and the atomic difference  $\omega_{32}$ , then the transition probability  $W_1$  becomes constant in time

$$W_1 = \frac{1}{4} |\mu E (C_1 + C_2)|^2 \quad (11.4)$$

To appreciate more fully this result, let us consider another possible set of selection rules. Let us assume that each field  $E_j$  couples equally the upper level 3 to the two lower states

$$\langle \varphi_j | er E_a | \varphi_3 \rangle = \langle \varphi_j | er E_b | \varphi_3 \rangle = \mu E, \quad j = 1, 2 \quad (11.5)$$

This could be the case if  $\omega_2 - \omega_1 \ll \ll \omega_3$ . In this case, using again the condition of equal detuning  $\omega_{31} - \omega_a = \omega_{32} - \omega_b$ , the probability of transition between the upper state and the state  $\Phi$  becomes

$$W_2 = \frac{|\mu E|^2}{4} |C_1(1 + e^{i\omega_{12}t}) + C_2(1 + e^{-i\omega_{12}t})|^2 \quad (11.6)$$

There is no way in which this function can become time-independent: it is and remains a periodic function of time with period  $T = 2\pi/\omega_{12}$ . This shows how critical the selection rules become in the three-level case.

Let us consider again the first case which yields the transition probability  $W_1$ . An interesting situation occurs if the superposition state is  $\Phi_- = C_1(\varphi_1 - \varphi_2)$ , i.e.,  $C_1 = -C_2$ . In this case  $W_1 = 0$  as a result of *maximum destructive interference*. Indeed, the vanishing of  $W_1$  results from the relations  $|C_1|^2 = |C_2|^2 = -C_1 C_2^* = -C_1^* C_2$ . Physically, this means that an atom which is initially in the upper state will be unable to decay in the state  $\Phi_-$  via a dipole-mediated transition. Conversely, an atom which is initially in the state  $\Phi_-$  will remain in that state. Such states are called *trap states*<sup>1</sup>.

There still remains to produce the superposition state  $\Phi(\mathbf{r}, t) = C_1(t)\varphi_1(\mathbf{r}) + C_2(t)\varphi_2(\mathbf{r})$ . In quantum mechanics, the states  $\Phi_{\pm} = \frac{1}{\sqrt{2}}(\varphi_1 \pm \varphi_2)$  appear in the study of the eigenstates of a two-level atom interacting resonantly with a single mode of the electromagnetic field. In that context, there is a unitary operator which maps the unperturbed basis  $\{\varphi_1, \varphi_2\}$  into the eigenstates of the total Hamiltonian  $\{\Phi_-, \Phi_+\}$ . These two states have a different energy due to the Stark splitting. It is easily verified that the state  $\Phi_+$  has a nonzero transition probability with the upper state 3, as should be. As a result, it appears that what matters is the amount of atomic population in the upper level and in the combination state  $\Phi_+$ . The surprise is that situations can be

<sup>1</sup>O. Kocharovskaya, Phys. Rep. **219**, 175 (1992); P. Mandel, Contemp. Physics **34** (1993) 235; E. Arimondo, in Progress in Optics **XXXV**, edited by E. Wolf (Elsevier, Amsterdam, 1996) 257.

conceived (and realized experimentally<sup>2</sup>) where there is an inversion of population between the upper state and  $\Phi_+$ , and therefore gain or even lasing, while there is no population inversion between the upper state and the lower states  $\varphi_1$  and  $\varphi_2$ . This phenomenon is referred to as gain without inversion or lasing without inversion.

## 11.2 Semiclassical formulation

In this section, we formulate more rigorously the scheme which was described in Section 11.1. We can use the semiclassical formulation developed in Chapter 1 since it is based on a quantum description of matter and a classical description of the electromagnetic fields. This is sufficient to include atomic interference effects.

The procedure is similar to that used for the two-level medium. The electric field and atomic polarization are decomposed as follows

$$E_{tot} = \frac{1}{2} [E_a e^{i(k_a x - \omega_a t)} + E_b e^{i(k_b x - \omega_b t)} + c.c.] \quad (11.7)$$

$$P_{tot} = N [P_a e^{i(k_a x - \omega_a t)} + P_b e^{i(k_b x - \omega_b t)} + c.c.] \quad (11.8)$$

Let us consider the atomic scheme of Fig. 11.1. It is described by the wave function  $\Psi$  with the properties

$$i\hbar \frac{\partial \Psi}{\partial t} = H\Psi = (H_0 + V)\Psi \quad (11.9)$$

$$\Psi = a_1 \varphi_1 + a_2 \varphi_2 + a_3 \varphi_3 \quad (11.10)$$

$$1 = |a_1|^2 + |a_2|^2 + |a_3|^2 \quad (11.11)$$

$$H_0 \varphi_k = \hbar \omega_k \varphi_k, \quad V = -erE_{tot} \quad (11.12)$$

In the dipole approximation, the matrix elements of the perturbation are

$$V_{12} = 0, \quad V_{13} = -\mu_{13} E_{tot}, \quad V_{23} = -\mu_{23} E_{tot} \quad (11.13)$$

With these expressions, we can derive the evolution equations for the coefficients  $a_k$  in  $\Psi$

$$i\hbar \partial_t a_1 = \hbar \omega_1 a_1 - \mu_{13} a_3 E_{tot} \quad (11.14)$$

$$i\hbar \partial_t a_2 = \hbar \omega_2 a_2 - \mu_{23} a_3 E_{tot} \quad (11.15)$$

$$i\hbar \partial_t a_3 = \hbar \omega_3 a_3 - \mu_{32} a_2 E_{tot} - \mu_{31} a_1 E_{tot} \quad (11.16)$$

---

<sup>2</sup>A. Nottelmann, C. Peters, and W. Lange, Phys. Rev. Lett. **70**, 1783 (1993); E.S. Fry, Xingfu Li, D. Nikonov, G. G. Padmabandu, M.O. Scully, A.V. Smith, F.K. Tittel, Ching Wang, S.R. Wilkinson, and Shi-Yao Zhu, Phys. Rev. Lett. **70**, 3235 (1993); W. E. van der Veer, R. J. J. van Diest, A. Dönszelmann, and H. B. van Linden van den Heuvell, Phys. Rev. Lett. **70**, 3243 (1993).

The next step is the derivation of evolution equations for the density matrix. Using the definition  $\rho_{kl} = a_k a_l^*$  and Eqs. (11.14)-(11.16), it is easy to derive the evolution equations

$$i\hbar\partial_t\rho_{31} = \hbar(\omega_3 - \omega_1)\rho_{31} + \mu_{31}(\rho_{33} - \rho_{11})E_{tot} - \mu_{32}\rho_{21}E_{tot} \quad (11.17)$$

$$i\hbar\partial_t\rho_{32} = \hbar(\omega_3 - \omega_2)\rho_{32} + \mu_{32}(\rho_{33} - \rho_{22})E_{tot} - \mu_{31}\rho_{12}E_{tot} \quad (11.18)$$

$$i\hbar\partial_t\rho_{21} = \hbar(\omega_2 - \omega_1)\rho_{21} + \rho_{23}\mu_{31}E_{tot} - \mu_{23}\rho_{31}E_{tot} \quad (11.19)$$

At this point, we use the fact that  $\omega_a \simeq \omega_{31}$  and  $\omega_b \simeq \omega_{32}$  to introduce slowly varying envelopes  $\sigma_{pq}$

$$\rho_{31} = \sigma_{31}e^{i(k_a x - \omega_a t)}, \quad \rho_{32} = \sigma_{32}e^{i(k_b x - \omega_b t)} \quad (11.20)$$

For the low frequency coherence  $\rho_{21}$ , the slowly varying envelope  $\sigma_{21}$  is

$$\rho_{21} = \sigma_{21}e^{i(\omega_b - \omega_a)t - i(k_b - k_a)x} \quad (11.21)$$

Using the rotating wave approximation, which amounts to neglect fast oscillating terms, these definitions lead to the evolution equations

$$i\hbar\partial_t\sigma_{31} = \hbar(\omega_{31} - \omega_a)\sigma_{31} + n_{31}\frac{\mu_{31}}{2}E_a - \sigma_{21}\frac{\mu_{32}}{2}E_b \quad (11.22)$$

$$i\hbar\partial_t\sigma_{32} = \hbar(\omega_{32} - \omega_b)\sigma_{32} + n_{32}\frac{\mu_{32}}{2}E_b - \sigma_{12}\frac{\mu_{31}}{2}E_a \quad (11.23)$$

$$i\hbar\partial_t\sigma_{21} = \hbar(\omega_{21} - \omega_a + \omega_b)\sigma_{21} + \sigma_{23}\frac{\mu_{31}}{2}E_a - \sigma_{31}\frac{\mu_{23}}{2}E_b^* \quad (11.24)$$

where we have used the notation  $n_{pq} = \rho_{pp} - \rho_{qq}$  for the population differences. As a final step, we introduce phenomenologically the damping rates for the three coherence functions. This leads to the set of equations

$$\partial_t\sigma_{31} = -(\gamma_{31} + i\delta_a)\sigma_{31} - in_{31}\frac{\mu_{31}}{2\hbar}E_a + i\sigma_{21}\frac{\mu_{32}}{2\hbar}E_b \quad (11.25)$$

$$\partial_t\sigma_{32} = -(\gamma_{32} + i\delta_b)\sigma_{32} - in_{32}\frac{\mu_{32}}{2\hbar}E_b + i\sigma_{12}\frac{\mu_{31}}{2\hbar}E_a \quad (11.26)$$

$$\partial_t\sigma_{21} = -[\gamma_{21} + i(\delta_a - \delta_b)]\sigma_{21} - i\sigma_{23}\frac{\mu_{31}}{2\hbar}E_a + i\sigma_{31}\frac{\mu_{23}}{2\hbar}E_b^* \quad (11.27)$$

where  $\delta_a = \omega_{31} - \omega_a$  and  $\delta_b = \omega_{32} - \omega_b$ . An essential feature is that although the electromagnetic field couples only level 3 to levels 1 and 2, there appears a low frequency coherence  $\sigma_{21}$  even though the  $2 \Leftrightarrow 1$  transition has been assumed to be forbidden.

The closure of the semiclassical theory implies the relations between the components  $P_j$  of the polarization and the density matrix are

$$P_a = \mu_{13}\rho_{31}e^{i(\omega_a t - k_a x)} \equiv \mu_{13}\sigma_{31}, \quad P_b = \mu_{23}\rho_{32}e^{i(\omega_b t - k_b x)} \equiv \mu_{23}\sigma_{32} \quad (11.28)$$

Therefore, in the slowly varying envelope approximation, the two field equations are

$$(\partial_x + v_a^{-1} \partial_t + \kappa_a) E_a = (iN\mu_{13}\omega_a/v_a \varepsilon'_a) \sigma_{31} \quad (11.29)$$

$$(\partial_x + v_b^{-1} \partial_t + \kappa_b) E_b = (iN\mu_{23}\omega_b/v_b \varepsilon'_b) \sigma_{32} \quad (11.30)$$

where  $v_{a,b} = c/n_{a,b}$  and  $n_{a,b}$  is the refractive index of the passive medium at frequency  $\omega_{a,b}$ .

To be complete, we should write the evolution equations for the populations  $\rho_{jj}$ . However, these equations are not necessary for the remaining of this chapter.

### 11.3 Electromagnetically induced transparency (EIT)

In this section, we consider the following problem: assuming  $E_b$  to be a strong field, how does it affect the optical properties of the 3 – 1 transition? To answer this question, we consider Eqs. (11.25) - (11.27) for the induced atomic coherence. In steady state, we have

$$\sigma_{31} = -\frac{i\mu_{31}}{2\hbar} \frac{E_a n_{31}}{\gamma_{31} + i\delta_a} + \frac{i\mu_{32}}{2\hbar} \frac{E_b \sigma_{21}}{\gamma_{31} + i\delta_a} \quad (11.31)$$

$$\sigma_{32} = -\frac{i\mu_{32}}{2\hbar} \frac{E_b n_{32}}{\gamma_{32} + i\delta_b} + \frac{i\mu_{31}}{2\hbar} \frac{E_a \sigma_{12}}{\gamma_{32} + i\delta_b} \quad (11.32)$$

$$\sigma_{21} = \frac{i(\mu_{23}E_b)^* \sigma_{31}}{2\hbar[\gamma_{21} + i(\delta_a - \delta_b)]} - \frac{i\mu_{31}E_a \sigma_{23}}{2\hbar[\gamma_{21} + i(\delta_a - \delta_b)]} \quad (11.33)$$

At this point, we introduce four simplifications:

1. We assume that the populations  $\rho_{kk}$  do not change much under the influence of the applied fields:  $\rho_{kk} \simeq n_k^{(0)}$ . It is not easy to justify this simplification, except for the fact that it is validated by the full calculation made without that approximation. It is in fact a version of the linear approximation introduced for the two-level model in Sec. 2.1 via Eq. (2.3).
2. Without external fields we have  $n_3^{(0)} = n_2^{(0)} e^{-\beta\hbar\omega_{32}}$  and  $n_2^{(0)} = n_1^{(0)} e^{-\beta\hbar\omega_{21}}$ . Hence  $n_1^{(0)} \gg n_2^{(0)} \gg n_3^{(0)}$ . Therefore, we introduce the simplification  $n_1^{(0)} = 1$  and  $n_3^{(0)} = n_2^{(0)} = 0$  which is surely valid at room temperature in the absence of driving field.

3. Since the field  $E_b$  is an intense field which drives the atomic system and  $E_a$  is a weak field, we only retain in the solutions of Eqs. (11.31)-(11.33) terms linear in the weak field  $E_a$  but make no simplification with respect to the strong driving field.
4. The field  $E_b$  is resonant with the atomic transition it drives:  $\delta_b = 0$ .

With these simplifications, the solutions of equations (11.31)-(11.33) are easily found to be

$$\sigma_{31} = \frac{i2\hbar\mu_{31}E_a(\gamma_{12} + i\delta_a)}{4\hbar^2(\gamma_{21} + i\delta_a)(\gamma_{31} + i\delta_a) + |\mu_{32}E_b|^2} \quad (11.34)$$

$$\sigma_{21} = -\frac{(\mu_{31}E_a)^* \mu_{32}E_b}{4\hbar^2(\gamma_{21} - i\delta_a)(\gamma_{31} - i\delta_a) + |\mu_{32}E_b|^2} \quad (11.35)$$

$$\sigma_{32} = \frac{i\mu_{13}E_a}{2\hbar\gamma_{32}}\sigma_{21} \quad (11.36)$$

Thus the susceptibility at the transition 3 – 1 as influenced by the intense field  $E_b$  driving the 3 – 2 transition is

$$\begin{aligned} \chi &= \frac{P_a}{E_a} = \frac{\mu_{13}\sigma_{31}}{E_a} = \frac{i2\hbar|\mu_{31}|^2(\gamma_{12} + i\delta_a)}{4\hbar^2(\gamma_{21} + i\delta_a)(\gamma_{31} + i\delta_a) + |\mu_{32}E_b|^2} \\ &= i\frac{|\mu_{31}|^2}{2\hbar\gamma_{31}} \frac{\gamma + i\delta}{(\gamma + i\delta)(1 + i\delta) + |\mu_{32}E_b/2\hbar\gamma_{31}|^2} \end{aligned} \quad (11.37)$$

with the dimensionless parameters  $\gamma = \gamma_{21}/\gamma_{31}$  and  $\delta = \delta_a/\gamma_{31} = (\omega_{31} - \omega_a)/\gamma_{31}$ . The real and imaginary parts of the susceptibility (11.37) are

$$\chi' = \frac{|\mu_{31}|^2}{2\hbar\gamma_{31}} \frac{\delta(\gamma^2 + \delta^2 - \Omega^2)}{(\gamma - \delta^2 + \Omega^2)^2 + \delta^2(\gamma + 1)^2} \quad (11.38)$$

$$\chi'' = \frac{|\mu_{31}|^2}{2\hbar\gamma_{31}} \frac{\gamma^2 + \delta^2 + \gamma\Omega^2}{(\gamma - \delta^2 + \Omega^2)^2 + \delta^2(\gamma + 1)^2} \quad (11.39)$$

with the dimensionless field amplitude defined by  $\Omega = |\mu_{32}E_b|/2\hbar\gamma_{31}$ .

The way in which  $E_b$  influences the 3 – 1 transition is displayed in Fig. 11.2. We see that for a weak driving field ( $\Omega \ll 1$ ), the susceptibility has qualitatively the same shape as for the two-level medium (see Fig. 2.1). This means that the system is transparent ( $\chi' = 0$ ) where the absorption is maximum ( $\chi'' = 1$ ). As the driving field increases, a dip appears in  $\chi''$  at the point of transparency and finally it practically reaches zero. At  $\delta = 0$ ,

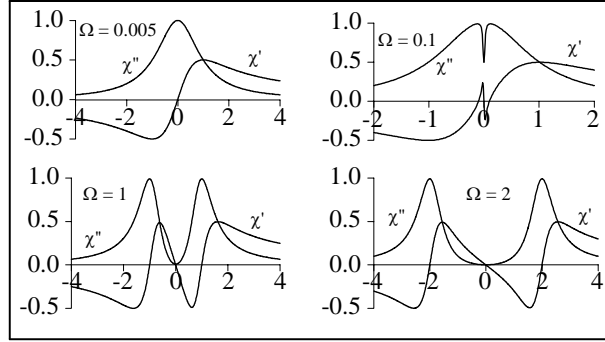


Figure 11.2: Real and imaginary parts of the susceptibility at the 3-1 transition as a function of  $\delta = (\omega_{31} - \omega_a) / \gamma_{31}$ , the normalized detuning between the atomic energy difference  $\omega_{31}$  and the probe field frequency  $\omega_a$ . Units of the susceptibility are  $|\mu_{31}|^2 / (2\hbar\gamma_{31})$ . Four different values of the field  $\Omega = |\mu_{32}E_b| / (2\hbar\gamma_{31})$  driving the 3-2 transition are chosen. The ratio  $\gamma_{21}/\gamma_{31}$  is  $10^{-2}$ .

$\chi'' = \gamma / (\gamma + \Omega^2) \rightarrow \gamma / \Omega^2$  in the limit  $\Omega \gg \gamma$ . Thus the absorption coefficient at the 3 – 1 transition becomes close to zero as the driving field at the 3 – 2 transition increases. In this way, atomic interference leads to a reduction of the absorption coefficient at  $\delta = 0$ . The deformations of  $\chi'$  and  $\chi''$  under the influence of  $\Omega$  preserve the property that zeroes of  $\chi'$  correspond to extrema of  $\chi''$ . The phenomenon of (near) cancellation of the absorption at transparency is known as *electromagnetically induced transparency* (EIT). It was first predicted theoretically<sup>3</sup>. The first experimental observation was reported by the same group the next year<sup>4</sup>. They used a 10 cm cell containing a gas of neutral Sr ( $5 \times 10^{15}$  atoms/cm<sup>3</sup>). The transition which was probed was the  $5s5p^1P_1 - 4d5d^1D_2$  transition at 337.1nm. In the absence of another field, the cell absorption at that frequency was  $e^{-20}$ . In the presence of a strong field driving the  $4d5p^1D_2 - 4d5d^1D_2$  transition at 570.3nm, the absorption of the cell was reduced to  $e^{-1}$ .

The obvious advantage of this scheme over the saturation bleaching is that in the latter case the medium is made transparent by saturation and this requires the use of intense fields. Since there is dispersion and nonlinearity, the beam which eventually succeeds in traversing the medium has lost significant power and beam quality: the field distribution in the plane transverse to the propagation direction is highly inhomogeneous. This is unacceptable for many applications. On the contrary, in the EIT scheme, it is an adjacent transition

<sup>3</sup>S.E. Harris, J.E. Field, and A. Imamoglu, Phys. Rev. Lett. **64** (1990) 1107.

<sup>4</sup>K.J. Boller, I. Imamoglu, and S.E. Harris, Phys. Rev. Lett. **66** (1991) 2593.

which is strongly driven. Furthermore, the EIT scheme allows the use of a driving field at a different frequency than the probed transition. This is can be exploited to drive at a low frequency and probe at a higher frequency.

## 11.4 Slow light

One observation about EIT as displayed in Fig. 11.2 is that the slope of  $\chi'$  close to  $\delta = 0$  changes sign and can be very steep. Therefore, one should expect that properties depending on that slope will manifest a markedly different behavior in the case of EIT. One such property is the group velocity or the group refractive index defined by Eq. (2.47). In this case,  $\partial n / \partial k = 0$  so that we are left with

$$v_g \equiv \frac{\partial \omega}{\partial k} = \frac{c}{n + \omega \frac{\partial n}{\partial \omega}} \equiv \frac{c}{n_g} \quad (11.40)$$

This leads to an unexpected consequence of EIT, namely the possibility to control the speed of light, to cancel it and even to make it negative<sup>5</sup>. Of course, this does not refer to the phase velocity but only to the group velocity. Still, it is the group velocity which is relevant for many applications since that is the velocity which affects the speed of the wave packet, i.e., the transport of energy. Using the expression (11.38) for the real part of the susceptibility and the definition  $n = \sqrt{1 + \chi'}$ , it is easy to verify that close to the resonance ( $\delta = 0$ ) the refractive index  $n$  and the group refractive index  $n_g$  are given by the following expansions

$$n = n_0 + n_1 \delta + \mathcal{O}(\delta^2) = 1 - \frac{|\mu_{31}|^2}{4\hbar\gamma_{31}} \frac{\Omega^2 - \gamma^2}{(\gamma - \Omega^2)^2} \delta + \mathcal{O}(\delta^2) \quad (11.41)$$

$$n_g = n_{0g} + \mathcal{O}(\delta) = 1 + \frac{|\mu_{31}|^2}{4\hbar\gamma_{31}} \frac{\omega_{31}}{\gamma_{31}} \frac{\Omega^2 - \gamma^2}{(\gamma - \Omega^2)^2} + \mathcal{O}(\delta) \quad (11.42)$$

To avoid jumping too quickly to wrong conclusions, it should be clear that the expansion in powers of  $\delta$  converges if and only if the coefficient of  $\delta^n$  is smaller than the coefficient of  $\delta^{n-1}$ . Otherwise,  $n$  and  $n_g$  must be used without approximations. The double constraint of  $|n_1 \delta| \ll n_0$  and  $n_{0g} \gg 1$  leads to the condition  $|\delta| \ll \omega_{31} / \gamma_{31}$ , which is physically realizable.

From Eqs. (11.41)-(11.42) it is seen that in the conditions of EIT for which the expressions (11.38)-(11.39) hold for the susceptibility, the refractive index

---

<sup>5</sup>A review of this topic is presented in *Slow, ultraslow, stored, and frozen light*, A.B. Maysko, O. Kocharovskaya, Yu. Rostovtsev, G.R. Welch, A.S. Zibrov, and M.O. Scully, Adv. Atom. Mol. Opt. Phys. **46** (2001) 191-242.

equals unity on resonance while the group refractive index can be made very large in the domain  $|\delta| \ll \omega_{31}/\gamma_{31}$ . Thus, we arrive at the following situation on resonance:

- In the absence of a driving field ( $\Omega = 0$ ), the refractive index equals unity but the absorption is maximum: the probe field  $E_a$  suffers maximum absorption, which may make the medium opaque to the radiation at the frequency  $\omega_a$ .
- Applying a strong driving field to excite the adjacent coherence between levels 3 and 2 has the effect of modifying the optical properties of the coherence between levels 3 and 1, resulting in a transparency of the medium at the frequency  $\omega_a$  since  $\chi''(\omega_a) \simeq 0$  without dispersion since  $n = 1$ .
- When this is realized, and if the condition  $|\delta| \ll \omega_{31}/\gamma_{31}$  is verified, the group refractive index is very large, which means that the group velocity is very small. Light propagating in these conditions is called slow or ultraslow light<sup>6</sup>. Group velocities of a few meters per second in the visible range are now realized without problems in various media (gas and solid-state) at room temperature.
- If the medium is inhomogeneous, there is a further source of reduction since in that case the group velocity is given by the complete expression (2.47)

$$v_g \equiv \frac{\partial \omega}{\partial k} = \frac{c - \omega \frac{\partial n}{\partial k}}{n + \omega \frac{\partial n}{\partial \omega}} \quad (11.43)$$

- Under suitable conditions, the group velocity can vanish<sup>7</sup> and even become negative. This has been achieved experimentally<sup>8</sup>. A positive/negative group velocity means that the wave packet moves in the

---

<sup>6</sup>L.V. Hau, S. E. Harris, Z. Dutton, and C. H. Behroozi, *Nature (London)* **397**, 594 (1999); M. Kash, V. Sautenkov, A. Zibrov, L. Hollberg, G. Welch, M. Kukin, Y. Rostovsev, E. Fry, and M. Scully, *Phys. Rev. Lett.* **82**, 5229 (1999); D. Budker, D. F. Kimball, S. M. Rochester, and V. V. Yashchuk, *Phys. Rev. Lett.* **83**, 1767 (1999).

<sup>7</sup>M.D. Lukin, S. F. Yelin, and M. Fleischhauer, *Phys. Rev. Lett.* **84**, 4232 (2000); A. E. Kozhokin, K. Mølmer, and E. Polzik, *Phys. Rev. A* **62**, 033809 (2000); O. Kocharovskaya, Yu. Rostovtsev, and M. O. Scully, *Phys. Rev. Lett.* **86**, 628 (2001).

<sup>8</sup>C. Liu, Z. Dutton, C. H. Behroozi, and L.V. Hau, *Nature* **409**, 490 (2001); D. F. Phillips, A. Fleischhauer, A. Mair, R. L. Walsworth, and M.D. Lukin, *Phys. Rev. Lett.* **86**, 783 (2001); A. Mair, J. Hager, D. F. Phillips, R. L. Walsworth, and M. D. Lukin, *Phys. Rev. A* **65**, 031802R (2002); A.V. Turukhin, V. S. Sudarshanam, and M. S. Shahriar, J. A. Musser, B. S. Ham, and P. R. Hemmer, *Phys. Rev. Lett.* **88**, 023602 (2002); A. S. Zibrov, A. B. Matsko, O. Kocharovskaya, Y.V. Rostovtsev, G. R. Welch, and M. O. Scully, *Phys. Rev. Lett.* **88**, 103601 (2002).

forward/backward direction. Controlling the sign of the group velocity may have potential applications to an all-optical read/write process.